POLITECNICO DI MILANO

FACOLTÀ DI INGEGNERIA DEI SISTEMI

Corso di Laurea Specialistica in Ingegneria Matematica

A MODEL FOR CELL GROWTH IN BATCH BIOREACTORS

Relatore

Dott. Nicola Parolini

Tesi di laurea di

Susanna Carcano

matricola 721016

Anno Accademico 2009/2010

Contents

List of Figures

Introduction

The use of animal cells for the production of recombinant proteins used in human therapy has gained great relevance at both development and application level in industrial production processes.

Today, in particular, Chinese hamster ovary (CHO) cells are the most commonly used mammalian hosts in biological and medical research and commercially in large scale recombinant protein production. CHO cells are a cell line derived from the ovary of the Chinese hamster. These cells are widely used for the production of therapeutic proteins such as prothrombin, a glycoprotein precursor of thrombin, that is necessary for the coagulation of blood, and thrombopoietin, a glycoprotein hormone that regulates the production of platelets by the bone marrow. The CHO cell line is widely used as it is known for being a highly stable host with respect to the expression of heterologous genes and for its immense adaptive ability.

Despite the significant advances and improvement during the last past decade in cell line development, as well as in medium optimization, process monitoring and control, the current paradigms of cell line development remain, to large extent, empirical [12], and the development of cultures for this type of cells still presents a series of problems. These difficulties primarily stem from our inadequate understanding of the biology and physiology of mammalian cells. Secondly, there is a considerable variability and very little understanding of the sources of variation in mammalian cell culture processes. Moreover, actually there are no reliable methods for predicting or modeling the growth characteristics and production capabilities in large-scale bioreactors. Indeed, the cells selected and characterized in bench-top reactors may not behave similarly in large-scale bioreactors, despite employing identical process parameters.

These problems can be faced in distinct ways. The first approach consists in the genetic manipulation of the cell. It is possible, for example, to enhance cell viability and to modify and improve its metabolic pathways in order to reduce the production of toxic by-product and to increase the production of recombinant proteins. The second approach consists in the improvement of the culture strategies, for example by modifying the bioreactor operative conditions or the culture medium composition. Fed-batch strategies for the addition of metabolic substrates and the elimination of the inhibitory compounds have also been considered; however, both these strategies require a high degree of instrumentation to be carried out in an optimal way. While the first approach, thanks to the sequencing of mammalian genomes, is based on the exact knowledge of the gene-coding and regulatory element sequences of the organism, the second approach is actually completely empirical, that is based on experimental observations.

In predicting the cell growth behavior, the use of mathematical models is gaining more and more attention because it guarantees an increasing insight into the process. For process design and optimization, simulation studies can be very useful to reduce the number of expensive and time-consuming experiments. Accumulating sufficient data on the dynamics of cells growth, in fact, requires an extensive amount of work and it is costly. In addiction, even if data can describe cell growth, they provide little insight into the relationship between physiological processes and growth or survival. One way this link can be made is through the use of mathematical models.

An investigation of bioreactor performance and cell growth behavior might conventionally be carried out in an almost entirely empirical manner. In this approach, the bioreactor behavior should be studied under practically all combinations of possible operating conditions and the results then expressed as series of correlations, from which the resulting performance might hopefully be estimated for any given set of new operating conditions. This empirical procedure can be carried out in a very routine way and is reasonably simple to set up. While this might seem to be rather convenient, the procedure has actually many disadvantages, since very little real

understanding of the process would be obtained. Moreover very many experiments would be required in order to obtain correlations that would cover every process.

Compared to this, the modeling approach attempts to describe both actual and potential bioreactor performance, by means of well-established theory, which describes, in mathematical terms, a working model for the process. In carrying out a modeling exercise, it is necessary to consider the nature of all the important parameters of the process, their effect on the process and how each parameter can be defined in quantitative terms. Thus the very act of modeling is one that forces a better understanding of the process, since all the relevant theory must be critically assessed. In addition, the task of formulating theory into terms of mathematical equations is also a very positive factor that forces a clear formulation of basic concepts.

Once formulated, the model can be solved and the behavior predicted by the model compared with experimental data. Any differences in performance may be used to further redefine or refine the model until good agreement is obtained. Once the model is established, it can then be used, with reasonable confidence, to predict performance under different process conditions, and it can also be used for such purposes as process design, optimization and control. An input of experimental data is, of course, required in order to assess or validate the model, but the quantity of experimental data required, when compared to that of the empirical approach, is considerably reduced. Apart from this, the major advantage gained is the increased understanding of the process that one obtains simply by carrying out the modeling exercise.

Starting from these introductive considerations, our purpose is to develop a mathematical model to describe CHO cell growth dynamics as a function of the culture medium composition and the bioreactor operative conditions. In this study, we follow a deterministic approach: we investigate the physical and chemical properties of the process of CHO cell growth in order to understand which are the governing factors. In particular, we analyze deeply cell physiology, paying particular attention to the the mechanism of metabolism that allows the cell to grow, maintain and reproduce. Then we try to understand in which way the environmental properties, like temperature and concentrations of nutrients, and the bioreactor operative conditions can in-

fluence cell growth dynamics. Consequently, the model that we are going to introduce, is based on the investigation of some of the most important mechanisms that govern the cell growth process.

This work has been carried out in collaboration with the Chair of Modeling and Scientific Computing (CMCS), the Cellular Biotechnology Laboratory (LBTC) and the Hydraulic Machines Laboratory (LMH) of the EPFL in the framework of the project *Fluid dynamics and mixing behavior in orbitally shaken bioreactors for mammalian cell cultivation* (Sinergia Research Proposal 2009-2011), approved by the Swiss National Science Foundation (FNS). In particular, we will refer to some of the experiments carried out at the LBTC in order to obtain important experimental information.

The work is structured in five chapters. In Chapter 1 we present and discuss the state of the art on cell growth models in order to detect the advantages and the limits related to the application of the most popular models in the literature before presenting our own cell growth model.

In Chapter 2 we analyze the most important characteristics of CHO cells, in particular focusing on cell metabolism and on the main environmental factors that affect cell growth process.

In Chapter 3 we describe the main properties of CHO cell culture and we introduce in particular a model for the batch fermenter.

In Chapter 4 we present a new model for cell growth which is based on the analysis and on the considerations made in the previous chapters. In this model the cell dynamics is function of time, substrates concentrations and temperature. Later on, the model is extended in order to take into account the spatial dependance.

In Chapter 5 we discuss the most significant numerical results obtained with the models introduced in the previous chapter and we make some comparison with the experimental results.

Introduzione

L'impiego di cellule animali per la produzione di proteine a scopo terapeutico ha acquistato una grande importanza sia a livello di ricerca, sia a livello industriale.

Oggi, in particolare, le cellule CHO (Chinese Hamster Ovary cells) sono le cellule maggiormente utilizzate nella ricerca medica e nella produzione di proteine su larga scala. Questo tipo di cellule è utilizzato ad esempio per la produzione di protrombina, una glicoproteina precursore della trombina, necessaria per la coagulazione del sangue, e della trombopoietina, una glicoproteina che regola la produzione di piastrine nel midollo osseo.

Nonostante i significativi progressi e miglioramenti compiuti nel corso degli ultimi dieci anni nello sviluppo di colture cellulari, così come nell'ottimizzazione del mezzo di coltura, nel monitoraggio e nel controllo del processo, i correnti paradigmi relativi allo sviluppo di colture cellulari sono essenzialmente di carattere empirico. La progettazione di colture presenta ancora una serie di problematiche. Queste difficoltà derivano principalmente da una inadeguata ed incompleta conoscenza delle caratteristiche fisiologiche delle cellule dei mammiferi. In secondo luogo, c'è una notevole variabilità ed comprensione una molto limitata dei fattori che influenzano il processo di coltura cellulare. Infine, ad oggi, non esistono metodi accurati per predire e modellare la dinamica del processo.

Questa tipologia di problemi può essere affrontata in differenti modi. Il primo approccio consiste nella manipolazione genetica delle cellule. E' possibile infatti incrementarne la probabilità di sopravvivenza e migliorarne il metabolismo in modo tale da ridurre la produzione di sostanze tossiche e aumentare la produzione di proteine. Il secondo approccio consiste nel migliorare le strategie di coltura, per esempio modificando le condizioni ope-

rative del bioreattore o la composizione del mezzo di coltura. Sono state anche considerate strategie basate sull'aggiunta di sostanze nutritive e sulla rimozione di sostanze inibitrici. Entrambe queste strategie richiedono però una complessa e costosa strumentazione per essere applicate in maniera efficace ed ottimale.

Mentre il primo approccio, grazie al sequenziamento del genoma dei mammiferi, è basato sull'esatta conoscenza del codice genetico ed in particolare delle sequenze che influiscono sulle funzioni regolatrici sull'organismo, il secondo approccio è attualmente basato su conoscenze di tipo empirico, cioè su osservazioni sperimentali.

Nel predire la dinamica del processo di crescita cellulare, l'utilizzo di modelli matematici sta guadagnando sempre maggiore attenzione in quanto garantisce una migliore e più profonda conoscenza del processo. Le simulazioni numeriche, applicate alla progettazione e all'ottimizzazione del processo, possono essere estremamente utili per ridurre il numero dei costosi e lunghi esperimenti attualmente necessari per sviluppare una tecnologia efficiente. Inoltre, nonostante i dati sperimentali raccolti siano utili per descrivere il processo, essi non forniscono maggiori informazioni sulle relazioni che intercorrono tra fisiologia cellulare, condizioni operative e produzione di cellule e proteine. Uno dei modi possibili per approfondire queste relazioni è basato sull'uso di modelli matematici.

Lo studio del rendimento di un bioreattore e del processo di crescita cellulare può essere portato avanti adottando un approccio quasi interamente empirico. Il comportamento del bioreattore dovrebbe essere analizzato in tutte le possibili condizioni operative ed i risultati quindi espressi come serie di correlazioni, dalle quali stimare il rendimento per ogni dato insieme di nuove condizioni operative. Questa procedura empirica risulta essere ragionevolmente semplice, ma non favorisce una reale comprensione del processo. Inoltre per poter ottenere informazioni relative ad ogni possibile condizione operativa è necessario un gran numero di esperimenti.

Al contrario un approccio di tipo modellistico ha lo scopo di descrivere il rendimento attuale e potenziale del bioreattore sulla base di teorie accettate che descrivono, in termini matematici, il processo. Per formulare il mod-

ello, è necessario considerare la natura di tutti i più importanti parametri ed il loro effetto sul processo, cercando di darne una definizione in termini quantitativi. L'esercizio stesso di modellazione, di conseguenza, stimola una migliore comprensione del processo.

Una volta formulato, il modello può essere risolto ed il comportamento previsto dal modello confrontato con i risultati sperimentali. Ogni differenza riscontrata può essere sfruttata per ridefinire o raffinare il modello finché non si ottiene un buon accordo con i risultati attesi. Una volta riconosciuta l'affidabilità del modello, questo può essere applicato per predire il rendimento in differenti condizioni operative, per la progettazione, l'ottimizzazione e il controllo del processo.

Anche adottando un approccio modellistico sono necessari dati sperimentali per validare il modello, ma la quantità di informazioni richieste è inferiore se confrontato con quella necessaria adottando un approccio interamente empirico. Il maggiore vantaggio risulta comunque essere quello di una più profonda comprensione dei meccanismi alla base del processo.

Partendo da queste considerazioni introduttive, l'obiettivo di questa tesi è stato lo sviluppo un modello matematico per descrivere il processo di crescita delle cellule CHO in funzione della composizione del mezzo di coltura e delle condizioni operative del bioreattore. Nello sviluppo del modello si è deciso di adottare un approccio di tipo deterministico: si sono analizzate le proprietà fisiche e chimiche del processo di crescita cellulare con l'obiettivo di comprendere quali fossero i fattori determinanti. Sono stati analizzati i principali aspetti della fisiologia cellulare, in particolare i processi metabolici che permettono alla cellula di crescere, mantenersi e riprodursi. In seguito si è cercato di comprendere le modalità in cui le condizioni ambientali, come temperatura e concentrazione di nutrienti, e le condizioni operative del bioreattore possono influenzare la dinamica del processo. In conclusione, il modello così sviluppato è dunque basato sull'analisi di alcuni dei principali meccanismi che governano il processo di crescita cellulare.

Questo lavoro è stato portato avanti in collaborazione con il Laboratorio CMCS (Chair of Modeling and Scientific Computing) ed il Laboratorio LBTC (Laboratoire de Biotechnologie Cellulaire) dell'Ecole Polytechnique

Fédérale de Lausanne (EPFL) nell'ambito del progetto *"Fluid dynamics and mixing behavior in orbitally shaken bioreactors for mammalian cell cultivation"* finanziato dalla Swiss National Science Foundation (FNS). In particolare la validazione del modello è stata svolta in collaborazione con il Laboratorio LBTC, che ha messo a disposizione i risultati delle prove sperimentali effettuate per ricavare alcune importanti informazioni relative al processo analizzato.

Il lavoro è strutturato in cinque capitoli. Nel Capitolo 1 è presentato e discusso lo stato dell'arte sui modelli di crescita cellulare con l'obiettivo di individuare i principali vantaggi e limiti legati all'applicazione dei modelli più diffusi in letteratura.

Nel Capitolo 2, vengono analizzate le principali caratteristiche delle cellule CHO; in particolare vengono studiati in dettaglio il metabolismo cellulare e i più importanti fattori ambientali che influenzano il processo di crescita cellulare.

Nel Capitolo 3, vengono descritte le proprietà che contraddistinguono le colture di cellule CHO e viene introdotto un opportuno modello matematico per il bioreattore.

Nel Capitolo 4, viene presentato un nuovo modello di crescita cellulare basato sulle analisi e sulle considerazioni discusse nei capitoli precedenti. Il modello introdotto descrive la dinamica cellulare in funzione del tempo, della concentrazione di nutrienti e della temperatura. In seguito, il modello è ampliato al fine di considerare la dipendenza del fenomeno dalla profondità e dal moto del mezzo di coltura.

Nel Capitolo 5, infine, vengono discussi i più significativi risultati numerici ottenuti applicando i modelli introdotti nel capitolo precedente.

Chapter 1

State of the art on cell growth models

1.1 Introduction

The growth of bacteria and cells has been the subject of much study over the years and in the scientific literature we can quite easily find different examples of cell growth models. In this chapter we want to introduce and compare some of the most popular models, in order to detect the advantages and the limits related to the application of each one before developing our own cell growth model.

Various types and classifications of models are possible. For example, we can divide models into *empirical* and *mechanistic models*. Empirical models are essentially pragmatic, and simply describe a set of data in a convenient mathematical relationship with no consideration of underlying phenomena. On the contrary, mechanistic models are build up from theoretical bases and, if they are correctly formulated, can allow the response to be interpreted in terms of known physical, chemical and biological phenomena. In one sense, if this approach is adopted, it follows that the parameters in such models might be readily interpretable properties of the system under study, and that the mathematical form of the model would enable interpretation of the interactions between those factors. Interpretability of model parameters is a feature highly valued by many authors in the predictive microbiology

literature. Although the development of predictive microbiology has seen the embedding of more and more mechanistic elements in the models, or at least the development of models whose structure and parametrization reflects known or hypothesized phenomena, in practice many models currently available, that we are going to introduce now, are not purely empirical nor purely mechanistic.

Cell growth models can be divided into *structured*, *unstructured* and *segregated models* [5]. A structured model attempts to explicitly describe intracellular processes in both a structural and physiological sense, and thus offers the most realistic representation of a cell. Structured models are usually single-cell models that look in some detail at individual processes and reactions. However, whereas cell behavior to varying growth conditions is not thoroughly understood, a structured model is not applicable to most of cell lines, for example to CHO cells. Therefore, the majority of the kinetic models in literature are categorized as unstructured: they rely on the global relationships between cell growth and environmental properties of the culture, and neglect intracellular processes. A third type of models are the segregated ones, which consider different stages of cell cycle and therefore a distribution of cell stages in a culture, without structuring the cell composition. In the most realistic, but most complex situation, models can be both structured and segregated.

The differences among these models can be better described by their different balance regions, as shown in Figure 1.1. In the non structured-non segregated model, the balance region is the total biomass volume; the structured model, instead, considers as balance regions different compartments inside the cell; finally, in the segregated model, the balance regions are different biomass parts.

Consistently with the widely accepted terminology introduced in [2], we term those models that describe the response of microorganisms to a single set of conditions over time as *primary models*. Models that describe the effect of environmental conditions, e.g., physical and chemical features, on the values of the parameters of a primary model are referred to as *secondary models*.

(a) Non structured - non segregated model

(b) Structured - non segregated model

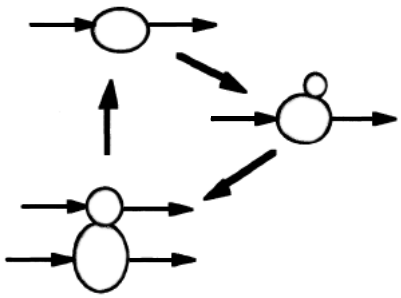

(c) Non structured - segregated model

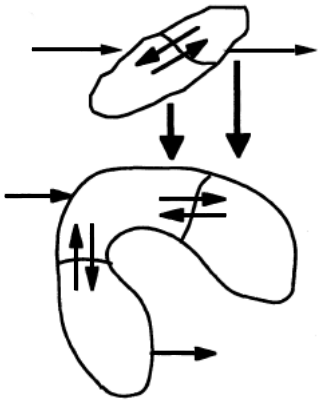

(d) Structured - segregated model

Figure 1.1: Balance regions for different types of kinetic models (from [5])

In this chapter we adopt this last classification to introduce the most popular cell growth models in the literature. First, we are going to present some example of primary model, then we will deeply describe the Monod model, probably the most applied secondary model, and different derived secondary models. Finally, we will briefly introduce some aspects of the structured approach.

1.2 Simple microbial kinetics: primary models

The models that we present in this section are known as primary models. A primary model for cell growth aims to describe the kinetics of the process with as few parameters as possible, while still being able to accurately describe the distinct stages of growth.

1.2.1 The Malthusian model

The simplest cell growth model is the Malthusian model [17], that is often referred to as *exponential law*. Under ideal conditions for growth, when a batch fermentation is carried out, it can be observed experimentally that the quantity of biomass, and therefore also its concentration, increases exponentially over time. This behavior can be explained by the fact that all cells have the same probability to multiply. Thus the overall rate of biomass formation is proportional to the biomass itself. This leads to an autocatalytic reaction, which is described by a first order rate expression as

$$r_X = \mu X,$$

where r_X is the rate of cell growth (kg cell/m^3·h), X is the cell concentration (kg cell/m^3) and μ is a kinetic growth constant (1/h), called *specific growth rate*. For a batch system, this is equivalent to

$$\frac{dX}{dt} = \mu X(t).$$

The analytical solution of this simple, first order differential equation is shown in Figure 1.2 and it is of the form

$$X(t) = X_0 \exp(\mu t),$$

where X_0 is the initial cell concentration at time $t = 0$. The cell concentration that is obtained from the Malthusian model has the rather unrealistic feature of getting larger without bound as t increases: the model ignores that cells require resources to grow and that these resources are limited. Basically, the Malthusian model does not fulfill the *first kinetic principle* proposed by Penfold and Norris [20], namely that the cell growth rate μ is best described by a saturation type of curve.

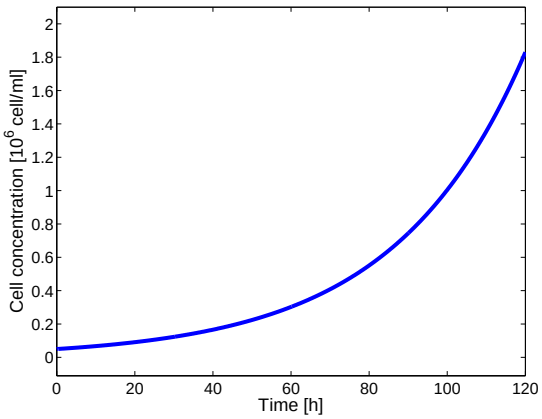

Figure 1.2: Solution of the Malthusian model with $X_0 = 0.3 \cdot 10^5$ [cell/ml] and $\mu = 0.03$ [1/h]

1.2.2 The logistic model

A second model that we can introduce is the logistic model [28], that was first published by Pierre-Francois Verhulst in 1838 after he read Malthus' work. It takes the following form:

$$\frac{dX}{dt} = \mu X\left(1 - \frac{X}{K}\right),$$

where now, besides μ, there is a second parameter K (kg cell/m^3), often called *carrying capacity*, which is the maximum concentration of cells that the environment can support. The logistic equation has the major disadvantage that the carrying capacity K cannot be measured other than by growing the organism until it stops growing. Moreover, there is no theoretical underpinning for it.

The logistic equation can be integrated exactly and has solution (Figure 1.3):

$$X(t) = \frac{K}{1 + CK\exp(-\mu t)},$$

where $C = 1/X_0 - 1/K$ is determined by the initial condition X_0.

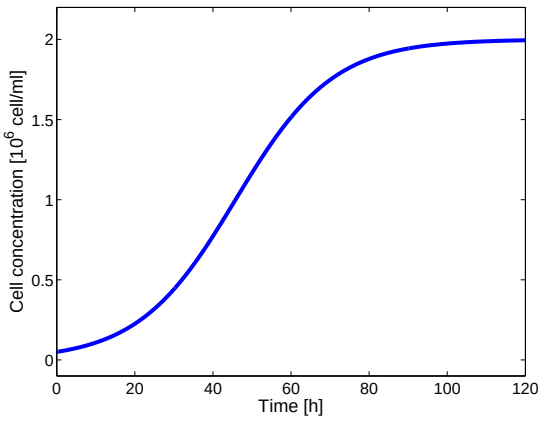

Figure 1.3: Solution of the logistic model with $X_0 = 0.3 \cdot 10^5$ [cell/ml], $\mu = 0.08$ [1/h] and $K = 2 \cdot 10^6$ [cell/ml]

1.2.3 The Gompertz model

The Gompertz function [8] is a sigmoid function, as the logistic curve. As the previous model, the curve shows a slowest growth at the start and at the end of the time period. In contrast to the logistic function in which both the asymptotes are approached by the curve symmetrically, in the Gompertz model the future value asymptote of the function is approached much more gradually by the curve than the lower valued asymptote.

The Gompertz curve has the following expression (Figure 1.4):

$$X(t) = a\exp[-b\exp(-ct)].$$

It is possible to verify immediately that a is the upper asymptotic value, b is the x displacement and c sets the growth rate. Moreover, the initial cell concentration is $X_0 = a\exp(-b)$.

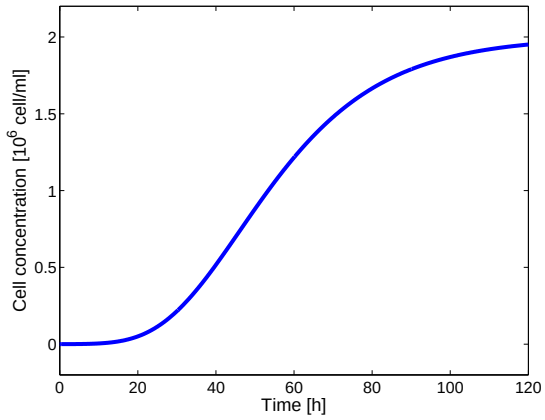

Figure 1.4: Solution of the Gompertz model with $a = 2 \cdot 10^6$ [cell/ml], $b = 10$, $c = 0.05$ [1/h]

1.2.4 The modified logistic and the modified Gompertz models

Sigmoidal functions have been the most popular ones used to fit microbial growth data since these functions consist of three phases, similar to the microbial growth curve. The most commonly used in the literature are the modified logistic model [18]:

$$\log X(t) = A + \frac{C}{1 + \exp(-B(t - M))}$$

and the modified Gompertz model:

$$\log X(t) = A + C \exp\big(- \exp[-B(t - M)]\big),$$

where $X(t)$ is the number of cells at time t, and A, B, C and M are model parameters. The original logistic and Gompertz functions are considered to be mechanistic; however, the modified functions are empirical: it is difficult, in fact, to give an interpretation of the model parameters, that have to be statistically estimated from experimental results.

The Gompertz equation and its modified version have been used extensively by researchers to fit a wide variety of growth curves from different microorganisms with good results [33]. There are, however, some limitations

associated with the use of these functions: the Gompertz rate μ_{max} is always the maximum rate, regardless of the actual culture medium composition, and it occurs at an arbitrary point of inflection; thus the generation time is not estimated properly. In addition, since the slope of the function cannot be zero, the lower asymptote must be lower than the inoculum level, giving a negative lag phase duration for some data sets.

1.3 Secondary models

Secondary models describe cell growth dynamics as a function of environmental conditions. The development of secondary models is based on the knowledge of the effects of the environmental conditions on the cell behavior. In particular we present those models that introduce the relationship between cell growth, substrate concentration and temperature.

1.3.1 The Monod model

During the last half century, the concepts in microbial growth kinetics have been dominated by the relatively simple semi-empirical model proposed by Monod [19]. The Monod model differs from the primary models in the way that it introduces the concept of a growth controlling substrate. This substrate is called *limiting substrate* to indicate that the microbial growth rate is dictated by the actual concentration of a particular metabolite. Whereas there is a causal relationship between the exhaustion of the limiting substrate and the end of growth, the Monod model may be considered deterministic.

In the 1930s and 1940s, Jacques Monod performed experiments on bacteria feeding on a single limiting nutrient in order to see if the logistic equation accurately described bacterial growth. He found it did not and therefore he developed a new model to describe his results. If $S(t)$ denotes the concentration (kg/m^3) of the nutrient in the media at time t, his experiments suggested that the specific growth rate

$$\mu = \mu_{max} \frac{S}{K_S + S} \tag{1.1}$$

seemed to best fit the data. Consequently, the dynamics of the cell concen-

tration $X(t)$ is described by

$$\frac{dX}{dt} = \mu_{max} \frac{S}{K_S + S} X(t).$$

The expression (1.1) is often called the Monod function. As a function of S it is monotonically increasing with limit μ_{max} as $S \to \infty$. The parameter μ_{max} is therefore called *maximum specific growth rate* and K_S is called *half-saturation constant*, or affinity constant, because when $S(t) = K_S$ the specific growth rate becomes $\frac{\mu_{max}}{2}$, that is half the maximum specific growth rate. The key feature of the Monod function is that the specific growth rate increases with nutrient concentration S as expected, but it levels out at low nutrient concentrations. For high substrate concentration, the relation (1.1) approaches zero order and the rate of reaction is thus independent of substrate concentration and is constant at the maximum value. In this case the growth is said to be in conditions of non-limiting nutrients.

The link between growth and substrate utilization was made by Monod, who linearly related the specific rate of biomass growth and the specific rate of substrate consumption through the *yield coefficient* Y_{XS}, a measure for the conversion efficiency of a growth substrate into cell material. The relation between cell growth and substrate consumption is given by

$$\frac{dS}{dt} = -\frac{1}{Y_{XS}} \frac{dX}{dt},$$

where

$$Y_{XS} = \frac{dX}{dS}.$$

The complete Monod model is then composed by two coupled differential equations with two model parameters:

$$\begin{cases} \dfrac{dX}{dt} = \mu_{max} \dfrac{S}{K_S + S} X(t) \\ \dfrac{dS}{dt} = -\dfrac{1}{Y_{XS}} \mu_{max} \dfrac{S}{K_S + S} X(t), \end{cases} \tag{1.2}$$

that can be solved if the initial values X_0 and S_0 are given. In Figure 1.5 the solution for the cell and the substrate concentrations is plotted: we can observe that cell growth gradually stops as the substrate is consumed.

Although very simple, the Monod model often describes experimental data for growth rates reasonably well.

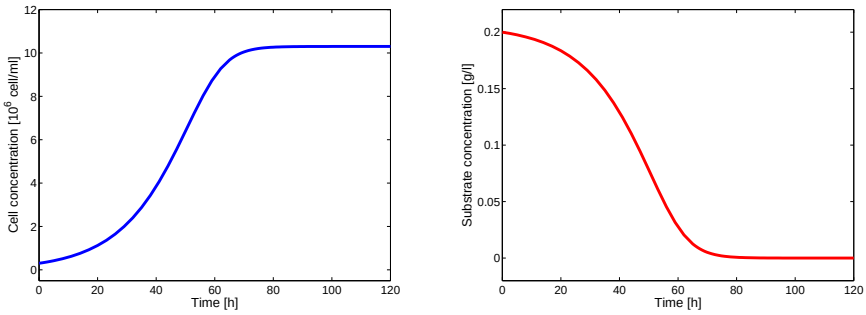

Figure 1.5: Solution of the Monod model with $X_0 = 0.3 \cdot 10^5$ [cell/ml], $S_0 = 0.2$ [g/l], $\mu_{max} = 0.1$ [1/h], $K_S = 0.1$ [g/l], $Y_{XS} = 0.1$

Biological meaning of μ_{max} and K_S

A comment on the biological meaning of the parameters K_S and μ_{max}, which are used to characterize microbial growth for given growth conditions, is necessary.

The maximum specific growth rate μ_{max} is a characteristic of all organisms and it is related to their ability to reproduce themselves in nutritional conditions of plenty. It is simply defined as the increase of biomass per unit time under optimal feeding conditions, in which there are not limiting nutrients.

While the interpretation of μ_{max} as the maximum specific growth rate is straightforward, the biological meaning of K_S is less obvious. The empirical constant K_S is the substrate concentration at which organisms are substrate limited to a growth rate of half the prevailing maximum value. This constant is closely related to the mechanism of transport of the substrate over the cell membrane, so it depends on cell membrane properties and intracellular conditions, on the type of transporter proteins in the cell and on the substrate properties. For this reason, the value of K_S can be interpreted as a reflection of the affinity of the cell towards the substrate S.

The values of these model parameters depend primarily on properties of the organism itself, which are determined by its genome. Moreover, because of the adaptive ability of organisms, both μ_{max} and K_S can vary with the

environmental conditions, for example with the nature of the growth medium and the duration of exposure to it, with temperature and pressure. For these reasons the values of μ_{max} and K_S have to be estimated for each specific couple cell-substrate and under constant conditions of temperature, pressure and medium composition.

1.3.2 Modified Monod models

Starting from the Monod model, different growth rate expressions have been proposed in the literature in order to model more complex situations. In this section we analyze the most common modified Monod models.

Multiple-substrate Monod kinetics

If we want to describe the influence of many substrates, for example two substrates S_1 and S_2, we can consider the following form of the Monod equation:

$$\mu = \mu_{max}\left(\frac{S_1}{K_{S_1} + S_1}\right)\left(\frac{S_2}{K_{S_2} + S_2}\right).$$

In this model either substrate may be limiting under conditions when the other substrate is in excess. In Figure 1.6 we can observe that cell growth stops when the second substrate is totally exhausted, even if the first substrate has been only partially consumed. An example of such kinetics is the simultaneous requirement of glucose and oxygen by aerobically growing organism.

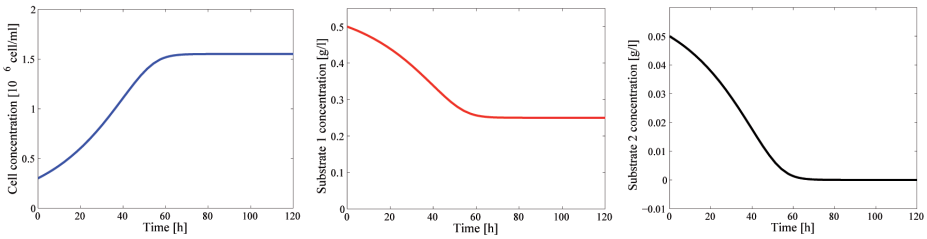

Figure 1.6: Solution of the multiple-substrate Monod model with $X_0 = 0.3 \cdot 10^5$ [cell/ml]

Double-Monod kinetics

The Monod equation can also be written for two substrates that can be used by the cell with parallel reactions:

$$\mu = \mu_{max}\left(\frac{1}{k_1 + k_2}\right)\left(k_1\frac{S_1}{K_{S_1} + S_1} + k_2\frac{S_2}{K_{S_2} + S_2}\right).$$

We can observe that each substrate allows a different maximal growth rate (Figure 1.7). An example of this kinetics is the parallel use of alternative carbon substrates, such as glucose and glutamine.

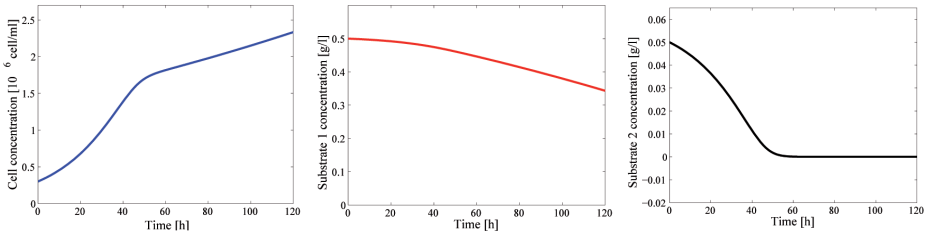

Figure 1.7: Solution of the double-Monod model with $X_0 = 0.3 \cdot 10^5$ [cell/ml]

Diauxic Monod growth

In a medium containing two carbon sources, cells can display a growth curve that is called diauxic. Diauxic growth can be observed in many organisms. Monod first observed this phenomenon when he grew *Escherichia Coli* in a medium containing glucose and lactose. Under these conditions, glucose is first utilized as energy source and after the exhaustion of glucose, lactose is utilized. This led him to conclude that some bacteria preferentially utilize certain carbon substrates.

Diauxic Monod growth can be modeled, for two substrates S_1 and S_2, by the relation

$$\mu = \mu_{max}^{(1)}\frac{S_1}{K_{S_1} + S_1} + \mu_{max}^{(2)}\frac{S_2}{K_2 + S_2 + \frac{S_1^2}{K_I}}.$$

In this way the consumption of substrate S_2 will be inhibited until S_1 is exhausted, for suitably low values of inhibition constant K_I (Figure 1.8).

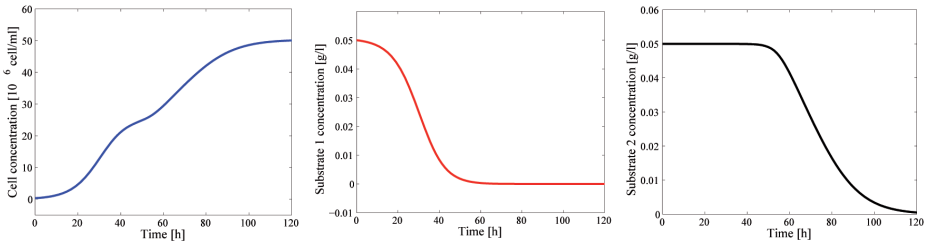

Figure 1.8: Solution of the diauxic Monod model with $X_0 = 0.3 \cdot 10^5$ [cell/ml]

Maintenance substrate uptake

The classical Monod equation does not consider the fact that cells may need substrate, or may synthesize product, even when they do not grow. In fact cells require energy just to maintain cellular viability and replace degraded proteins, even when they are not dividing. For this reason, the original Monod equation was modified by introducing the terms of maintenance, expressed as *maintenance rate* m, originally proposed in [10], and by assuming that the per unit mass maintenance energy is constant.

The maintenance factor m (kg substrate/kg cells·h) is defined as the mass of substrate that one unit of biomass requires for non-growth functions in one unit time. The total substrate utilization for cell maintenance is, of course, taken to be proportional to the total quantity of cells, and therefore for a batch reactor it is proportional to the cell concentration X. If we introduce the maintenance substrate uptake in the classic Monod model (1.2) we obtain

$$\begin{cases} \dfrac{dX}{dt} = \mu_{max} \dfrac{S}{K_S + S} X(t) - m\, Y_{XS}\, X(t) \\ \dfrac{dS}{dt} = -\dfrac{1}{Y_{XS}} \mu_{max} \dfrac{S}{K_S + S} X(t). \end{cases} \tag{1.3}$$

The solution of the model (1.3) is plotted in Figure 1.9. We can see that, when the substrate is exhausted, cell growth stops and, since cells don't have any energy source to maintain, they start dying.

A literature survey has shown that the rate of maintenance energy m is similar for many microorganisms [25] and does not depend significantly on the nature of the carbon source used in catabolism to generate the maintenance energy. This is understandable because maintenance relates to biomass

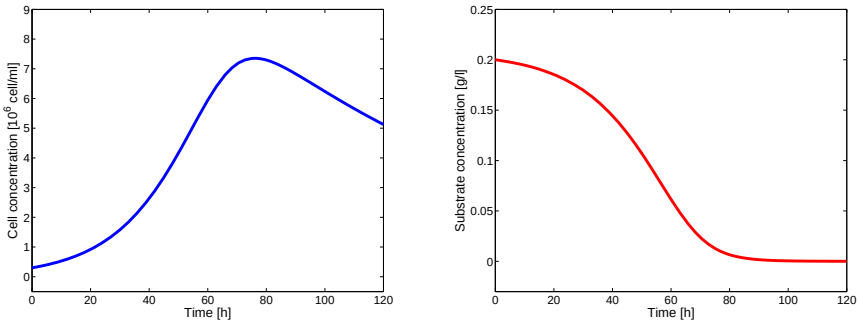

Figure 1.9: Solution of the Monod model with the maintenance substrate uptake with $X_0 = 0.3 \cdot 10^5$ [cell/ml] and $m = 0.01$ [kg substrate/kg cells·h]

which has already been synthesized and for which viability must be maintained; it does not relate to new biomass that is being formed. It is obvious that the energy needed for maintenance is generated in a catabolic reaction, where catabolic substrates and products are involved. Hence maintenance is not only characterized by m, but the generation of this energy leads to associated chemical maintenance rates of all the catabolic substrates and products which are consumed and produced in the catabolic reaction.

Moreover it has been observed from experimental results that the maintenance energy is negligible during the growth phase, that is when cells are dividing, and it becomes relevant only when growth is inhibited [30].

1.3.3 Secondary models based on the Arrhenius law

In order to introduce the temperature dependance on the specific growth rate, the empirical Arrhenius-van't Hoff relationship is often considered

$$\mu = A \exp\left(\frac{\Delta E_a}{RT}\right),$$

where the parameters may be interpreted as follows:

- A is the constant related to the number of collisions between reactants per unit time;
- E_a is the activation energy;
- $R = 8.314\ \mathrm{J/K \cdot mol}$ is the gas constant;

- T is the temperature in Kelvin degrees.

This law is well established in chemistry to describe the effects of temperature on the rate of chemical reactions. If the logarithm of rate is plotted against T, the resulting plot is a straight line over temperature ranges relevant to microbial growth, as shown in Figure 1.10.

It has been argued that because all life processes are the result of chemical reactions, the growth rate of organisms should also be described by Arrhenius kinetics. Within a narrow range of temperature this is true. In fact if we plot also the estimated effect of temperature on microbial growth rate for a cell, we can see that in a limited range of temperature, termed *normal physiological range* (NPR), the microbial growth rate follows the Arrhenius model's prediction. At temperatures above or below the NPR, microbial growth rate deviates markedly from that predicted by the Arrhenius model (Figure 1.10).

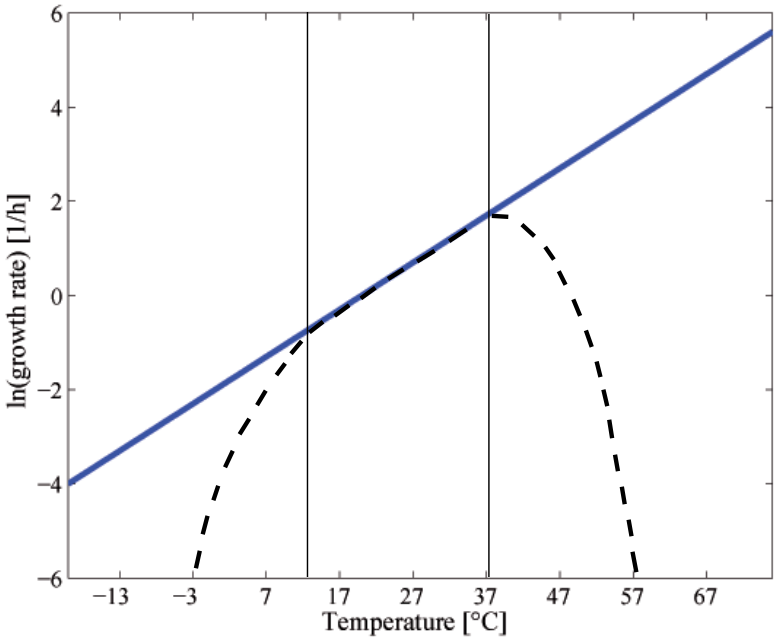

Figure 1.10: Effect of temperature on reaction rate predicted using the Arrhenius law (solid line) and the estimated effect of temperature on the cell growth rate (dashed line)

A range of secondary models, based on adherence to the reaction kinetics described by the Arrhenius model, but including terms to account for the observed deviations, have been proposed. These models can be divided into those based on mechanistic modifications of the Arrhenius model and those based on empirical modifications.

An example of the first class of models is represented by the model proposed by Hinshelwood [11]. This model is based on the hypothesis that at high temperatures denaturation of enzymes involved in cell metabolism takes place and cell growth is inhibited. The model has the following form:

$$\mu = A \exp\left(-\frac{E_a}{RT}\right) - B \exp\left(-\frac{E_{a,high}}{RT}\right),$$

where A and B are pre-exponential factors (1/h), E_a is the activation energy of cell growth (J/mol) and $E_{a,high}$ is the activation energy of the high-temperature denaturation of the rate-limiting enzyme.

In practice, few of these modified models have been routinely applied in predictive microbiology, possibly because the models are highly nonlinear and parameter estimates are difficult to determine. Furthermore the concept that a single enzyme is rate-limiting under all environmental conditions seems questionable. Finally, several studies demonstrated that empirical models provide an equally good fit as those mechanistic models, and are usually easier to work with. In the literature there are different examples of empirical model for the dependance of the cell growth rate on temperature. Many of them expresses the growth rate as a polynomial function of temperature and without any physical or chemical interpretation [27].

1.3.4 The gamma concept

The idea of dimensionless growth factors, now known as *gamma concept*, was introduced in predictive microbiology by Zwietering [34]. The gamma concept relies on the observation that

- many factors that affect microbial growth rate act independently;
- the effect of each measurable factor on growth rate can be represented by a discrete term that is multiplied by terms for the effect of all other growth rate affecting factors;

- the effect on growth rate of any factor can be expressed as a fraction of the maximum growth rate.

Under completely optimal conditions each microorganism has a reproducible maximum growth rate. As any environmental factor becomes suboptimal the growth rate declines. The relative inhibitory effect of a specific environmental variable is described by a growth factor *gamma*, a dimensionless measure that has a value between 0 and 1.

The relative inhibitory effect can be determined from the distance between the optimal level of the factor and the minimum (or maximum) level that completely inhibits growth. In the gamma model approach, the reference growth rate is μ_{max}, so that the reference levels of every environmental factor are those that are the optimum for growth rate.

If this approach is adopted, the problem shifts from the modeling of the cell growth rate to the modeling of the effects of each inhibitory factor on cell kinetics.

1.4 Structured kinetic models

In many cases the characterization of biological activity by considering only the total biomass is insufficient for a true model representation, in particular under varying environmental conditions. It has been proved experimentally that variations of temperature during cell growth cause the composition and behavior of the cell to change, for example in terms of maximum specific growth rate and substrate uptake, that unstructured models can not simulate. It has also been verified that a variation in the biomass activity per unit biomass concentration may be caused by morphological changes, variation of enzyme content of the cells or accumulation of intracellular storage materials.

Such variations in biomass activity and composition require a complex description of the cellular metabolism and a structured approach to the modeling of cell kinetics. Models that are based on a compartmental description of the cell mass are called structured models. These models look in some details at individual cell processes and reactions, in order to obtain a more realistic description of the behavior of the cell. In particular they focus on the cell physiology, that includes the cell mechanism and the cell interaction

with its environment, and are built up starting from appropriate intracellular mass balances.

However, in general it is very difficult experimentally to obtain sufficient mechanistic knowledge about the cell physiology and metabolism for the development of a realistic structured model. Parameter estimation may be almost impossible because it is difficult to take direct measurement of quantities and properties related to one single cell, whose dimension is often lower than 1μm. Moreover, the mechanism of cell growth is complex and not yet completely understood. For this reason, unstructured models are more desirable than structured ones, that are seldom used for design or control.

1.5 Conclusions

The idea that the relationship between μ and S is best described by a saturation type of curve has been widely accepted [20]: at high substrate concentrations the organisms should grow at a maximum rate μ_{max} independent of the substrate concentration. Although Monod model fulfills the requirement, the fact that even Monod own data did not indisputably support his proposed mathematical model gave rise to many more studies. A variety of other mathematical expressions have been put forward to describe this hyperbolic curve. However, the development of structured mechanistic models for quantifying microbial growth kinetics is still limited because the mechanism of cell growth is complex and not yet completely understood. Therefore, most of the proposed growth models are unstructured and empirical. In principle, three methods are used to design such refined equations for the growth kinetics of cells:

- incorporating additional constants into the original Monod model that provided corrections of, for example, substrate or product inhibition;
- proposing different kinetics concepts, resulting in both empirical and mechanistic models;
- describing the influence of physicochemical factors on the Monod growth parameters.

These approaches give rise to new empirical models, such that presented in the previous sections, that however partially move away from the ideal of creating a completely mechanistic model, in which each parameter has its physical or chemical meaning. In the literature there are only a few examples of cell growth models applied to batch culture system that includes multiple nutrients, metabolites and toxic by-products with adequate accuracy [14, 30] and, up to our knowledge, there are no examples of models that take into account the spatial dependance of the cell growth process.

Chapter 2

Characterization of CHO cells physiology

2.1 Introduction

Chinese hamster was first used as laboratory specimen in 1919 in place of mice for typing *Pneumococci*. Subsequent efforts in the mid-20th century led to the development of spontaneous hereditary diseases due to inbreeding, spurring research interest in hamster genetics. It was noted during that time that the low chromosome number of Chinese hamsters ($2n = 22$) made them particularly useful models in tissue culture studies. In 1957, for the first time, an ovary cell from a female Chinese hamster was isolated and established in culture plates. It soon became obvious that these cells were quite resilient and lent themselves to in vitro cultivation with relatively fast generation times.

Until the later part of the 20th century, isolation and characterization of mammalian cell mutants for cytogenetic studies was challenging exercise, fraught with failures because, unlike microbes, mammalian cells are generally diploid, so have two homologous copies of each chromosome. However, CHO cells have, thereafter, been used in numerous biomedical studies ranging from analysis of intermediary metabolism and cell cycle to toxicology studies, so much so, that they have been termed as the mammalian equivalent of the model bacterium, *Escherichia Coli*. Among the historically important medical and cell biology studies conducted in CHO, it was the early work

involving mutagenesis of these cells that facilitated their migration from laboratory benches to industrial reactors. These mutants exhibited particular nutritional requirements for maintaining growth and viability over long culture periods.

While the primary reason behind the isolation of these mutants was fundamental research, it was fortuitous that the nutritional requirements of these cells could be put to use for selection of cells expressing exogenous proteins. This ability of transfect, select, amplify and express biologically active proteins soon became an immense boon for pharmaceutical companies involved in the business of large-scale protein therapeutic synthesis. The immense adaptive ability of CHO cells and their ease of maintenance have been exploited in many fields of basic biomedical research. The most important factors that enable the adoption of CHO cells as the industry workhorse are their adaptability and their ease of genetic manipulation. CHO cells are quite adaptable and can grow to very high density in suspension cultures that are scaled up to 10.000 liters bioreactors.

One of the major challenges in using CHO and other mammalian cell lines as recombinant protein production hosts is that the volumetric yields of protein produced from processes using these cells are relatively low. The productivity of mammalian cell culture processes is typically about 10-100 fold lower than what can be achieved using microbial host systems [12]. This requires the construction and the maintenance of very large and costly production facilities. This is one of the reasons why it is of great interest the expansion of culture volumes and the optimization of culture strategies for higher yields.

Despite the significant advances and improvement during the last past decade in cell line development, these are still a lot of difficulties related to these technologies, primarily stemmed from an inadequate understanding of the biology and physiology of mammalian cells. First, their metabolic characteristics, especially the energy metabolism and regulation modes, have not been well recognized. It has been noted, for example, that the cells have consumption rates of the principal sources of carbon and energy far above the rates strictly required to give support to the cellular metabolism. As a result, situations of exhaustion of metabolites and accumulation of toxic

by-products are frequently reached, with the consequent initiation of the programmed cell death apoptosis. Finally, there is only an empirical knowledge about the environmental factors that determine variations in the cell growth process.

The purpose of this chapter is to analyze the most important characteristic of CHO cells growth, focusing in particular on cell physiology and metabolism. Due to the lack of knowledge about the mechanism related to cell behavior, we will take some important information from experimental results. This analysis is useful for the identification of which aspects and factors related to cell growth should be taken into account in our new model.

2.2 Cell growth curve

The curve which represents the cell concentration in the culture as a function of time is called *growth curve*. A typical cell growth curve is shown in Figure 2.1.

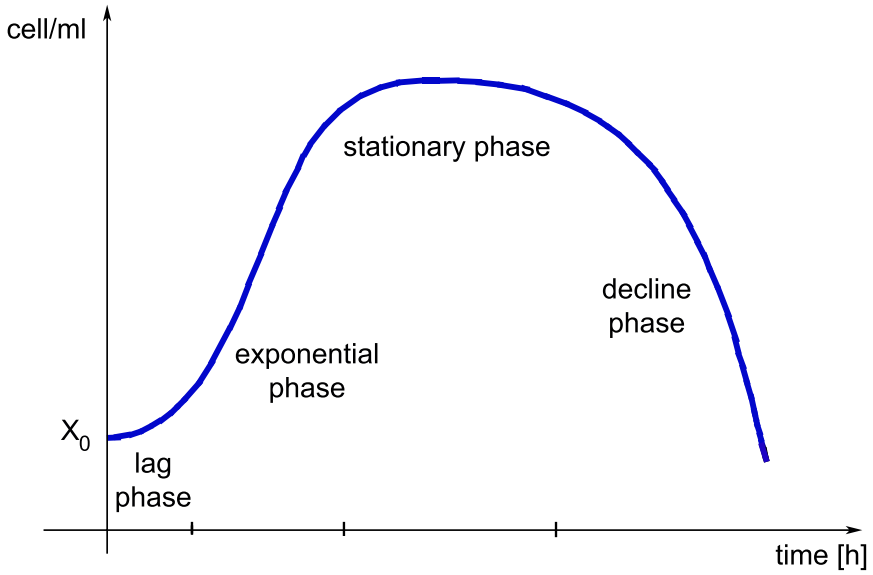

Figure 2.1: Cell growth curve

The cell growth curve can be divided into a number of distinct phases,

referred to as the *lag*, *exponential*, *stationary* and *death phase* respectively. Each of these phases is characterized by a different growth rate and can be influenced by different factors:

- *lag phase:* the beginning of the growth is generally delayed because of the changing of environment. Cells have to rearrange their metabolism and to adapt it to the new environment, for example to a different temperature or nutrient concentration. Lag phase is relatively poorly understood. However, it is known that factors affecting the occurrence and extent of the commonly observed initial lag phase are the initial cell concentration, the past environment, the new environment, the magnitude of the environmental change, the rate of the environmental change, the growth status of the inoculated cell culture, and the variability between individual cell lag phases. In conclusion, these environmental changes may involve nutritional and chemical, as well as physical, changes. The lag phase can last from minutes to several hours. The length of the lag phase can be controlled to some extent because it is dependent on the type of medium as well as on the initial inoculum size. For instance, if the inoculum is taken from a stationary phase culture and is placed into fresh medium, there will be a lag phase as the stationary phase cells adjust to the new conditions and shift physiologically from stationary phase cells to exponential phase cells. Similarly, if the inoculum is transferred from a medium with glutamine as substrate to a new medium with only glucose as the sole carbon source, a lag phase will be observed while the cells reorganize and shift physiologically to synthesize the appropriate enzyme for glucose metabolism;

- *exponential phase:* in this phase the cells have adjusted to their new environment and multiply rapidly. Growth rate is virtually independent of nutrient concentration, as nutrient are in excess. The exponential phase is characterized by the most rapid growth possible under the actual conditions of the system. During exponential growth the rate of increase of cells in the culture is proportional to the number of cells present at any particular time. The exponential phase ends due to either depletion of one or more essential nutrients, the accumulation

of toxic by-products of growth or the reaching of a saturation limit of cell concentration;

- *stationary phase:* it can be defined as a state in which, even if cells still grow and divide, there is no net growth. In this phase growth is balanced by an equal number of cells dying. There are several reasons why a culture may reach the stationary phase. One common reason is that the carbon and energy source becomes completely used up. When carbon source is exhausted, it does not necessarily mean that all growth stops. This is because dying cells can lyse and provide a source of nutrients. A second reason why stationary phase may be observed is that waste products build up to a point where they begin to inhibit cell growth or are toxic to cells. This generally occurs in cultures with high cell density. As a result of nutrient stress, stationary phase cells are generally smaller and rounder than cells in the exponential phase. Even if the cell concentration is constant, the environment keeps changing because of the accumulation of toxic by-product produced by cell functions different from growth;

- *decline phase:* the growth rate becomes smaller than the death rate due to a lack of nutrients and toxic products increasing. It results in a net loss of viable cells. The death phase is often exponential, although the rate of cell death is usually slower than the rate of growth during the exponential phase.

The growth phases that are of most interest to microbiologist, and in particular to biologist involved in the development of cell cultures for production of recombinant proteins, are the lag phase, the exponential phase and the time to onset of the stationary phase. In particular there is not a great interest in modeling the death phase because, if it is known that after a certain time the stationary phase, hence the maximal cell concentration, is reached, then the growth process will be interrupt at that time. For these reasons in the development of our model we will focus mainly on the modeling of the lag, the exponential and the stationary phase.

2.3 Cellular metabolism

Cellular metabolism can be defined as the sum of all the processes involved in energy conversion in the cell. They regulate cellular conditions such that a state of a metabolic homeostasis, that is a stable supply of energy and metabolites, is maintained.

Metabolic processes are organized into complex sequences of controlled chemical reactions referred to as *metabolic pathways*, that form the basis of all cellular activities. Many different pathways are responsible for nutrient processing, energy acquisition and energy conversion in the cell. Metabolic pathways can be broadly categorized as *anabolic* and *catabolic*. Anabolic pathways are energy-requiring (endoergonic) pathways that result in synthesis of complex biomolecules such as proteins, nucleic acid and membranes from smaller ones. In contrast, catabolic pathways are energy-releasing (exergonic) pathways that break down molecules into smaller components.

The ensemble of catabolic processes in the cell, in which molecules are oxidized to carbon dioxide and water, is termed *cellular respiration*. Cellular respiration, also known as oxidative metabolism, is one of the key ways a cell gains useful energy. It includes *anaerobic pathways*, that do not require molecular oxygen, and *aerobic pathways*, that directly or indirectly require molecular oxygen.

Energy released from cellular respiration has to be converted in some form that is useful to drive energy-requiring processes in the cell. In most cases, the energy that is used by most processes is stored in adenosine triphosphate (ATP) molecule, that consists of three phosphate attached to the ribose of adenosine. The energy is obtained from ATP through the hydrolysis process, in which the ATP molecule is split by reacting with a molecule of water. Hydrolysis of ATP is an exergonic reaction with a standard free energy change (δG^0) of -7.3 kcal/mol. This is the energy which is available to do work. Cellular reactions do not occur under standard conditions; thus, the actual amount of energy released is likely greater than the calculated δG^0. In any case, it is clear that hydrolysis of ATP releases a substantial packet that can be used to drive endoergonic reactions. To maintain usable energy, the cell must continually resynthesize ATP. Synthesis of ATP is an energy requiring process, that is fed by the catabolic reactions that comprise cellular respira-

tion. Hence, ATP acts as an intermediary that transfers energy from cellular respiration to the energy-requiring processes in the cell.

In the model that we are going to present in the next chapters, we want to take into account both the anaerobic and the aerobic respiration. Consequently in this section we analyze these chemical processes in order to derive information that may be useful for the development of our model. In particular we consider the main catabolic reactions that involve as energy source glucose and glutamine, that are known to be the most important carbon and energy source for animal cells [23].

2.3.1 Glycolysis

The first step in cellular respiration is glycolysis, that includes the initial reactions required for carbohydrate metabolism [29]. Glycolysis is a series of cytosolic reactions that converts one molecule of glucose to two 3-carbon pyruvate molecules (Figure 2.2):

$$Glucose + 2ADP + 2Pi + 2NAD^+ \rightarrow$$
$$2Pyruvate + 2ATP + 2NADH + 2H^+ + 2H_2O.$$

Glycolysis is a 10-step process, in which usable energy is stored in two ATP molecules and in two pairs of high energy electrons passed to nicotinamide adenine dinucleotide (NAD^+). Two ATP represent only a small percentage of the total energy that can be obtained from the glucose molecule (686 kcal/mol), and the final product, pyruvate, still contains the bulk of the total energy initially present in the glucose molecule. Nonetheless, glycolysis is a pivotal pathway in cellular respiration because it is the initial step for oxidation of glucose, and it generates energy under anaerobic conditions. Anaerobic metabolism, in fact, can be critically important when oxygen availability is limited.

If glycolysis were to continue indefinitely, all of the NAD^+ would be used up, and glycolysis would stop. To allow glycolysis to continue, the cell must be able to oxidize $NADH$ back to NAD^+.

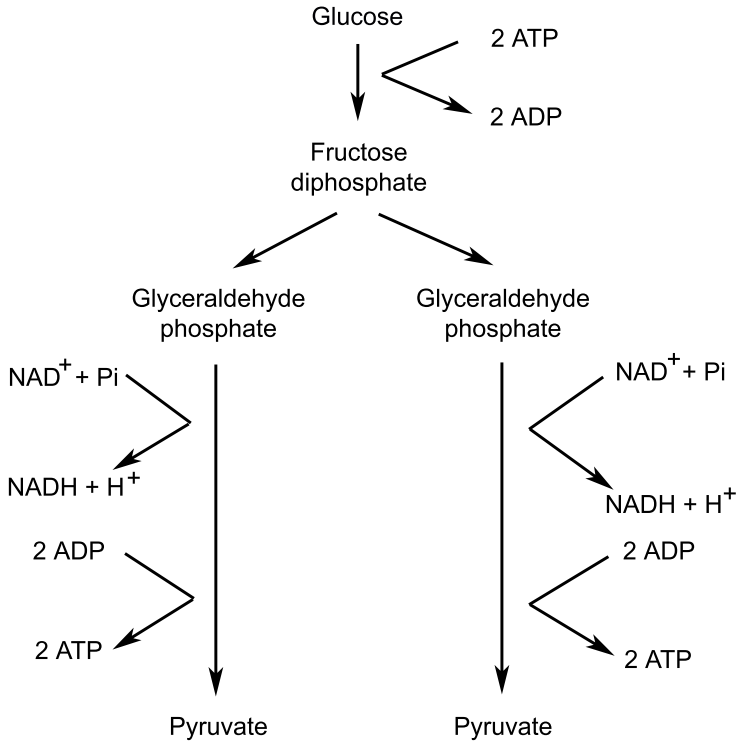

Figure 2.2: Glycolysis pathway

Molecules produced during glycolysis can enter different pathways. In fact, pyruvate, the end product of glycolysis, can enter the anaerobic process of fermentation or it can be converted to acetyl coenzyme A (acetyl-CoA) and enter aerobic respiration. The employment of pyruvate will be determined by the availability of oxygen.

2.3.2 Anaerobic respiration

In the absence of oxygen, NAD^+ is regenerated when $NADH$ passes electrons to pyruvate, forming lactate, but without producing ATP [29]. This process is called lactate fermentation (Figure 2.3):

$$Pyruvate + NADH + H^+ \rightarrow Lactate + NAD^+.$$

This anaerobic fermentation allows cell to use glucose as its only energy

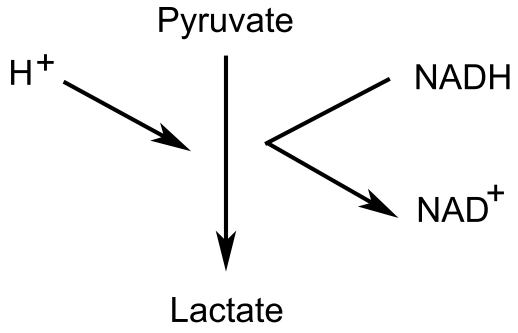

Figure 2.3: Lactic fermentation

resource, because it reconverts $NADH$ back to NAD^+ that is needed by glycolysis. If we assume that all the products of glycolysis, namely pyruvate, $NADH$ and H^+, are instantaneously converted to lactate and NAD^+ through lactic fermentation, the overall reaction of anaerobic respiration can be simplified as follows (Figure 2.4):

$$Glucose + 2ADP + 2Pi \rightarrow 2Lactate + 2H_2O + 2ATP.$$

Plant and yeast cells also use fermentation under anaerobic conditions but in these cells the electrons are not passed to pyruvate. Pyruvate is first decarboxylated to acetaldehyde, which is then reduced by electrons from

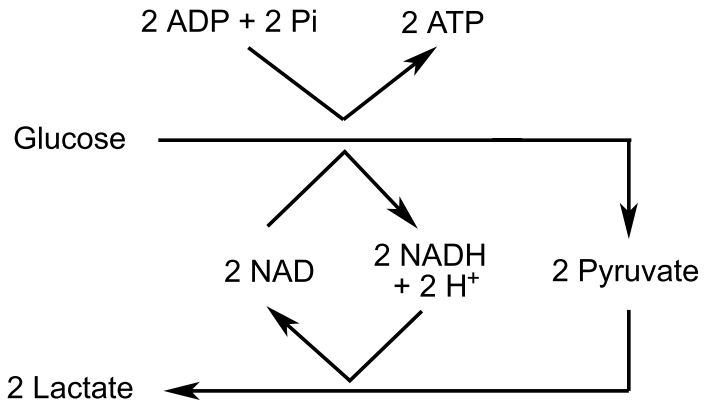

Figure 2.4: Anaerobic respiration

$NADH$ to form ethanol. Because the process yields ethanol, it is called alcoholic fermentation. This kind of fermentation, carried out by yeast and plant cells, is used, for example, to make bread, wine and beer.

2.3.3 Aerobic respiration

Anaerobic fermentation, that converts glucose to lactate, releases only a small portion of the total energy available in the glucose molecule. However, if oxygen is available, glucose can be completely oxidized and a much larger amount of energy can be extracted. In presence of oxygen, pyruvate produced during glycolysis is transported into the matrix of the mitochondrion and it is involved in four different processes: pyruvate decarboxylation, tricarboxylic acid (TCA) cycle, electron transport chain and oxidative phosphorylation [29].

The first step of this process is pyruvate oxidative decarboxylation (Figure 2.5):

$$Pyruvate + CoA + NAD^{+} \rightarrow acetyl - CoA + CO_2 + NADH.$$

In this reaction, pyruvate is converted to acetyl-CoA and carbon dioxide, thanks to the Coenzyme A (CoA). Oxidation of pyruvate to acetyl-CoA is a highly exergonic process. Then acetyl-CoA is committed to entering the

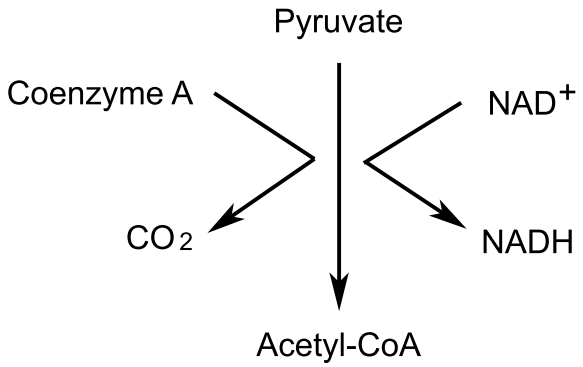

Figure 2.5: Pyruvate oxidative decarboxylation

TCA cycle, where it is fully oxidized to carbon dioxide:

$$Acetyl - CoA \ + \ 2H_2O \ + \ 3NAD^+ \ + \ FAD \ + \ ADP \ + \ Pi \ \rightarrow$$

$$2CO_2 \ + \ 3NADH \ + \ 3H^+ \ + \ FADH_2 \ + \ CoA + ATP.$$

The TCA cycle is an eight-step cycle (Figure 2.6). The only usable energy produced in the TCA cycle is that stored in one molecule of ATP. This molecule of ATP is in addition to the two ATP produced by glycolysis. Thus, the complete oxidation of one molecule of glucose generates $4ATP$, $10NADH$ and $2FADH_2$. The energy in these stored electrons can be converted in ATP and NAD^+ thanks to the electron transport chain and the oxidative phosphorylation, that require molecular oxygen.

The theoretical maximum ATP yield for complete oxidation of a molecule of glucose is 38 ATP. If one assumes that hydrolysis of ATP in the cell yields approximately 10 kcal/mol, then oxidation of glucose provides 380 kcal/mol of usable energy. Whereas the δG^0 for oxidation of glucose is 686 kcal/mol, the efficiency of energy conservation in aerobic respiration is about 55.4 %.

In the hypothesis that we made in the previous section, the overall reaction of oxidation of glucose can be simplified as follow:

$$Glucose \ + \ 6O_2 \ \rightarrow \ 6CO_2 \ + \ 6H_2O \ + \ 38ATP.$$

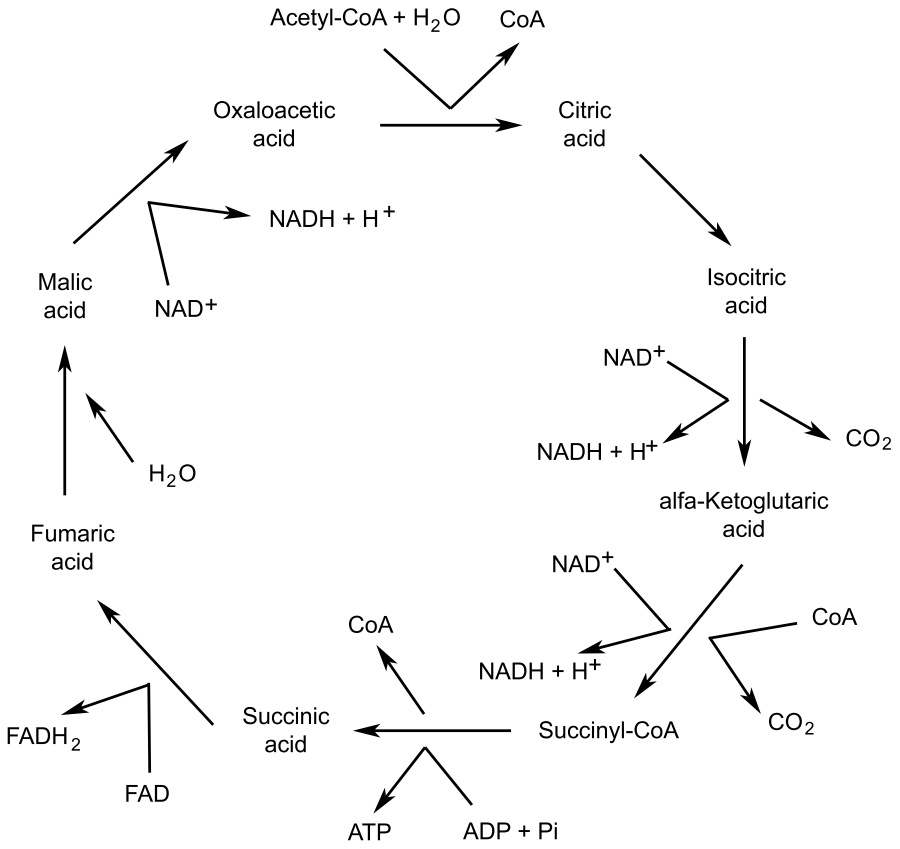

Figure 2.6: TCA cycle

2.3.4 Glutamine oxidation

Glutamine is one of the twenty amino acids and has a variety of biochemical functions, in particular it is an important cellular energy source, next to glucose. Therefore glutamine is commonly added to the media in cell culture.

Glutamine is involved in three different metabolic reactions [9]. The first one is a single-step reaction: in presence of oxygen, glutamine oxidizes and the products of this reaction are carbon dioxide, ammonia and lactate:

$$Glutamine \ + \ 2O_2 \ \rightarrow \ 2CO_2 \ + \ 2NH_3 \ + Lactate.$$

Glutamine is also involved in two reactions that have respectively alanine and aspartate as intermediate products. The first two-step reaction has alanine as intermediate product:

$$Glutamine \ + \ 3O_2 \ \rightarrow \ 2CO_2 \ + \ NH_3 \ + \ Alanine$$

$$Alanine \ + \ H_2O \ \rightarrow \ CO_2 \ + \ NH_3 \ + \ Lactate,$$

while the second two-step reaction involves aspartate as intermediate product:

$$Glutamine \ + \ 3O_2 \ \rightarrow \ CO_2 \ + \ NH_3 \ + \ Aspartate$$

$$Aspartate \ + \ H_2O \ \rightarrow \ CO_2 \ + \ NH_3 \ + Lactate.$$

In order to simplify the model, we suppose that all the aspartate and the alanine produced in the first step of the reactions are consumed instantaneously in the second step, so that the concentration of both alanine and aspartate in the culture medium is constant at every time. This hypothesis is supported by the fact that alanine and aspartate need only water, which is not a limiting-substrate, to react and produce carbon dioxide, ammonia and lactate. However, this hypothesis is quite strong and depends on the chemical properties of these substances, therefore it should be tested with appropriate experiments. Under this hypothesis, the two-step reactions become

$$Glutamine \ + \ 3O_2 \ \rightarrow \ 3CO_2 \ + \ 2NH_3 \ + \ Lactate$$

and

$$Glutamine \ + \ 3O_2 \ \rightarrow \ 2CO_2 \ + \ 2NH_3 \ + \ Lactate.$$

In conclusion, if we want to consider in our model the metabolic pathways introduced in this section, we need to take into account the concentrations of three substrates, that are glucose, glutamine and oxygen, and the concentrations of three toxic by-products, that are carbon dioxide, lactate and ammonia. In order to build up the model that describes the dynamics of these metabolites, we will consider the stoichiometric coefficients of the reactions that we have just introduced. However, it is necessary to underline that the reactions proposed in this chapter are ideal and simplified reactions and not the actual reactions that take place in the cells. For example, there are evidences that glutamine is not totally converted into lactate by the cell, but it is also partially deaminated and used to produce other amino acids. In fact, unless the amino acids like glutamine are taken up by the cells in "right" stoichiometric ratios, conversions among them will be necessary to meet the cellular needs.

2.4 Environmental factors

Before moving to the description of the cell growth model, it is necessary to detect which environmental factors influence the cell kinetics. In this section, in particular, we want to analyze the effect on cell growth of temperature, oxygen concentration and pH of the culture medium.

2.4.1 Temperature

Animal cells are most commonly cultured at 37°C. However, since the culture temperature would affect such cellular events as growth, viability, protein synthesis and metabolism, it is an important factor which has been widely studied to realize an efficient process for protein production by animal cell culture [7]. It has been shown in the previous section that cellular metabolism consists of a network of reactions. Whereas it is known that these individual biochemical reactions are temperature dependent, the fundamental question of whether cell growth kinetics is temperature dependent must be asked. To determine this, many comparisons of growth kinetics at different temperatures were carried out in the literature.

With appropriate experiments it has been verified that the specific growth

rate is temperature-dependent (Figure 2.7) and, in particular, the maximum specific growth rate was found at 37°C [13, 32]. Temperatures above 37°C decrease cell growth capacity by lowering the specific growth rate and the maximum cell concentration, while at temperatures above 39°C cell growth stops and cell viability decreases dramatically. Moreover temperatures below 37°C decrease growth capacity non linearly by lowering the specific growth rate, while at temperatures below 35°C cell division is inhibited but cells maintain a high viability over time, medium consumption is suppressed and the production of toxic by-products is lowered [7].

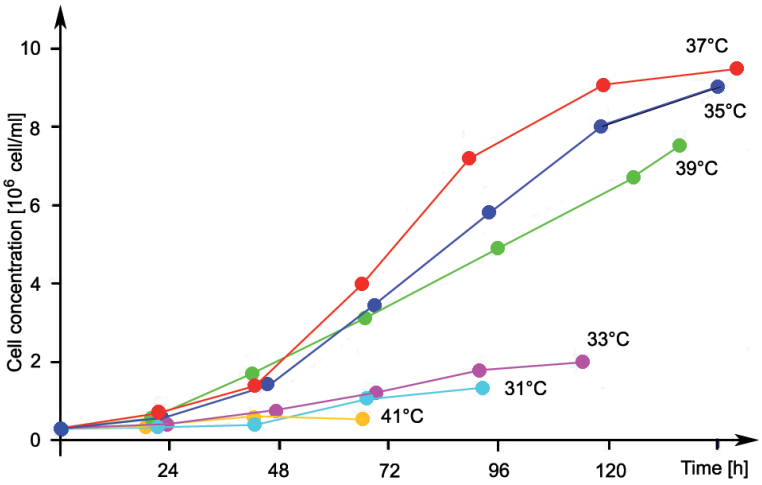

Figure 2.7: Cell concentration at different temperatures (from [1])

2.4.2 Oxygen concentration

In the previous section, it has been shown that cells can obtain energy both from aerobic and from anaerobic respiration. However, we have also estimated that glucose oxidation produces an amount of ATP that is approximately 20 times larger than the amount produced by anaerobic glucose consumption. This is the reason of the decrease in viability and the suppression of growth in anoxic conditions [1], namely in absence of oxygen in the atmosphere above the culture medium (Figure 2.8). Moreover, it has been proved that the continuous exposure of CHO cells to an atmosphere of 98% of oxygen (hyperoxia) induces a disturbance of energy metabolism that results in growth inhibition after an initial doubling [24].

Finally, it has been proven that a variation of the oxygen concentration between 5% and 35% does not affect significantly cell growth and viability [1]. However, usually cell culture is carried on with 20% of oxygen concentration in the gas phase.

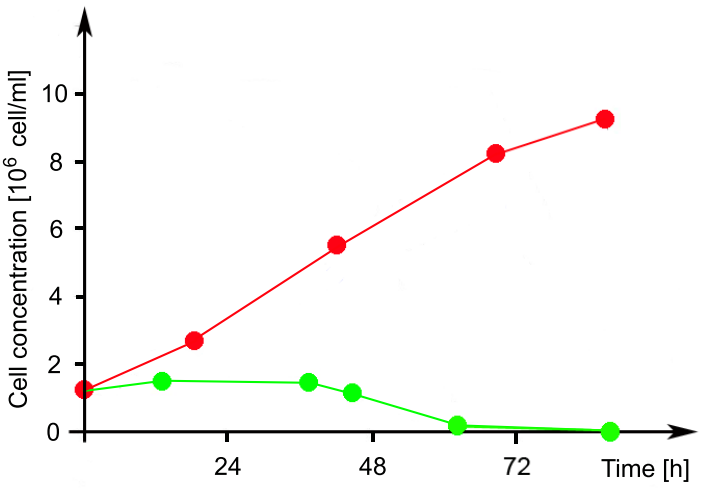

Figure 2.8: Cell concentration at different oxygen concentrations: 20 % (red) and anoxia (green) (from [1])

2.4.3 pH

The pH is commonly considered a good indicator for cell metabolism, whereas it depends directly on the concentration of toxic by-products of cell growth that dissociate in water. In CHO culture medium, the pH is mainly determined by the concentrations of carbon dioxide and lactate, which cause the reduction of the pH.

In particular, experiments have demonstrated a marked decrease in survival of CHO cells when they are incubated under oxygen-limited conditions at low pH. Lethal effects are observed when the pH becomes lower than 6.4. In CHO cells, glucose consumption and lactate production are suppressed as the pH of the medium is lowered from 7.0 to 6.0, confirming that glycolysis is inhibited at low pH. Thus, one possible explanation for the cell death observed under conditions of hypoxia and acidity is that cells incubated in hypoxia, a condition in which aerobic respiration is inhibited, and low pH,

a condition in which glycolysis is inhibited, might die of energy deprivation [22]. These conditions often occur in bioreactors when the oxygenation of the culture medium is not efficient (Figure 2.9).

In order to limit the reduction of the pH in the culture medium, bicarbonate is often introduced in the bioreactor [26].

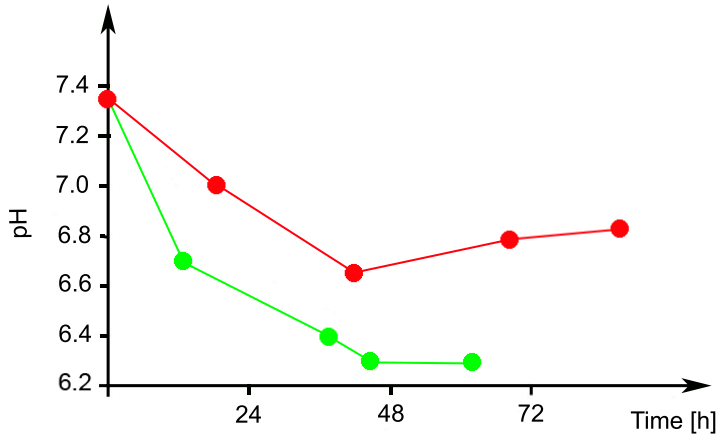

Figure 2.9: pH at different oxygen concentrations: 20 % (red) and anoxia (green) [1]

Chapter 3

Batch bioreactor modeling

3.1 Introduction

In the previous chapter we analyzed some aspects of CHO cell growth kinetics primarily related to the type of cell and its physiology, focusing in particular on the cell metabolism and on the interactions between cells and environment. However, it is necessary to highlight that the environmental properties like oxygen concentration and pH are mainly determined by the type of culture system. The consumption and production rates, for example, depend upon the level of concentrations, and it has been proven that concentration levels in the culture system depend on its type and operation mode. Different operation modes can lead to different rates of cell growth, to different rates of product formation and hence to substantially different productivity. In this chapter we are going to analyze the CHO cell culture system, focusing in particular on the relationship between the mode of operation and the properties of the culture environment.

3.2 CHO cell culture

Cell culture is the complex process by which cells are grown under controlled conditions. Cells are maintained at an appropriate temperature and gas mixture in a bioreactor, that is a vessel in which a chemical reaction is carried out involving organisms and biochemical substances.

The mode of bioreactor operation depends on the type of cell line. CHO cells, in particular, can be grown in suspension, without been attached to

a surface, in vessels called shaken bioreactors under batch conditions (Figure 3.1). This implies that the bioreactor is first charged with medium, inoculated with cells, and the cells are allowed to grow for a sufficient time, such that the culture achieves the required cell density or the optimum product concentrations. The bioreactor contents are finally discharged and the bioreactor is prepared for a fresh charge of medium.

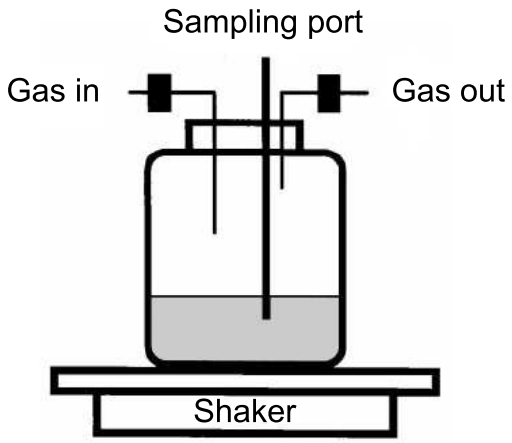

Figure 3.1: Shaken bioreactor under batch conditions

During the period of cell growth, no additional material is either added to or removed from the bioreactor, apart from minor adjustments needed for control of pH or foam, the removal of samples and, of course, a continuous supply of air needed for aerobic metabolism. Concentrations of biomass, nutrients and products thus change continuously with respect to time, as the various constituents are either produced or consumed during the time course of the reaction.

Although it has been over two decades since the employment of CHO cell culture in recombinant therapeutic production, and a decade since cell culture bioprocessing was proclaimed to be a "mature technology", the new surge in the quantities of products required and the phenomenally high investment cost for a manufacturing plant have spurred a new drive to enhance cell culture bioprocess technology and modeling.

Both physical and biological information are required in the design and

interpretation of biological reactor performance. Physical factors that affect the general hydrodynamic environment of the bioreactor include such parameters as liquid flow pattern and circulation time, air distribution efficiency and gas holdup volume, oxygen mass transfer rates, intensity of mixing and the effects of shear. These factors are affected by the bioreactor and agitator geometries and by physical property effects, such as liquid viscosity. They have a large effect on both liquid and gas phase hydrodynamics. It has been proved that there are considerable interactions between the bioreactor hydrodynamic conditions and the cell biokinetics, morphology and physiology. For example, in large scale bioreactors, some cells may suffer local starvation of essential nutrients owing to a combination of long liquid circulation time and an inadequate rate of nutrient supply, caused by inadequate mixing or inefficient mass transfer. Agitation and shear effects can affect cell morphology and hence liquid viscosity, which will also vary with cell density. This means that the process of cell growth affects the bioreactor hydrodynamics in a very complex and interactive manner. Changes in the cell physiology, such that the cell processes are switched from production of biomass to that of a secondary metabolite or product, can also be affected by selective limitation on the quantity and rate of supply of some essential nutrient in the medium. This can in turn be influenced by the bioreactor hydrodynamics and also by the mode of the operation of the bioreactor. These are the reasons why it is not possible to develop a cell growth model without considering the coupling between cell kinetics and bioreactor hydrodynamics.

3.3 Bioreactor classification

The various types of bioreactor can be classified according to the mode of operation as *batch*, *semi-continuous* or *continuous reactors*.

As mentioned in the previous section, in a batch reactor all the materials needed by the cell culture are introduced at the beginning of the process and there is no introduction or removal of substances or fresh medium.

In semicontinuous or fed batch operation, additional substrate is fed into the bioreactor, thus prolonging operation by providing an additional continuous supply of nutrients to the cells. No material is removed from the reactor, apart from normal sampling, and therefore the total quantity of ma-

terial within the reactor will increase as a function of time. However, if the feed is highly concentrated, then the reactor volume will not change much and can be regarded as essentially constant.

In continuous operation, fresh medium is added continuously to the bioreactor, while at the same time depleted medium is continuously removed. The rates of addition and removal are such that the volume of the reactor contents is maintained constant. The depleted material contains any products that have been excreted by the cells and, in the case of suspended-cell culture, also contains effluent cells from the bioreactor.

Otherwise, on the basis of the mixing technology, we can distinguish three main bioreactor types: *stirred tank*, *airlift* and *orbitally shaken bioreactor*.

The stirred tank reactor is composed of a vessel and a mixer, such as a stirred or a turbine, usually mounted with a shaft at the top of the vessel to achieve mixing inside the tank. This is the most popular in industry and represents a well established technology.

In the airlift reactor the culture medium is kept mixed and gassed by the introduction of air or another gas mixture at the base of the vessel equipped either with a draught tube or another device by which the reactor volume is separated into a gassed and an ungassed region with different density, thus generating a vertically circulating flow. In general, these reactors are less expansive than the stirred tank bioreactors, however the mixing properties are likely to be more critical.

The orbitally shaken bioreactor is a vessel, usually cylindrical, put in motion by a shaker. The mixing is archived by the fluid motion resulting from friction force which is exerted by the liquid-contacting vessel wall, and most of all, by the high inertial forces due by the shaking movement of the tank. The shaken bioreactors have been widely used in the biotechnological field since they are easily to handle and inexpensive. In spite of their large practical importance, very little is known about the characteristic properties of shaken cultures. These are the reasons why in the last years many studies about cell growth have been carried out using this alternative technology [31] and models for shaken bioreactors have been recently proposed [4].

In this work, in particular, we focus on cell growth in shaken bioreactors under batch conditions.

3.4 Balance equations for the batch fermenter

As advanced in the previous section, CHO cells are cultivated mainly under batch conditions. Inherent in this system is that the cell environment and hence the cell composition and physiological state change during the culture period.

Starting from an inoculum X_0 at $t = 0$ and an initial quantity of limiting substrate S_0 at $t = 0$, the biomass will grow, perhaps after a short lag phase, and consume substrate. As the substrate becomes exhausted, the growth rate will slow and become zero when substrate is completely depleted. If we suppose that the volume V of the bioreactor is constant, we obtain the following general balances:

- total volume balance
$$\frac{dV}{dt} = 0,$$
- substrate balance
$$\frac{dS}{dt} V = r_S V,$$
- biomass balance
$$\frac{dX}{dt} V = r_X V.$$

Suitable rate expressions for r_S and r_X and the specification of the initial conditions would complete the batch fermenter model, which describes the growth process.

These balances can be applied to all the components of the culture medium that are neither added nor removed from the bioreactor, for example glucose, glutamine and cells, but they can not be applied to substances, like oxygen and carbon dioxide, that are exchanged between the culture medium and the atmosphere. Therefore in the next section we are going to analyze the mass transfer process in order to complete the batch fermenter model.

3.5 Mass transfer

The bioreactor is a multiphase system in which the transport of material between the gaseous phase and the liquid phase plays an essential role. Usually one of the reactants is transferred from one phase into a second

phase, in which the reaction takes place. The typical example is the aeration of the bioreactor culture medium and the supply of oxygen to the cells.

Concentration gradients are the driving forces for mass transfer. Actual concentration gradients in the very near vicinity of the gas-liquid interface, under mass transfer conditions, are very complex. They result from an interaction between the mass transfer process and the local fluid hydrodynamics, which changes gradually from stagnant flow, close to the interface, to perhaps fully-developed turbulence within each of the bulk phases.

According to the Two-Film Theory [15], the actual concentration profiles can be approximated by linear gradients. A thin film of fluid is assumed to exist at either side of the interface. Away from these films, each fluid is assumed to be in fully developed turbulent flow. There is therefore no resistance to mass transfer throughout each relevant phase. At the phase interface itself, it is assumed that there is no resistance to mass transfer, and the interfacial concentrations, C_{Gi} and C_{Li}, are therefore in local equilibrium with each other. All the resistance to mass transfer must occur within the films. In each film, the flow of fluid is assumed to be stagnant, and mass transfer is assumed to occur only by molecular diffusion and therefore to be described by Fick's law, which says that the flux j_A (mol/s·m^2) for the molecular diffusion of the component A is given by

$$j_A = -D\,\frac{dC}{dZ},$$

where D is the molecular diffusion coefficient (m^2/s) and dC/dZ is the steady state concentration gradient (mol/m$^3\cdot$m). Thus applying the same concept to mass transfer across the two films we obtain:

$$j_A = D_G\,\frac{C_G - C_{Gi}}{Z_G} = D_L\,\frac{C_L - C_{Li}}{Z_L},$$

where D_G and D_L are the effective diffusivity of each film and Z_G and Z_L are the respective thickness of the two films. The above equations can be expressed in terms of mass transfer coefficient k_G and k_L (m^2/s) for the gas and liquid films:

$$j_A = k_G\,(C_G - C_{Gi}) = k_L\,(C_{Li} - C_L).$$

The total rate of mass transfer Q (mol/s) is given by

$$Q = j_A \mathcal{A},$$

where $\mathcal{A}$ is the total interfacial area available for mass transfer. Thus we obtain

$$Q = k_G\mathcal{A}\,(C_G - C_{Gi}) = k_L\mathcal{A}\,(C_{Li} - C_L).$$

Since the mass transfer coefficient k_i and the interfacial area $\mathcal{A}$ depend on the same hydrodynamic conditions and system physical properties, they are frequently combined and referred to as a "$k_L\mathcal{A}$ value" or "$k_G\mathcal{A}$ value", or more properly as *mass transfer capacity coefficients*.

In the above theory, the interfacial concentrations C_{Gi} and C_{Li} can not be measured, and are therefore of relatively little use, even if the values of the film coefficient were known. For this reason, by analogy to the film equations, overall mass transfer rate equations are defined, based on overall coefficients of mass transfer, K_G and K_L, and overall concentration driving force terms:

$$Q = K_G\mathcal{A}(C_G - C_G^*) = K_L\mathcal{A}(C_L^* - C_L).$$

Here, C_G^* and C_L^* are the respective equilibrium concentrations, corresponding to the bulk phase concentrations C_L and C_G respectively.

Equilibrium relationships for gas-liquid systems, at low concentrations of component A, usually obey Henry's law, which is a linear relation between gas partial pressure, p_A, and equilibrium liquid phase concentration, C_{LA}^*:

$$p_A = H_A C_{LA}^*,$$

where H_A (bar·m^3/kg) is the Henry's law constant for component A in the medium. Henry's law is generally accurate for gases with low solubility, such as of oxygen in water or in culture media.

For gases of low solubility, such as oxygen and carbon dioxide in water, the concentration gradient through the gas film is very small, compared to that within the liquid film. This results from the relatively low resistance to mass transfer in the gas film, as compared to the much greater resistance to mass transfer in the liquid film. The main resistance to mass transfer is predominantly within the liquid film. This causes a large jump in concentration $C_{Li} - C_L$, since the resistance is almost entirely on the liquid side of the interface.

At the interface, the liquid concentration C_{Li} is in equilibrium with that of the gas, C_{Gi}, and since C_{Gi} is very close in magnitude to the bulk gas concentration, C_{Li} must then be very near to equilibrium with the bulk gas phase concentration C_G. This is known as liquid film control and corresponds to the situation where the overall resistance to mass transfer resides almost entirely within the liquid phase. The overall mass transfer capacity coefficient is $K_L\mathcal{A}$. Hence the overall mass transfer rate equation used for slightly soluble gases in terms of the specific interfacial area a (interfacial area per unit liquid volume) is

$$Q = K_L a \left(C_L^* - C_L\right) V_L,$$

where C_L^* is in equilibrium with C_G, as given by Henry's law:

$$C_G = HC_L^*.$$

Mass transfer coefficients in bioreactor are therefore generally referred to in terms of K_L *values* or K_La *values* for the case of mass transfer capacity coefficients.

Generally the K_La value depends on the mode of bioreactor operation, for example, the dimensions of the vassel and the shaken velocity, and it can be estimated from experimental results.

3.5.1 Oxygen and carbon dioxide balances for gas-liquid transfer

In order to characterize aeration efficiency, to predict dissolved oxygen concentration, or to follow the biological activity, it is necessary to develop models which include expressions for the rate of oxygen transfer and the rate of oxygen uptake by the cells. Well-mixed phase region, in which the oxygen concentration can be assumed uniform, can be described by simple balancing methods. Situations in which spatial variations occur require more complex models. The following generalized oxygen balance equation is derived for well-mixed phases, using the well mixed tank concept.

If V_L is the total volume of the liquid phase we obtain

$$\frac{dO_2}{dt} V_L = K_L^{O_2} a(O_2^* - O_2)V_L.$$

Here O_2^* is the equilibrium solubility of oxygen corresponding to the oxygen partial pressure in the gas phase P_{O_2} and is calculated by Henry's law, according to the relationship:

$$O_2^* = \frac{P_{O_2} n_{H_2O}}{H_{O_2}},$$

where n_{H_2O} is the molar concentration of water and H_{O_2} is the Henry constant for oxygen, which depends on temperature. In this balance we are neglecting the consumption of oxygen by the cells.

In the same way we can derive the balance equation for the carbon dioxide concentration in the batch bioreactor:

$$\frac{dCO_2}{dt} V_L = K_L^{CO_2} a(CO_2^* - CO_2)V_L.$$

3.5.2 Models for oxygen transfer in large scale bioreactors

Large-scale industrial bioreactors can generally be expected to exhibit deviations from the idealized flow conditions of perfect mixing. Thus the assumption of completely mixed liquid phase may not be valid. Little experimental information is available on concentration inhomogeneities or concentration gradients within large bioreactors. Residence time distribution information, from which a physical and mathematical model could be established, is also generally not available.

Convection currents within the liquid phase of a bioreactor are usually caused by the mechanical energy inputs of agitation and aeration. It is often reasonable to assume that slowly changing quantities, such as biomass concentration, substrate concentration, pH and temperature are uniform within the whole mass of bioreactor liquid. Oxygen must be considered, however, as a rapidly changing substrate, owing to its low solubility in culture media. It is therefore necessary to consider that differences in oxygen transfer and uptake will create oxygen concentration gradients throughout the reactor. The possibility that oxygen transfer parameters can vary with the dimensions and the conditions in which the bioreactor works, like rotational speed, introduces a much greater degree of complexity to the problem of modeling the bioreactor.

Chapter 4

A new cell growth model

4.1 Introduction

The purpose of this chapter is to present a new model for cell growth. In particular the first step is to derive an expression for the cell growth rate as a function of the environmental properties that we have analyzed in the previous sections. Then, we derive the rates for the substrates consumption and the products formation as a function of the cells dynamics. In this first model, that we are going to introduce in the next section, we neglect the spatial dependance of the concentrations of cells and metabolites and we consider only the time dependance. Thus, we refer to it as *0D model*.

Later on, we extend the 0D model in order to consider the effect of the distance between cells and the culture medium surface. In particular, we expect a dependance of the aerobic growth rate from the depth of the medium, whereas oxygen diffuses in the medium through the fluid surface. This model will be referred to as *1D model*.

Finally, we present a *3D model* in which we introduce the transport effect on cell growth. We expect that the dynamics of the fluid would help the mixing of the metabolites in the medium and the exchange of oxygen and carbon dioxide between the gas phase and the liquid phase, thus enhancing cell growth. In this work, we consider a transport field $\mathbf{u}$ in the cell growth model, without solving the fluid problem. The coupling of the growth model with the real free-surface hydrodynamics in the bioreactor is envisaged, however its implementation goes beyond the objective of this work.

4.2 0D model

It has been shown that the kinetic behavior of microorganism can be described by the values of biomass specific rates, namely the specific rate of substrate consumption, the specific cell growth rate and the specific rate of product formation. The values of these rates depend on properties of the organism itself, which are determined by its genome, as well as on environmental conditions, such as the concentrations of compounds in the extracellular environment.

It is obvious that a decrease in the extracellular substrate concentration will lead, at sufficiently low concentration, to a decrease in the biomass specific substrate uptake rate. Since the substrate uptake rate and the specific cell growth rate are intimately linked, it also follows that the cell growth rate decreases at lower substrate concentration. Finally the rate of product formation is also expected to change. Thus, the aim is to find the algebraic functions, called the *kinetic functions*, which describe how the rates depend on the environmental conditions.

The kinetic functions are algebraic equations describing how changes in extracellular environment modify the value of the rate r_i of the component i of the culture medium that we are considering.

These functions are nonlinear and should in principle contain the effects of all different concentrations present in the growth medium on r_i. Because the growth medium contains so many (> 30) different compounds, the complete kinetic function for each r_i would be very complex. Such complexity would prohibit practical use, both with respect to the determination of the function itself as well as the determination of the values of the kinetic parameters and with respect to the application in mathematical models. Fortunately, a general property of biological systems allows considerable simplification: during an experiment several of these factors are usually kept constant. For example, the extracellular concentrations of some of the substrates, such as water, are so high that the rates can be considered independent of the extracellular concentration values.

However, it is always possible to identify one, or more, substrates that can be considered limiting-nutrients. For example, as mentioned in the previous chapters, an exceeding concentration of oxygen can be toxic for CHO

cells. Moreover it has been proved that an excessive metabolic flux and excretion of toxic by-products is diminished greatly when the external concentrations of glucose and glutamine are low. Therefore, it is critical that the glucose and glutamine concentrations in a bioreactor are controlled at a low level so as to decrease the lactate and ammonia accumulation [16] and that the oxygen concentration in the gas phase above the culture medium is maintained at constant, quite low, level.

In the case of CHO cells, three limiting-nutrient components of the culture medium can be identified:

- glucose Glc;
- glutamine Gln;
- oxygen O_2.

Each of them is involved in more than one metabolic pathway: under the hypothesis introduced in the previous chapters and assuming that all the other substances, enzymes and metabolites involved are not limiting-components, the reactions can be simplified as follows:

- aerobic consumption of glucose

$$Glc + 6O_2 \rightarrow 6CO_2 + 6H_2O, \tag{4.1}$$

- anaerobic consumption of glucose

$$Glc \rightarrow 2Lac + 2H_2O, \tag{4.2}$$

- aerobic consumption of glutamine

$$3Gln + 8O_2 + 2H_2O \rightarrow 7CO_2 + 6Amm + 3Lac. \tag{4.3}$$

Whereas water (H_2O) can be neglected since it is not a limiting-component of the culture medium, the products that we have to introduce in the model are

- lactate Lac;

- ammonia Amm;
- carbon dioxide CO_2.

In conclusion, our model has to describe the dynamics of seven component, i.e. cells, three substrates and three products, which are coupled through the reactions (4.1), (4.2) and (4.3).

4.2.1 Cell growth rate

As introduced in the previous chapter, we consider a constant volume V of culture medium in which we have an initial cell concentration X_0. Whereas in a batch culture there is no introduction or removal of cells during the process, the balance equation for the cells is:

$$\begin{cases} \dfrac{dX}{dt}V = r_X V \\ X(0) = X_0, \end{cases} \tag{4.4}$$

where r_X is the cell growth rate. The equation (4.4) can be written introducing the specific growth rate $\mu_X = \dfrac{r_X}{X}$:

$$\begin{cases} \dfrac{dX}{dt} = \mu_X X \\ X(0) = X_0. \end{cases} \tag{4.5}$$

The expression for the specific growth rate that we are now introducing is based on the following considerations:

- in presence of oxygen, the cell takes energy from the aerobic reactions of glucose and glutamine, which release an higher amount of energy respect to the anaerobic respiration;
- the anaerobic respiration takes always place, also in presence of oxygen, but the process is inhibited until oxygen becomes limited;
- the rate of cell growth changes when the cell shifts from aerobic and anaerobic respiration; because of the different amount of energy released in these two processes, we expect that cell growth would be faster during aerobic respiration than during anaerobic respiration;
- the inhibition of cell growth is due to substrate exhaustion.

If we assume that aerobic and anaerobic respirations determine different growth rates, we can decompose the specific growth rate into two terms:

$$\mu_X = \mu_{max}\big(\gamma_{aer}\ \mu_{aer} + \gamma_{anaer}\ \mu_{anaer}\big),$$

with $\gamma_{aer} + \gamma_{anaer} = 1$. The coefficient μ_{max} (1/h) is the maximum specific growth rate, and it is function of all the environmental conditions except the metabolites concentrations.

The term μ_{aer} represents the cell growth rate due to aerobic respiration, while μ_{anaer} is the rate due to anaerobic respiration. These rates have the properties that, under non-limiting nutrient conditions, they approach 1. The constants γ_{aer} and γ_{anaer} help expressing the growth rate as a weighted mean between the growth rate that we would have if we had only aerobic respiration and the growth rate under anaerobic conditions. For example, if $\gamma_{aer} = 0.8$ and $\gamma_{anaer} = 0.2$, under non limiting conditions, the specific growth rate approaches the maximum specific growth rate and cell growth is attributable to aerobic respiration for the 80% and to anaerobic respiration for the 20%.

If we assume that the anaerobic consumption of glucose is inhibited at high concentrations of oxygen, we can introduce the following expression for the specific anaerobic growth rate:

$$\mu_{anaer} = \frac{Glc}{K_{anaer} + Glc + \frac{O_2^2}{K_I}},$$

where Glc is the glucose concentration, O_2 the oxygen concentration, K_I is the inhibition parameter and K_{anaer} is the affinity constant for anaerobic consumption of glucose. We can observe that this term becomes zero when glucose is exhausted and approaches 1 when glucose is in excess and the oxygen concentration is low.

In order to take into account in the expression of the aerobic growth rate μ_{aer} of both the glucose and the glutamine consumption, we introduce the following decomposition:

$$\mu_{aer} = \gamma_{Glc}\ \mu_{Glc} + \gamma_{Gln}\ \mu_{Gln},$$

where the coefficients γ_{Glc} and γ_{Gln}, with $\gamma_{Glc} + \gamma_{Gln} = 1$, have the same meaning of γ_{aer} and γ_{anaer}.

The expression for μ_{Glc} is based on the consideration that the cell, in order to obtain energy from glucose oxidation, needs both glucose and oxygen at the same time. Thus μ_{Glc} depends on the product of glucose and oxygen concentrations as follows:

$$\mu_{Glc} = \left(\frac{Glc}{K_{Glc} + Glc}\right)\left(\frac{O_2}{K_{O_2} + O_2}\right).$$

We can observe that if either oxygen or glucose runs out, the growth rate due to aerobic consumption of glucose becomes zero, while if both glucose and oxygen are in excess, μ_{Glc} approaches 1.

In the same way, we define the growth rate due to glutamine oxidation:

$$\mu_{Gln} = \left(\frac{Gln}{K_{Gln} + Gln}\right)\left(\frac{O_2}{K_{O_2} + O_2}\right).$$

In conclusion, the model for μ_X that we have introduced considers the inhibitory effect on cell growth due to substrate consumption and exhaustion. In particular, if all the substrates are not limiting-nutrients, the specific cell growth rate will approach μ_{max}, while as the substrates are consumed, the growth rate becomes zero.

4.2.2 Substrate uptake rate

The dynamics of the substrates that we are considering, namely glucose, glutamine and oxygen, is coupled with the cell dynamics through the adimensional yield coefficients Y_S, that represents the amount of cells produced for unit of substrate S consumed.

The generic balance equation for the substrate S has the following expression:

$$\begin{cases} \dfrac{dS}{dt} = r_S = -\dfrac{1}{Y_S}\,\mu_{X|S}\,X \\ S(0) = S_0, \end{cases} \tag{4.6}$$

where $\mu_{X|S}$ is the specific cell growth rate due to the substrate S consumption. Starting from the expression for μ_X, we can derive the consumption rates for glucose, glutamine and oxygen.

Glucose consumption rate

Whereas glucose consumption is related both to aerobic oxidation and anaerobic metabolism, its balance equation becomes:

$$\begin{cases} \dfrac{dGlc}{dt} = -\mu_{max}\left(\dfrac{1}{Y_{Glc}}\,\gamma_{aer}\,\gamma_{Glc}\,\mu_{Glc} + \dfrac{1}{Y_{anaer}}\,\gamma_{anaer}\,\mu_{anaer}\right)X \\ Glc(0) = Glc_0, \end{cases} \tag{4.7}$$

where Y_{Glc} is the amount of cells produced thanks to glucose aerobic consumption and Y_{anaer} is the amount of cells produced thanks to glucose anaerobic consumption. We can observe that the glucose consumption would be zero either when the cell concentration is zero or when glucose concentration is zero.

Glutamine consumption rate

Glutamine is involved in aerobic respiration and its balance equation takes the following form:

$$\begin{cases} \dfrac{dGln}{dt} = -\mu_{max}\,\dfrac{1}{Y_{Gln}}\,\gamma_{aer}\,\gamma_{Gln}\,\mu_{Gln}\,X \\ Gln(0) = Gln_0, \end{cases} \tag{4.8}$$

where Y_{Gln} is the amount of cells produced for unit of glutamine consumed. Glutamine consumption is zero either when cell concentration is zero, or when glutamine or oxygen are zero.

Oxygen consumption rate

Oxygen dynamics is related only to aerobic respiration and, if we neglect the oxygen transfer between gas phase and liquid phase, it can be described by the following balance equation:

$$\begin{cases} \dfrac{dO_2}{dt} = -\mu_{max}\,\gamma_{aer}\left(\dfrac{1}{Y_{O_2|Glc}}\,\gamma_{Glc}\,\mu_{Glc} + \dfrac{1}{Y_{O_2|Gln}}\,\gamma_{Gln}\,\mu_{Gln}\right)X \\ O_2(0) = O_{20}. \end{cases} \tag{4.9}$$

The yield coefficients $Y_{O_2|Glc}$ and $Y_{O_2|Gln}$ represent the amount of cells produced for unit of oxygen consumed respectively through glucose and glutamine oxidation. The value of these yield coefficients are dependent on the yield coefficients for glucose and glutamine. In fact, from the stoichiometric

coefficients of the reactions introduced in the previous section, we know that we need 6 moles of oxygen to oxidize 1 mole of glucose and we need 2 moles of oxygen to oxidize 1 mole of glutamine.

If we consider the consumption of oxygen through the glucose aerobic reaction, whereas for one mole of glucose the cell consumes 6 moles of oxygen, we obtain:

$$Y_{O_2|Glc} = \frac{X \text{ produced}}{O_2 \text{ consumed}}\bigg|_{Glc} = \frac{X \text{ produced}}{Glc \text{ consumed}} \cdot \frac{Glc \text{ consumed}}{O_2 \text{ consumed}} = \frac{1 \cdot M_{Glc}}{6 \cdot M_{O_2}} Y_{Glc},$$

where M_{Glc} and M_{O_2} are the molar masses of glucose and oxygen respectively. In the same way we can express the yield coefficient $Y_{O_2|Gln}$ as a function of the glutamine yield coefficient Y_{Gln}:

$$Y_{O_2|Gln} = \frac{X \text{ produced}}{O_2 \text{ consumed}}\bigg|_{Gln} = \frac{1 \cdot M_{Gln}}{2 \cdot M_{O_2}} Y_{Gln},$$

where M_{Gln} is the molar mass of glutamine.

As introduced in the previous chapter, the batch culture system is characterized by the exchange of oxygen between the culture medium and the atmosphere above the liquid. If we introduce the mass transfer term in the balance equation for the oxygen (4.9), we obtain:

$$\begin{cases} \dfrac{dO_2}{dt} = & -\mu_{max}\, \gamma_{aer} \left(\dfrac{1}{Y_{O_2|Glc}}\, \gamma_{Glc}\, \mu_{Glc} + \dfrac{1}{Y_{O_2|Gln}}\, \gamma_{Gln}\, \mu_{Gln} \right) \\ & +K_L^{O_2} a \big(O_2^* - O_2\big) X \\ O_2(0) = & O_{20}. \end{cases} \tag{4.10}$$

4.2.3 Product formation rate

As done in the previous section for the substrate consumption, we can derive the rate of product formation from the cell growth rate μ_X. The generic balance equation for the product P has the following form:

$$\begin{cases} \dfrac{dP}{dt} = r_P = \dfrac{1}{Y_P}\, \mu_{X|P}\, X \\ P(0) = P_0, \end{cases} \tag{4.11}$$

where $\mu_{X|P}$ is the specific cell growth rate related to the product P formation. In this section we derive the balance equations for lactate, ammonia and carbon dioxide from the expression for μ_X.

Lactate production rate

Lactate is produced by the process of anaerobic respiration and by the process of glutamine oxidation. We obtain the following expression:

$$\begin{cases} \dfrac{dLac}{dt} = \mu_{max}\left(\dfrac{1}{Y_{Lac|Glc}}\,\gamma_{anaer}\,\mu_{anaer} + \dfrac{1}{Y_{Lac|Gln}}\,\gamma_{aer}\,\gamma_{Gln}\,\mu_{Gln}\right)X \\ Lac(0) = Lac_0. \end{cases} \tag{4.12}$$

The yield coefficients of lactate related to the anaerobic reaction $Y_{Lac|Glc}$ and to the aerobic reaction $Y_{Lac|Gln}$ depend on the glucose and glutamine yield coefficients:

$$Y_{Lac|Glc} = \left.\frac{X \text{ produced}}{Lac \text{ produced}}\right|_{Glc} = \frac{1 \cdot M_{Glc}}{2 \cdot M_{Lac}}\,Y_{Glc}$$

and

$$Y_{Lac|Gln} = \left.\frac{X \text{ produced}}{Lac \text{ produced}}\right|_{Gln} = \frac{3 \cdot M_{Gln}}{3 \cdot M_{Lac}}\,Y_{Gln}.$$

where M_{Lac} is the molar mass of lactate.

Ammonia production rate

Ammonia is produced only in the process of glutamine oxidation. We obtain the following balance equation:

$$\begin{cases} \dfrac{dAmm}{dt} = \mu_{max}\,\dfrac{1}{Y_{Amm|Gln}}\,\gamma_{aer}\,\gamma_{Gln}\,X \\ Amm(0) = Amm_0, \end{cases} \tag{4.13}$$

where the yield coefficient $Y_{Amm|Gln}$ is related to the glutamine yield coefficient Y_{Gln}:

$$Y_{Amm|Gln} = \left.\frac{X \text{ produced}}{Amm \text{ produced}}\right|_{Gln} = \frac{3 \cdot M_{Gln}}{6 \cdot M_{Amm}}\,Y_{Gln}.$$

where M_{Amm} is the molar mass of ammonia.

Carbon dioxide production rate

Carbon dioxide is produced both in the process of glucose oxidation and in the process of glutamine oxidation. Moreover, we have to consider the

exchange between the culture medium and the gas phase. We obtain:

$$\begin{cases} \dfrac{dCO_2}{dt} = & \mu_{max}\,\gamma_{aer}\left(\dfrac{1}{Y_{CO_2|Glc}}\,\gamma_{Glc}\,\mu_{Glc} + \dfrac{1}{Y_{CO_2|Gln}}\,\gamma_{Gln}\,\mu_{Gln}\right)X + \\ & +K_L^{CO_2}a\big(CO_2^* - CO_2\big) \\ CO_2(0) = & CO_{20}, \end{cases} \tag{4.14}$$

where the yield coefficient $Y_{CO_2|Glc}$ of carbon dioxide through glucose oxidation depends on glucose yield coefficient:

$$Y_{CO_2|Glc} = \frac{X \text{ produced}}{CO_2 \text{ produced}}\bigg|_{Glc} = \frac{1 \cdot M_{Glc}}{6 \cdot M_{CO_2}}\,Y_{Glc},$$

and the yield coefficient $Y_{CO_2|Gln}$ of carbon dioxide through glutamine oxidation depends on glutamine yield coefficient:

$$Y_{CO_2|Gln} = \frac{X \text{ produced}}{CO_2 \text{ produced}}\bigg|_{Gln} = \frac{3 \cdot M_{Gln}}{7 \cdot M_{CO_2}}\,Y_{Gln}.$$

where M_{CO_2} is the molar mass of carbon dioxide.

4.2.4 Remarks

The cell growth model introduced in this section consists of a system of seven ordinary differential equations (4.5), (4.7), (4.8), (4.10), (4.12), (4.13), (4.14), that are coupled through the reaction terms r_i.

The reaction rates are algebraic functions of the substrate concentrations Glc, Gln and O_2. The relationships between the concentrations and the rates are given by different types of model parameters:

- the fundamental yield coefficients Y_{Glc} and Y_{Gln};
- the derived yield coefficients $Y_{i|j}$, that depend on the fundamental yield coefficients through the stoichiometric coefficients;
- the weight coefficients γ_{aer}, γ_{anaer}, γ_{Gln} and γ_{Glc};
- the half-saturation constants K_{Glc}, K_{Glc}, K_{O_2} and K_{anaer};
- the maximum specific growth rate μ_{max};
- the mass transfer coefficients $K_L^{O_2}a$ and $K_L^{CO_2}a$.

Except for the derived yield coefficients, that are estimated from the stoichiometric coefficient of the metabolic reactions, these parameters should be estimated through appropriate experiments.

4.2.5 Numerical approximation

The 0D model introduced in the previous section is solved with MATLAB and in particular the solver *ode45*, which is based on an explicit Runge-Kutta formula. The results obtained from the 0D model are showed and discussed in the next chapter.

4.3 1D model

In his section we want to introduce in the cell growth model the spatial dependance, in particular the effect on the growth kinetics of the distance from the interface between the culture medium and the atmosphere.

The new model that we are now introducing will be referred to as *1D model*, whereas we take into account of only one spatial coordinate (Figure 4.1). While in the 0D model the effect of the hydrodynamics was included indirectly through the mass transfer coefficient $K_L a$, in the 1D model we are not able to consider this effect on the growth kinetics.

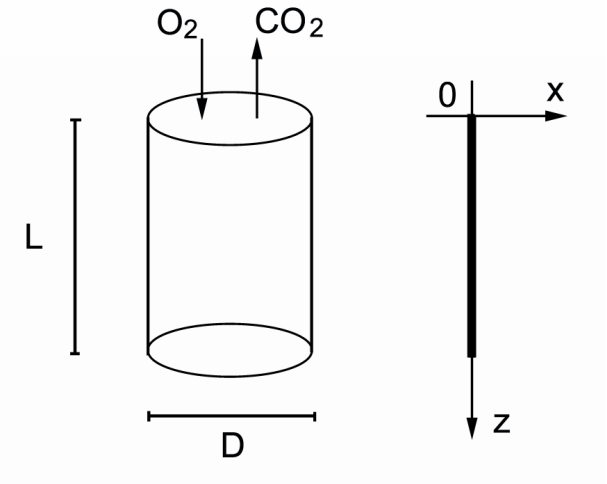

Figure 4.1: 1D domain

Our model is based on the following further hypotheses:

- the dependance of cell growth on the distance from the cylinder axis is negligible compared with the dependance on the distance from the fluid surface;
- the fluid is steady;
- at the beginning, the cell concentration and the concentrations of glucose, glutamine, oxygen and carbon dioxide are uniform in the culture medium, while the concentrations of lactate and ammonia are zero;
- all the substances diffuse in the culture medium: we define D_i the diffusivity coefficient of the substance i;
- cells diffusivity is negligible respect to the diffusivity of the other components; whereas the fluid is steady, this hypothesis implies that each cell is almost fixed in its initial position;
- oxygen and carbon dioxide diffuse from the gas phase to the liquid phase, and conversely; there is no exchange of cells, substrates and products between culture medium and atmosphere, except for oxygen and carbon dioxide.

The second hypothesis that we have introduced is the most restricting: in fact from experimental results we know that cell growth is strongly dependent on the fluid dynamics, which contributes to make the distribution of cells and substrates uniform in the medium.

In order to build up the model, we define the domain $\Omega = [0, L]$ and we suppose that the point $z = 0$ represents the interface between gas phase and culture medium, as shown in Figure 4.1. We obtain the following system of partial differential equations:

- Cell concentration X

$$\begin{cases} \dfrac{dX}{dt} - D_X \dfrac{d^2X}{dz^2} - \mu_X X = 0, & \text{in } \Omega,\ \forall\, t > 0 \\ X(z,0) = X_0(z), & \text{in } \Omega \\ \dfrac{d}{dz}X(0,t) = 0, & \forall\, t > 0 \\ \dfrac{d}{dz}X(L,t) = 0, & \forall\, t > 0 \end{cases} \tag{4.15}$$

- Glucose concentration Glc

$$\begin{cases} \dfrac{dGlc}{dt} - D_{Glc}\,\dfrac{d^2Glc}{dz^2} + \mu_{Glc}\,Glc = 0, & \text{in } \Omega,\ \forall\, t > 0 \\ Glc(z,0) = Glc_0(z), & \text{in } \Omega \\ \dfrac{d}{dz}Glc(0,t) = 0, & \forall\, t > 0 \\ \dfrac{d}{dz}Glc(L,t) = 0, & \forall\, t > 0 \end{cases} \tag{4.16}$$

- Glutamine concentration Gln

$$\begin{cases} \dfrac{dGln}{dt} - D_{Gln}\,\dfrac{d^2Gln}{dz^2} + \mu_{Gln}\,Gln = 0, & \text{in } \Omega,\ \forall\, t > 0 \\ Gln(z,0) = Gln_0(z), & \text{in } \Omega \\ \dfrac{d}{dz}Gln(0,t) = 0, & \forall\, t > 0 \\ \dfrac{d}{dz}Gln(L,t) = 0, & \forall\, t > 0 \end{cases} \tag{4.17}$$

- Oxygen concentration O_2

$$\begin{cases} \dfrac{dO_2}{dt} - D_{O_2}\,\dfrac{d^2O_2}{dz^2} + \mu_{O_2}\,O_2 = 0, & \text{in } \Omega,\ \forall\, t > 0 \\ O_2(z,0) = O_{20}(z), & \text{in } \Omega \\ O_2(0,t) = O_2^*, & \forall\, t > 0 \\ \dfrac{d}{dz}O_2(L,t) = 0, & \forall\, t > 0 \end{cases} \tag{4.18}$$

- Lactate concentration Lac

$$\begin{cases} \dfrac{dLac}{dt} - D_{Lac}\,\dfrac{d^2Lac}{dz^2} = r_{Lac}, & \text{in } \Omega,\ \forall\, t > 0 \\ Lac(z,0) = Lac_0(z), & \text{in } \Omega \\ \dfrac{d}{dz}Lac(0,t) = 0, & \forall\, t > 0 \\ \dfrac{d}{dz}Lac(L,t) = 0, & \forall\, t > 0 \end{cases} \tag{4.19}$$

- Ammonia concentration Amm

$$\begin{cases} \dfrac{dAmm}{dt} - D_{Amm}\,\dfrac{d^2Amm}{dz^2} = r_{Amm}, & \text{in } \Omega,\ \forall\, t > 0 \\ Amm(z,0) = Amm_0(z), & \text{in } \Omega \\ \dfrac{d}{dz}Amm(0,t) = 0, & \forall\, t > 0 \\ \dfrac{d}{dz}Amm(L,t) = 0, & \forall\, t > 0 \end{cases} \tag{4.20}$$

- Carbon dioxide concentration CO_2

$$\begin{cases} \dfrac{dCO_2}{dt} - D_{CO_2} \dfrac{d^2CO_2}{dz^2} = r_{CO_2}, & \text{in } \Omega,\ \forall\, t > 0 \\ CO_2(z,0) = CO_{20}(z), & \text{in } \Omega \\ CO_2(0,t) = CO_2^*, & \forall\, t > 0 \\ \dfrac{d}{dz} CO_2(L,t) = 0, & \forall\, t > 0. \end{cases} \tag{4.21}$$

The 1D model is composed of seven parabolic diffusion-reaction equations: whereas the rate coefficients μ_i depend on the unknown quantities, the equations are non linear and coupled through the reaction terms.

4.3.1 Remarks

Unlike the 0D model, in the 1D model we introduce the mass diffusivity D_i of each substance in water. It is possible to find the value of the diffusivity coefficients in the literature or to estimate them from the Einstein-Stokes equation:

$$D = \frac{k_B\, T}{6\, \pi\, \eta\, r},$$

where k_B is Boltzmann constant, T is the absolute temperature, η is water viscosity and r is the radius of the molecule.

The coefficient μ_i is the growth (or consumption) rate of the i-th substance. The specific cell growth rate μ_X has been already introduced in the previous section and in the 1D model it maintains the same expression of the 0D model. We can observe that, whereas the concentrations depend on the spatial coordinate z, now also the cell growth rate depends on z.

The specific consumption rate μ_S for the substrate S is defined as

$$\mu_S = -\frac{r_S}{S}$$

where r_S is the consumption rate for S introduced in the 0D model, while r_P is the same production rate introduced in the 0D model. We can observe that the production rate is independent from the concentration of P itself, therefore in the balance equations for the product P we don't have the reaction term but a forcing term coupled with the other equations.

In order to make the model well-posed, appropriate boundary conditions have been imposed to describe the mass exchanges between the culture medium and the external environment. In particular we use homogeneous Neumann conditions to impose the null flux at $z = L$ for each substance and at $z = 0$ for each substance except oxygen and carbon dioxide. Moreover, in agreement with the Two Film theory introduced in the previous chapter, we impose Dirichlet boundary conditions equal to the saturation values at $z = 0$ for oxygen and carbon dioxide.

Unlike the 0D model, the 1D model does not contain the mass transfer parameter $K_L a$, that measure the capacity of the fluid to exchange mass with the gas phase. The $K_L a$ is an experimental parameter that depends on the gas diffusivity coefficient, on the bioreactor geometry and on the bioreactor operational mode, in particular on the fluid dynamics. It is a "global" parameter, because, whereas in the 0D model the spatial dependance is not considered, it is as if the liquid phase would exchange mass with the gas phase in each point of its volume. Because of the hypothesis of steady fluid, in the 1D model the exchange of oxygen and carbon dioxide between gas phase and liquid phase is determined only by the Dirichlet boundary conditions and the gas diffusivity in water, but not by the fluid motion. Consequently, with the 1D model we do not expect the same results of the 0D model, since it is well known that the fluid dynamics highly affect the mixing and the mass exchanges in the bioreactor and hance the substances concentrations.

4.3.2 Numerical approximation

In order to solve the 1D model introduced in the previous section, the governing equations must be discretized in both space and time. The temporal discretization is based on a first-order semi-implicit scheme. We consider a uniform decomposition of the time interval $[0, T]$ into N_t subintervals. We denote the time step with $\Delta t = T/N_t$ and we use the index n to denote variables at time $t^n = n\Delta t$, with $n = 0, \ldots, N_t$.

The generic expression for the time evolution of cells and substrates is given by:

$$\frac{dS(t)}{dt} - D_S \frac{d^2 S(t)}{dz^2} + \mu_S(t) S(t) = 0.$$

where $\mu_S(t)$ represents the time dependent reaction coefficient.

If the time derivative is discretized using the backward finite differences, the first-order time discretization is given by:

$$\frac{S^{n+1}-S^n}{\Delta t} - D_S\frac{d^2S^{n+1}}{dz^2} + \mu_S(t^*)S(t^{**}) = 0.$$

If we consider $t^* = t^n$ and $t^{**} = t^{n+1}$, the time discretization can be referred to as semi-implicit, and we obtain:

$$\frac{1}{\Delta t}S^{n+1} - D_S\frac{d^2}{dz^2}S^{n+1} + \mu_S(t^n)S^{n+1} = \frac{1}{\Delta t}S^n.$$

In the same way, if we consider the generic expression for the time evolution of products:

$$\frac{dP(t)}{dt} - D_P\frac{d^2P(t)}{dz^2} = r_P(t),$$

and we apply the previous approach, we obtain:

$$\frac{1}{\Delta t}P^{n+1} - D_P\frac{d^2P^{n+1}}{dz^2} = \frac{1}{\Delta t}P^n + r_P^n.$$

We can observe that the semi-implicit time discretization permits to decouple the balance equations:

$$\begin{cases}
\frac{X^{n+1}}{\Delta t} - D_X\frac{d^2}{dz^2}X^{n+1} + \mu_X^n X^{n+1} = \frac{1}{\Delta t}X^n \\
\frac{Glc^{n+1}}{\Delta t} - D_{Glc}\frac{d^2}{dz^2}Glc^{n+1} + \mu_{Glc}^n Glc^{n+1} = \frac{1}{\Delta t}Glc^n \\
\frac{Gln^{n+1}}{\Delta t} - D_{Gln}\frac{d^2}{dz^2}Gln^{n+1} + \mu_{Gln}^n Gln^{n+1} = \frac{1}{\Delta t}Gln^n \\
\frac{O_2^{n+1}}{\Delta t} - D_{O_2}\frac{d^2}{dz^2}O_2^{n+1} + \mu_{O_2}^n O_2^{n+1} = \frac{1}{\Delta t}O_2^n \\
\frac{Lac^{n+1}}{\Delta t} - D_{Lac}\frac{d^2}{dz^2}Lac^{n+1} = \frac{1}{\Delta t}Lac^n + r_{Lac}^n \\
\frac{Amm^{n+1}}{\Delta t} - D_{Amm}\frac{d^2}{dz^2}Amm^{n+1} = \frac{1}{\Delta t}Amm^n + r_{Amm}^n \\
\frac{CO_2^{n+1}}{\Delta t} - D_{CO_2}\frac{d^2}{dz^2}CO_2^{n+1} = \frac{1}{\Delta t}CO_2^n + r_{CO_2}^n
\end{cases}$$

The spatial discretization is based on a finite-element approach. We consider the general equation for cells and substrates concentrations on the domain $\Omega = [0, L]$:

$$\frac{dS}{dt} - D_S\frac{d^2S}{dz^2} + \mu_S(z,t)S = 0, \tag{4.22}$$

with Dirichlet boundary conditions on Γ_D and homogeneous Neumann boundary conditions on Γ_N. We suppose that we are looking for a solution S in an appropriate space V and we derive the week formulation of (4.22) by multiplying for a test function v such that $v \in V$ and $v|_{\Gamma_D} = 0$:

Find $S \in V$ such that

$$\int_0^L \frac{dS}{dt}\, v\, dz + D_S \int_0^L \frac{dS}{dz}\, \frac{dv}{dz}\, dz + \int_0^L \mu_S(z,t)\, S\, v\, dz = 0$$

for all $v \in V$, with $v|_{\Gamma_D} = 0$.

We consider a uniform discretization $\mathcal{T}_h$ of the domain $\Omega = [0, L]$ into N_h subintervals K_i, with $i = 1, \ldots, N_h$, and we define $h = L/N_h$ their dimension. Moreover, we use the index i to denote variables in the node $z_i = ih$, with $i = 0, \ldots, N_h$. We introduce the space $X_h^1 = \{v_h \in C^0(\Omega) : v_h|_{K_i} \in P_1, \forall K_i \in T_h\}$, where P_1 is the space of polynomial function with grade 1, and the space $V_h = \{v_h \in X_h^1\} \subset V$. Finally, we consider a lagrangian base $\{\varphi_i, i = 0, \ldots, N_h\}$ for the space V_h.

The finite element formulation for the problem is:

Find $S_h \in V_h$ such that:

$$\int_0^L \frac{dS_h}{dt}\, v_h\, dz + D_S \int_0^L \frac{dS_h}{dz}\, \frac{dv_h}{dz}\, dz \int_0^L \mu_S(z,t)\, S_h\, v_h\, dz = 0 \qquad (4.23)$$

for all $v_h \in V_h$, with $v_h|_{\Gamma_D} = 0$.

If we express S_h as a linear combination of the base functions φ_j:

$$S_h = \sum_{j=0}^{N_h} S_j(t)\, \varphi_j(z)$$

and we impose that the equation (4.23) is valid for all $v_h \in V_h$, we obtain

$$\frac{d}{dt} \sum_{j=0}^{N_h} S_j(t) \int_0^L \varphi_j \varphi_i dz + D_S \sum_{j=0}^{N_h} S_j(t) \int_0^L \frac{d\varphi_j}{dz} \frac{d\varphi_i}{dz} dz + \sum_{j=0}^{N_h} S_j(t) \int_0^L \mu_S \varphi_j \varphi_i dz = 0$$

and then

$$\mathrm{M} \frac{d\mathbf{S}}{dt} + D_S \mathrm{A}\mathbf{S} + \mathrm{R}_S \mathbf{S} = 0,$$

where we have introduced the stiffness matrix

$$[\mathrm{A}]_{ij} = \int_0^L \frac{d\varphi_j}{dz}\,\frac{d\varphi_i}{dz}\,dz,$$

the mass matrix

$$[\mathrm{M}]_{ij} = \int_0^L \varphi_j\,\varphi_i\,dz$$

and the reaction matrix

$$[\mathrm{R}_S]_{ij} = \int_0^L \mu_S(z,t)\,\varphi_j\,\varphi_i\,dz.$$

Since we are using linear finite elements, the stiffness matrix and, in general, the reaction matrix will be tridiagonal while the mass matrix will be diagonal. In order to build up the reaction matrix, in particular, we need to introduce an integration rule in order to estimate its terms, because the reaction coefficient is not constant on the domain. We apply the trapezoidal rule, that is:

$$\int_a^b f(z)\,dz = \frac{b-a}{2}\,\big[f(a)+f(b)\big].$$

We can observe that, thanks to the properties of the linear finite elements, we obtain that

$$[\mathrm{R}_S]_{ij} = \begin{cases} 0 & \text{if } j \neq i, \\ h\,\mu_S(z_i,t) & \text{if } j = i. \end{cases}$$

In conclusion, the reaction matrix that we obtain is diagonal as if we applied the mass lumping technique to the reaction-diffusion problem [21]. Consequently we don't expect instabilities related to dominating reaction.

Finally, if we apply the semi-implicit time discretization already introduced, we obtain:

$$\frac{1}{\Delta t}\mathrm{M}\mathbf{S}^{n+1} + D_S\mathrm{A}\mathbf{S}^{n+1} + \mathrm{R}_S^n\mathbf{S}^{n+1} = \frac{1}{\Delta t}\mathrm{M}\mathbf{S}^n$$

In the same way, we can derive the finite element formulation for the general product equation:

$$\frac{dP}{dt} - D_P\,\frac{d^2P}{dz^2} = r_P(z,t). \tag{4.24}$$

We obtain

$$\mathrm{M}\frac{d\mathbf{P}}{dt} + D_P\mathrm{A}\mathbf{P} = \mathbf{r}_P(t)$$

and

$$\frac{1}{\Delta t}\mathrm{M}\mathbf{P}^{n+1} + D_P\mathrm{A}\mathbf{P}^{n+1} = \frac{1}{\Delta t}\mathrm{M}\mathbf{P}^{n} + \mathbf{r}_P^n,$$

where

$$r_{P,i} = \int_0^L r_P(z)\,\varphi_i\,dz = h\,r_P(z_i).$$

In conclusion, we obtain the following set of linear systems:

$$\begin{cases} \frac{1}{\Delta t}\mathrm{M}\mathbf{X}^{n+1} + D_X\mathrm{A}\mathbf{X}^{n+1} + \mathrm{R}_X^n\mathbf{X}^{n+1} = \frac{1}{\Delta t}\mathrm{M}\mathbf{X}^n \\ \frac{1}{\Delta t}\mathrm{M}\mathbf{Glc}^{n+1} + D_{Glc}\mathrm{A}\mathbf{Glc}^{n+1} + \mathrm{R}_{Glc}^n\mathbf{Glc}^{n+1} = \frac{1}{\Delta t}\mathrm{M}\mathbf{Glc}^n \\ \frac{1}{\Delta t}\mathrm{M}\mathbf{Gln}^{n+1} + D_{Gln}\mathrm{A}\mathbf{Gln}^{n+1} + \mathrm{R}_{Gln}^n\mathbf{Gln}^{n+1} = \frac{1}{\Delta t}\mathrm{M}\mathbf{Gln}^n \\ \frac{1}{\Delta t}\mathrm{M}\mathbf{O}_2^{n+1} + D_{O_2}\mathrm{A}\mathbf{O}_2^{n+1} + \mathrm{R}_{O_2}^n\mathbf{O}_2^{n+1} = \frac{1}{\Delta t}\mathrm{M}\mathbf{O}_2^n \\ \frac{1}{\Delta t}\mathrm{M}\mathbf{Lac}^{n+1} + D_{Lac}\mathrm{A}\mathbf{Lac}^{n+1} = \frac{1}{\Delta t}\mathrm{M}\mathbf{Lac}^n + \mathbf{r}_{Lac}^n \\ \frac{1}{\Delta t}\mathrm{M}\mathbf{Amm}^{n+1} + D_{Amm}\mathrm{A}\mathbf{Amm}^{n+1} = \frac{1}{\Delta t}\mathrm{M}\mathbf{Amm}^n + \mathbf{r}_{Amm}^n \\ \frac{1}{\Delta t}\mathrm{M}\mathbf{CO}_2^{n+1} + D_{CO_2}\mathrm{A}\mathbf{CO}_2^{n+1} = \frac{1}{\Delta t}\mathrm{M}\mathbf{CO}_2^n + \mathbf{r}_{CO_2}^n \end{cases} \tag{4.25}$$

These linear systems are implemented and solved using MATLAB. Thanks to the semi-implicit time discretization, the systems are decoupled and consequently they can be solved sequentially.

The algorithm can be synthesized as follows:

- `definition of the model parameters;`
- `definition of the initial values;`
- `construction of the mass matrix M and the stiffness matrix A;`
- `temporal loop: for n = 1 ... Nt do`
  - `loop on the systems: for i = 1 ... 7 do`
    - `construction of the reaction matrices R and the right-hand-side using the solution at the time step n-1;`
    - `imposition of the boundary conditions;`
    - `solution of the system i at the time step n;`
  - `end for;`
- `end for.`

Boundary conditions

We have observed in the previous section that, since the boundary conditions of all the balance equations are either homogeneous Neumann conditions or Dirichlet conditions, we obtain the same weak formulation for each variable, except for the reaction term. In particular the boundary terms that derive from the integration are all equal to zero. Consequently, the last step to be done before solving the system (4.25) is to impose the Dirichlet boundary conditions for the oxygen and the carbon dioxide concentrations on the interface between liquid and gas at $z = 0$. We decide to impose the boundary value directly by replacing the equation related to the node z_0 with

$$O_{2,0} = O_2^*$$

for the oxygen and

$$CO_{2,0} = CO_2^*$$

for the carbon dioxide. This approach requires only the modification of one row of the system and it is quite simple.

4.4 3D model

The development of the 3D model for the cell growth process requires the coupling of the growth model for the cells with the real free-surface hydrodynamics inside the bioreactor. While the extension of the cell growth model to a 3D domain is quite straightforward, the last problem requires the solution of the Navier-Stokes equations for an incompressible Newtonian fluid on a moving domain $\Omega \subset \mathbb{R}^3$:

$$\begin{cases} \rho\dfrac{\partial \mathbf{u}}{\partial t} - \mu\Delta\mathbf{u} + \rho\mathbf{u}\cdot\nabla\mathbf{u} + \nabla p = 0, & \text{in } \Omega(t),\ \forall\, t > 0 \\ \nabla\cdot\mathbf{u} = 0, & \text{in } \Omega(t),\ \forall\, t > 0 \\ \mathbf{u}(\mathbf{x},0) = \mathbf{u}_0(\mathbf{x}), & \text{in } \Omega(t) \\ \mathbf{u}(\mathbf{x},t) = \mathbf{g}(\mathbf{x},t), & \text{su } \Gamma_D(t),\ \forall\, t > 0 \\ \mu\dfrac{\partial \mathbf{u}}{\partial \mathbf{n}} - p\mathbf{n} = \mathbf{h}(\mathbf{x},t) & \text{su } \Gamma_N(t),\ \forall\, t > 0 \end{cases} \tag{4.26}$$

where $\mathbf{u}$ is the velocity field, p is the pressure, ρ is the fluid density and μ is the fluid viscosity.

The implementation of the real bioreactor hydrodynamics is quite complex and goes beyond our objective of testing the global properties of the cell growth model. Therefore in this work we do not solve the fluid dynamics and we suppose that the transport field $\mathbf{u}$ is known.

We assume that the fluid transports the cells, the substrates and the products and that the transport is passive, that is the fluid dynamics is not affected by the concentrations of the substances. This assumption is justified by the the fact that the cell density is similar to the water density [26]. Under this hypothesis, if we define Γ_{up} the interface between the liquid phase and the atmosphere, we obtain the following set of partial differential equations:

- Cell concentration X

$$\begin{cases} \dfrac{\partial X}{\partial t} - D_X\,\Delta X + \mathbf{u}\cdot\nabla X - \mu_X\,X = 0, & \text{in } \Omega,\ \forall\, t > 0 \\ X(\mathbf{x},0) = X_0(\mathbf{x}), & \text{in } \Omega \\ \dfrac{\partial}{\partial \mathbf{n}} X(\mathbf{x},t) = 0, & \text{su } \partial\Omega \end{cases} \tag{4.27}$$

- Glucose concentration Glc

$$\begin{cases} \dfrac{\partial Glc}{\partial t} - D_{Glc}\,\Delta Glc + \mathbf{u}\cdot\nabla Glc + \mu_{Glc}\,Glc = 0, & \text{in } \Omega,\ \forall\, t > 0 \\ Glc(\mathbf{x},0) = Glc_0(\mathbf{x}), & \text{in } \Omega \\ \dfrac{\partial}{\partial \mathbf{n}} Glc(\mathbf{x},t) = 0, & \text{su } \partial\Omega \end{cases} \tag{4.28}$$

- Glutamine concentration Gln

$$\begin{cases} \dfrac{\partial Gln}{\partial t} - D_{Gln}\,\Delta Gln + \mathbf{u}\cdot\nabla Gln + \mu_{Gln}\,Gln = 0, & \text{in } \Omega,\ \forall\, t > 0 \\ Gln(\mathbf{x},0) = Gln_0(\mathbf{x}), & \text{in } \Omega \\ \dfrac{\partial}{\partial \mathbf{n}} Gln(\mathbf{x},t) = 0, & \text{su } \partial\Omega \end{cases} \tag{4.29}$$

- Oxygen concentration O_2

$$\begin{cases} \dfrac{\partial O_2}{\partial t} - D_{O_2}\,\Delta O_2 + \mathbf{u}\cdot\nabla O_2 + \mu_{O_2}\,O_2 = 0, & \text{in } \Omega,\ \forall\, t > 0 \\ O_2(\mathbf{x},0) = O_2^*(\mathbf{x}), & \text{in } \Omega \\ \dfrac{\partial}{\partial \mathbf{n}} O_2(\mathbf{x},t) = 0, & \text{su } \partial\Omega \setminus \Gamma_{Up} \\ O_2(\mathbf{x},t) = O_2^*, & \text{su } \Gamma_{Up} \end{cases} \tag{4.30}$$

- Lactate concentration Lac

$$\begin{cases} \dfrac{\partial Lac}{\partial t} - D_{Lac}\,\Delta Lac + \mathbf{u}\cdot\nabla Lac = r_{Lac}, & \text{in } \Omega \\ Lac(\mathbf{x},0) = Lac_0(\mathbf{x}), & \text{in } \Omega \\ \dfrac{\partial}{\partial \mathbf{n}} Lac(\mathbf{x},t) = 0, & \text{su } \partial\Omega \end{cases} \tag{4.31}$$

- Ammonia concentration Amm

$$\begin{cases} \dfrac{\partial Amm}{\partial t} - D_{Amm}\,\Delta Amm + \mathbf{u}\cdot\nabla Amm = r_{Amm}, & \text{in } \Omega \\ Amm(\mathbf{x},0) = Amm_0(\mathbf{x}), & \text{in } \Omega \\ \dfrac{\partial}{\partial \mathbf{n}} Amm(\mathbf{x},t) = 0, & \text{su } \partial\Omega \end{cases} \tag{4.32}$$

- Carbon dioxide concentration CO_2

$$\begin{cases} \dfrac{\partial CO_2}{\partial t} - D_{CO_2}\,\Delta CO_2 + \mathbf{u}\cdot\nabla CO_2 = r_{CO_2}, & \text{in } \Omega \\ CO_2(\mathbf{x},0) = CO_2^*(\mathbf{x}), & \text{in } \Omega \\ \dfrac{\partial}{\partial \mathbf{n}} CO_2(\mathbf{x},t) = 0, & \text{su } \partial\Omega \setminus \Gamma_{Up} \\ CO_2(\mathbf{x},t) = CO_2^*, & \text{su } \Gamma_{Up} \end{cases} \tag{4.33}$$

The diffusivity coefficients D_i and the rates μ_i and r_i of the 3D model are exactly the same as the 1D model. The only differences between the two models are represented by the transport term $\mathbf{u}\cdot\nabla(\cdot)$ and the domain dimension.

We can observe that the main difference between the 0D model and the 3D model is that the compounds in the culture medium are transported by the fluid, thus helping the mixing of the substrates and the mass exchange between the liquid phase and the gas phase. However we want to highlight

that we are not considering the free-surface hydrodynamics, which is known to further enhance the mass exchange. As previously mentioned, the full coupling with the complete hydrodynamics of the flow inside the bioreactor is currently under development.

Moreover in our model we do not consider the effect of shear stresses on the cell physiology. It has been observed, in fact, that low shear stresses can increase cell activity, whereas high shear stresses can reduce cell viability.

In conclusion, the 3D model that we have presented allows us to understand how a better mixing of the compounds in the culture medium influences the dynamics of cell growth, but not the effect of the real bioreactor hydrodynamics.

4.4.1 Numerical approximation

In order to solve the 3D model introduced in the previous section, the equations are discretized both in time and in space with the same approach adopted for the 1D model discretization, that is with semi-implicit finite differences for time discretization and linear finite element for spatial discretization.

We obtain the following set of linear systems:

$$\begin{cases} \frac{1}{\Delta t}\mathrm{M}\mathbf{X}^{n+1} + D_X\mathrm{A}\mathbf{X}^{n+1} + \mathrm{B}^{n+1}\mathbf{X}^{n+1} + \mathrm{R}_X^n\mathbf{X}^{n+1} = \frac{1}{\Delta t}\mathrm{M}\mathbf{X}^n \\ \frac{1}{\Delta t}\mathrm{M}\mathbf{Glc}^{n+1} + D_{Glc}\mathrm{A}\mathbf{Glc}^{n+1} + \mathrm{B}^{n+1}\mathbf{Glc}^{n+1} + \mathrm{R}_{Glc}^n\mathbf{Glc}^{n+1} = \frac{1}{\Delta t}\mathrm{M}\mathbf{Glc}^n \\ \frac{1}{\Delta t}\mathrm{M}\mathbf{Gln}^{n+1} + D_{Gln}\mathrm{A}\mathbf{Gln}^{n+1} + \mathrm{B}^{n+1}\mathbf{Gln}^{n+1} + \mathrm{R}_{Gln}^n\mathbf{Gln}^{n+1} = \frac{1}{\Delta t}\mathrm{M}\mathbf{Gln}^n \\ \frac{1}{\Delta t}\mathrm{M}\mathbf{O}_2^{n+1} + D_{O_2}\mathrm{A}\mathbf{O}_2^{n+1} + \mathrm{B}^{n+1}\mathbf{O}_2^{n+1} + \mathrm{R}_{O_2}^n\mathbf{O}_2^{n+1} = \frac{1}{\Delta t}\mathrm{M}\mathbf{O}_2^n \\ \frac{1}{\Delta t}\mathrm{M}\mathbf{Lac}^{n+1} + D_{Lac}\mathrm{A}\mathbf{Lac}^{n+1} + \mathrm{B}^{n+1}\mathbf{Lac}^{n+1} = \frac{1}{\Delta t}\mathrm{M}\mathbf{Lac}^n + \mathbf{r}_{Lac}^n \\ \frac{1}{\Delta t}\mathrm{M}\mathbf{Amm}^{n+1} + D_{Amm}\mathrm{A}\mathbf{Amm}^{n+1} + \mathrm{B}^{n+1}\mathbf{Amm}^{n+1} = \frac{1}{\Delta t}\mathrm{M}\mathbf{Amm}^n + \mathbf{r}_{Amm}^n \\ \frac{1}{\Delta t}\mathrm{M}\mathbf{CO}_2^{n+1} + D_{CO_2}\mathrm{A}\mathbf{CO}_2^{n+1} + \mathrm{B}^{n+1}\mathbf{CO}_2^{n+1} = \frac{1}{\Delta t}\mathrm{M}\mathbf{CO}_2^n + \mathbf{r}_{CO_2}^n. \end{cases} \tag{4.34}$$

We have introduced the transport matrix B that is defined as:

$$[\mathrm{B}]_{ij}^{n+1} = \int_\Omega (\mathbf{u}^{n+1} \cdot \nabla\varphi_j)\, \varphi_i \, d\Omega.$$

where $\mathbf{u}^{n+1}$ is the assigned velocity field at time t^{n+1}.

As observed previously, the semi-implicit time discretization permits to decouple the linear systems, that can be solved sequentially.

The discretized equations are solved using LifeV [6], a finite element library providing implementation of mathematical and numerical methods. In particular we use the advection-diffusion-reaction solver, that we have opportunely extended in order to solve our problem. The decoupled equations that we obtained for each time step with the semi-implicit scheme are solved on the domain Ω, which is discretized using tetrahedral elements. Each linear equation is discretized at time t^n using linear finite elements (P1), that are implemented in the library. Moreover, the LifeV library implements the Interior Penalty method in order to stabilize the advection-dominated problem [3]. The algebraic problem (4.34) obtained from the discretization of the advection-diffusion-reaction equations is solved using the GMRES method. The linear systems are preconditioned using Ifpack, an object-oriented algebraic preconditioner package, and in particular Amesos, that implements the complete LU factorization.

4.5 Environmental factors

In this section we introduce in the previous models the effect of temperature on cell growth dynamics through two distinct terms. We first present a simple model for the maximum growth rate as a function of temperature. Moreover, we introduce the relationship between temperature and the saturation concentrations of oxygen and carbon dioxide. These expressions are exactly the same for the three models introduced in the previous sections.

Finally, we derive an estimate of the pH in the culture medium as a function of the concentrations of the main compounds in the medium.

4.5.1 Temperature dependance

Maximum growth rate μ_{max}

It has been highlighted in the previous chapters that cell metabolism and growth are highly influenced by temperature. If we consider cell growth as a chemical reaction, we can express the maximum specific cell growth rate

μ_{max} as a function of the temperature T using the Arrhenius equation, as proposed by [11]:

$$\mu_{max} = A \exp\left(-\frac{E_a}{RT}\right) - B \exp\left(-\frac{E_{a,high}}{RT}\right).$$

The Arrhenius law has four parameters that have to be estimated; in particular, if only one reaction is considered in the model, the coefficients E_a and $E_{a,high}$ can be interpreted respectively as the activation energy and the denaturation energy for the reaction. Consequently, whereas we consider three different reactions, if we apply the Arrhenius law to estimate the maximum specific growth rate in our model, we loose the mechanistic interpretation of its parameters. Moreover, if we try to apply this law in our model for CHO cells, it seems not to provide good results.

Thus, we introduce the following expression for μ_{max} as a function of the temperature T:

$$\mu_{max} = \mu_{opt} \exp\left(-\frac{(T - T_{opt})^2}{r^2}\right). \tag{4.35}$$

In the gaussian model (4.35) there are three parameters:

- T_{opt} is the optimal temperature for cell growth;
- r represents the size of the interval of temperature in which cell growth is not significantly inhibited by temperature;
- μ_{opt} represents the maximum specific growth rate at optimal temperature conditions.

The advantage of using the gaussian model instead of the Arrhenius law is related first to a more clear significance of the model parameters, even when the growth model include more than one substrate. Secondly, as suggested in [34], if we neglect the coefficient μ_{opt}, the temperature effect on cell growth is included in the model as an independent multiplicative factor that is equal to 1 under optimal temperature conditions, while it decreases to 0 when the environment moves away from optimal temperature conditions. Finally, the number of parameters to e estimated is reduced from four to three.

Gas solubility

Temperature influences the solubility of oxygen and carbon dioxide in water and consequently their saturation concentration. We have seen in the previous sections that the oxygen saturation concentration in water is given by the Henry's law:

$$O_2^* = \frac{P_{O_2} n_{H_2O}}{H_{O_2}},$$

where the Henry constant H_{O_2} depends on temperature through the Van't Hoff equation:

$$H(T) = H(T_s) \exp\left[- C\left(\frac{1}{T} - \frac{1}{T_s}\right)\right].$$

The constant T_s refers to the standard temperature, which is 289 K, T is the temperature of the fluid and C is a constant that depends on the considered gas. In particular for oxygen we have $C_{O_2} = 1700$ K and for carbon dioxide $C_{CO_2} = 2400$ K. Moreover at standard temperature it results $H_{O_2}(T_s) = 4.259 \cdot 10^4$ atm and $H_{CO_2}(T_s) = 0.163 \cdot 10^4$ atm.

4.5.2 pH estimation

If we want to recover an estimate of the pH in the culture medium, we need to take into account the effects of four of the main component of the medium:

- *Ammonia* NH_3: it is a base and in water it releases one hydroxyl anion OH^-:

  $$NH_3 \rightarrow NH_4^+ + OH^-$$

  The basic dissociation constant of ammonia is $Kb_{Amm} = 1.9 \cdot 10^{-5}$.

- *Lactic acid* $C_3H_6O_3$: it is an acid and in water it releases one hydrogen ion H^+:

  $$Lac \rightarrow Lac^- + H^+.$$

  The acid dissociation constant is $Ka_{Lac} = 1.3 \cdot 10^{-4}$.

- *Carbon dioxide* CO_2: it reacts with water forming carbonic acid H_2CO_3. The carbonic acid is a diprotic acid and its dissociation constants are

$Ka_{CA} = 4.3 \cdot 10^{-7}$ and $K_{a2} = 5.6 \cdot 10^{-11}$. In first approximation, we can neglect the second dissociation:

$$CO_2 + H_2O \rightarrow H_2CO_3 \rightarrow HCO_3^- + H^+,$$

- *Bicarbonate* HCO_3^-: the bicarbonate ion behaves like a base when it is in solution with a stronger acid and it behaves like an acid when it is in presence of a stronger base. The basic dissociation constant of bicarbonate is $Kb_B = 2.2 \cdot 10^{-8}$ and the acid dissociation constant is $K_a = 5.6 \cdot 10^{-11}$. In the culture medium, in first approximation, bicarbonate behaves like a base:

$$HCO_3^- + H_2O \rightarrow H_2CO_3 + OH^-.$$

If we want to calculate the pH of a solution of one acid and one base exactly, we have to resolve a system of coupled equations that express:

- acid number of moles balance;
- base number of moles balance;
- charge balance;
- acid dissociation equilibria;
- base dissociation equilibria;
- water dissociation constant.

For example, if we consider only the stronger acid and the stronger base that are dissolved in the culture medium, which in our case are lactic acid and ammonia, we need to solve the following set of coupled equations:

- acid and base dissociation equilibria:

$$\begin{cases} Kb_{Amm} = \dfrac{[Amm^+][OH^-]}{[Amm]} \\ Ka_{Lac} = \dfrac{[Lac^-][H^+]}{[Lac]} \end{cases}$$

- charge balance:

$$[Lac^-] + [OH^-] = [Amm^+] + [H^+]$$

- acid and base moles balances:

$$\begin{cases} C_a = [Lac] + [Lac^-] \\ C_b = [Amm] + [Amm^+] \end{cases}$$

  where C_a and C_b are the analytical concentration of the acid and the base respectively;

- water dissociation constant:

$$K_w = [H^+][OH^-]$$

  where K_w is the ion product of water.

The unknown quantities are the equilibrium concentrations $[OH^-]$, $[H^+]$, $[Lac^-]$, $[Amm+]$, $[Lac]$, $[Amm]$. If we manipulate the system, we obtain a fourth degree equation for $[H^+]$.

From this example we can understand that, even if we consider only one acid and one base, the system that we have to solve is complex and it is not possible to obtain the exact value of the pH. It becomes necessary to make some approximations.

Let us now consider the set of equations that we obtain if we consider the presence in the culture medium of both the two acids and the two basis:

$$\begin{cases} Kb_{Amm} = \dfrac{[Amm^+][OH^-]_{Amm}}{[Amm]} \\ Kb_B = \dfrac{[H_2CO_3][OH^-]_B}{[HCO_3^-]} \\ Ka_{Lac} = \dfrac{[Lac^-][H^+]_{Lac}}{[Lac]} \\ Ka_{CA} = \dfrac{[HCO_3^-][H^+]_{CA}}{[H_2CO_3]} \\ Cb_{Amm} = [Amm] + [Amm^+] \\ Cb_B = [H_2CO_3] + [HCO_3^-] \\ Ca_{Lac} = [Lac] + [Lac^-] \\ Ca_{CA} = [H_2CO_3] + [HCO_3^-] \\ K_w = ([H^+]_{Lac} + [H^+]_{CA})([OH^-]_{Amm} + [OH^-]_B) \\ (OH^-)_{Lac} + [OH^-]_B + [Lac^-] + [HCO_3^-] = \\ \qquad = [Amm^+] + [H_2CO_3] + [H^+]_{Lac} + [H^+]_{CA} \end{cases} \tag{4.36}$$

Now we suppose that the fraction of each acid and base that dissociates is negligible respect to the analytical concentration, e.g. $[Amm] \simeq Cb_{Amm}$. This assumption is correct because the acids and the basis that we are considering are weak ($Ka, Kb < 10^{-3}$).

The first fourth equations of the system (4.36) become:

$$\begin{cases} Kb_{Amm} = \dfrac{[Amm^+][OH^-]_{Amm}}{Cb_{Amm}} \\ Kb_B = \dfrac{[H_2CO_3][OH^-]_B}{Cb_B} \\ Ka_{Lac} = \dfrac{[Lac^-][H^+]_{Lac}}{Ca_{Lac}} \\ Ka_{CA} = \dfrac{[HCO_3^-][H^+]_{CA}}{Ca_{CA}} \end{cases} \tag{4.37}$$

Using the charge balance equations, from these relations we obtain the following expression for the unknown concentrations $[H^+]$ and $[OH^-]$:

$$\begin{aligned}\frac{Cb_{Amm}Kb_{Amm}}{[OH^-]_{Amm}} + \frac{Cb_BKb_B}{[OH^-]_B} + [H^+]_{Lac} + [H^+]_{CA} = \\ = [OH^-]_{Amm} + [OH^-]_B + \frac{Ca_{Lac}Ka_{Lac}}{[H^+]_{Lac}} + \frac{Ca_{CA}Ka_{CA}}{[H^+]_{CA}}\end{aligned} \tag{4.38}$$

Now we can define the total H^+ concentration:

$$[H^+] = [H^+]_{Lac} + [H^+]_{CA}$$

and the total OH^- concentration:

$$[OH^-] = [OH^-]_{Amm} + [OH^-]_B = \frac{K_w}{[H^+]}.$$

We obtain

$$\begin{aligned}\frac{Cb_{Amm}Kb_{Amm}[OH^-]_B + Cb_BKb_B[OH^-]_{Amm}}{[OH^-]_B[OH^-]_{Amm}} + [H^+] = \\ \frac{K_w}{[H^+]} + \frac{Ca_{Lac}Ka_{Lac}[H^+]_{CA} + Ca_{CA}Ka_{CA}[H^+]_{Lac}}{[H^+]_{Lac}[H^+]_{CA}}\end{aligned} \tag{4.39}$$

Now we suppose that the effects of lactic acid and carbonic acid on pH are comparable, so that $[H^+]_{Lac} \simeq [H^+]_{CA} \simeq [H^+]/2$, and, similarly, that the effects of bicarbonate and ammonia are comparable, $[OH^-]_B \simeq [OH^-]_{Amm} \simeq [OH^-]/2$. This hypothesis is quite strong and should be tested with appropriate experiments. We obtain the following second degree equation for the H^+ concentration:

$$\begin{aligned}2(Cb_{Amm}Kb_{Amm} + Cb_BKb_B)\frac{[H^+]}{K_w} + [H^+] = \\ \frac{K_w}{[H^+]} + 2(Ca_{Lac}Ka_{Lac} + Ca_{CA}Ka_{CA})\frac{1}{[H^+]}.\end{aligned} \tag{4.40}$$

From equation (4.40) we obtain an explicit estimate of the H^+ concentration in the medium:

$$[H^+] = \left[\frac{2K_w(Ca_{Lac}Ka_{Lac} + Ca_{CA}Ka_{CA}) + K_w^2}{K_w + 2(Cb_{Amm}Kb_{Amm} + Cb_BKb_B)}\right]^{1/2}, \tag{4.41}$$

and finally the pH:

$$pH = -\log_{10}[H^+]. \tag{4.42}$$

As mentioned in the previous chapter, the pH influences cell growth and, when it becomes lower than a critical value that depends on the cell physiology, growth is inhibited and cells start dying. In this work, however, since we are not modeling the death phase of the growth curve, we will not consider the pH as a factor that influences cell growth directly, but we will use the pH value in order to evaluate cells activity and to test our model.

Chapter 5

Numerical simulations

5.1 Preliminary remarks

In order to analyze and test the cell growth models introduced in the previous chapter, it is necessary to define some important properties of the culture system. In particular we refer to the experiments carried out at the Laboratoire de Biotechnologie Cellulaire (LBTC) of the EPFL [1, 26] to obtain information about standard operative conditions that are usually applied in CHO cell culture.

5.1.1 Cell culture

We consider suspension adapted CHO DG44 cells that are grown in serum-free ProCHO5 medium; the culture have the following properties:

- the cells are incubated in an orbital shaker and their initial concentration is $3 \cdot 10^5$ cell/ml;
- the atmosphere above the culture medium is maintained with a constant composition: the partial pressure of CO_2 is 5% and the partial pressure of oxygen is 20%;
- cell density is measured microscopically with a hemocytometer by the trypan blue exclusion method. Glucose, glutamine, lactate and ammonia concentrations are determined with a BioProfile 200 Analyzer;

- cells are cultivated in CultiFlask50 Bioreactor (Sartorius AG, Switzerland) with 10 ml of culture medium. The vessel is agitated at 180 rpm with 5 cm shaking diameter;
- the shaker is placed in a warm cabinet in order to control temperature.

5.1.2 Units of measurement

During the experiments, the concentrations of cells, substrates and products are measured with different techniques and the values of concentrations in the literature are given with different units of measurement. In order to make our model more clear, all the quantity are expressed using the International System of Units (SI). Therefore, to compare the results, we need to introduce the correct conversion rates.

Usually the cell concentration is measured in cells per milliliter. In order to convert the cell concentration in grams per liter, we have estimated the average cell density knowing that the biomass density is about 1.2 kg/m^3 and the cell diameter is about 15 μm [26]. Starting from these experimental estimates, we obtain that the cell volume is $1.77 \cdot 10^{-15}$ m^3 and the mass of one cell is about $2 \cdot 10^{-15}$ kg. Finally, we obtain the conversion factor for the cell concentration:

$$1 \ \frac{\text{cell}}{\text{ml}} = 2 \cdot 10^{-9} \ \frac{\text{kg}}{\text{m}^3} = 2 \cdot 10^{-9} \ \frac{\text{g}}{\text{l}}.$$

While glucose and lactate concentrations are measured in grams per milliliter, glutamine and ammonia concentrations are measured in millimoles per liter. To convert these values in grams per liter, it is simply necessary to know the molar masses of these chemical species, respectively $M_{Gln} = 146$ g/mol and $M_{Amm} = 17$ g/mol.

5.1.3 Values of parameters

In the development of the cell growth models, we have introduced some parameters. All these parameters can be estimate with appropriate experiments and several of them have already been estimated in the literature, for example the mass transfer coefficient $K_L a$. However, whereas these parameters are highly influenced by the experimental set up, the range in which they

can vary is often quite large. Consequently, for our simulations, we have selected a particular operative set up and, when possible, we have chosen the corresponding parameters values from the literature or, when these data were not available, we estimated an average value from different experimental results. Finally, when appropriate experimental results were available, we estimate the parameters values from them.

5.2 0D model

In this section we analyze the results obtained from the model under the following conditions:

- temperature $T = 37°C$;
- mass transfer coefficient $K_L a = 20$: this value has been estimated for the CultiFlask50 Bioreactor with 10 ml of culture medium at 180 rpm with 5 cm shaking diameter;
- initial cell concentration $X_0 = 3 \cdot 10^5$ cell/ml;
- initial glucose concentration $Glc_0 = 8.0$ g/l;
- initial glutamine concentration $Gln_0 = 0.74$ g/l;
- duration of the culture $T_{tot} = 120$ h;
- oxygen partial pressure $P_{O_2} = 20$ % and carbon dioxide partial pressure $P_{CO_2} = 5$ %.

In Figure 5.1 (left) we can observe that the stationary phase is reached after more than 4 days of culture and the maximal cell concentration is about $8.5 \cdot 10^6$ cell/ml. These values are comparable with the experimental results plotted in Figure 5.1 (right), where we can observe that the maximum cell concentration is about $9.0 \cdot 10^6$ cell/ml after 5 days of culture [1, 26]. The lag phase of the real growth curve is longer than the one obtained from the 0D model, thus suggesting that an accurate model for the lag phase should be introduced.

In Figure 5.2 we plot the results about the metabolites and the toxic by-products concentrations. We can observe that, as expected from experimental results, glutamine is completely consumed in the first 4 days of

culture and the model reproduces quite well the real glutamine dynamics. Moreover, as expected from experiments, glutamine is consumed faster than glucose. However, while from experimental results we expect that glucose is not completely consumed during the culture, from the model we obtain that this substrate is exhausted at the end of the process.

We can observe that the maximum ammonia and lactate concentrations are reached after 4 days of culture both in the model and in the experimental results. The maximum lactate concentration in the culture medium estimated by the model is 2.0 g/l, as expected from experimental results. The maximum ammonia concentration that we obtain from the model is 0.07 g/l, which is equal to 4.2 mmol/l, while the maximum concentration that is measured in the real culture is about 4.5 mmol/l [1, 26]. While the model results about the ammonia concentration reproduce quite well the real ammonia dynamics, the lactate formation obtained from the model is slower than the real one.

In Figure 5.3 we plot the oxygen and the carbon dioxide concentrations. We can observe that the oxygen is consumed during the cell growth phases and when cell growth stops its concentration approaches the saturation value. In the same way, the carbon dioxide is produced and accumulated in the first three days of culture and then it is released gradually to the atmosphere.

5.2.1 pH estimation

If we apply the equations (4.41) and (4.42) to estimate the pH in the culture medium at $T = 37°C$, we obtain the result plotted in Figure 5.4. If we compare the model results with the experimental results analyzed in Section 2.4.3, we can observe that the model calculates an underestimate of the real pH in the culture medium and the dynamics of the pH that the model simulates is partially correct. In fact, in Figure 5.4 we can observe that the pH diminishes quickly during the first day of culture and later on it remains almost constant. However, the model does not reproduce the increment of the pH in the last hours of the process, as we can observe from experimental results (Figure 2.9) [1, 26]. The differences between the experimental results and the model estimation could be probably related to the approximations that we have introduced in order to obtain a simple estimation of the pH from the compounds concentrations.

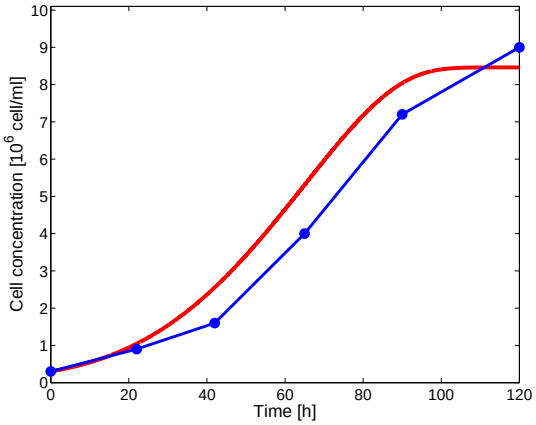

Figure 5.1: Cell growth: comparison between model results and experimental results (points) [1]

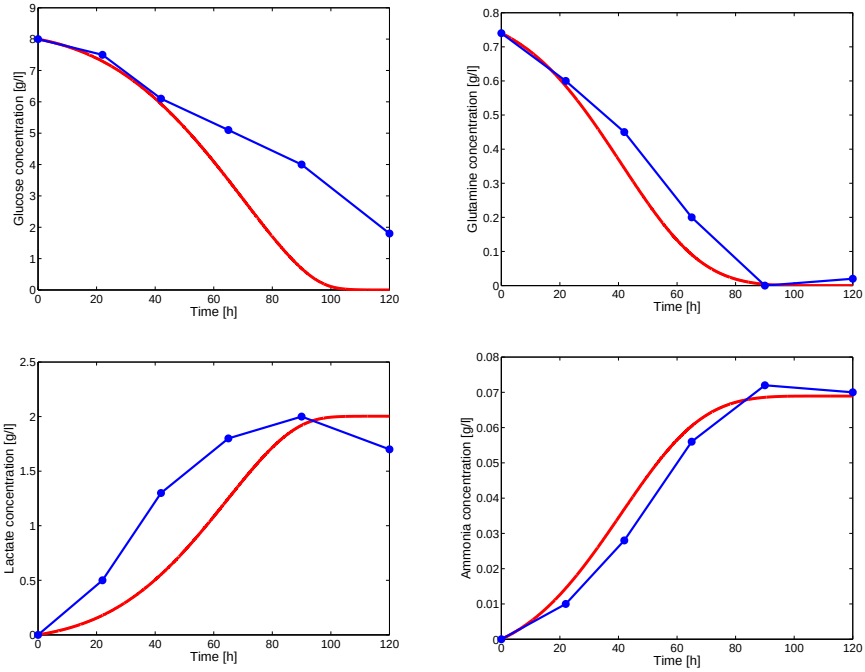

Figure 5.2: Cell metabolism: comparison between model results and experimental results (points) [1]

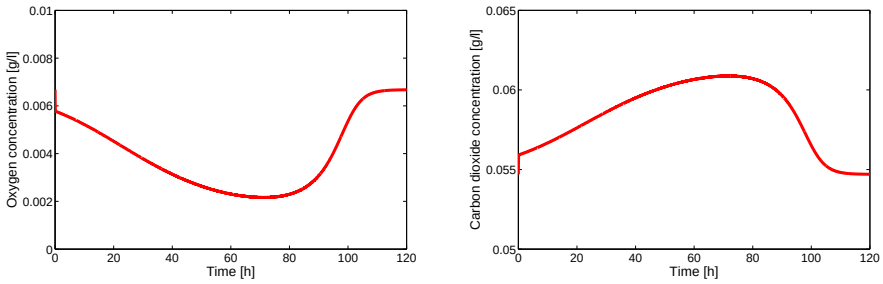

Figure 5.3: Cell metabolism: oxygen (left) and carbon dioxide (right) concentration

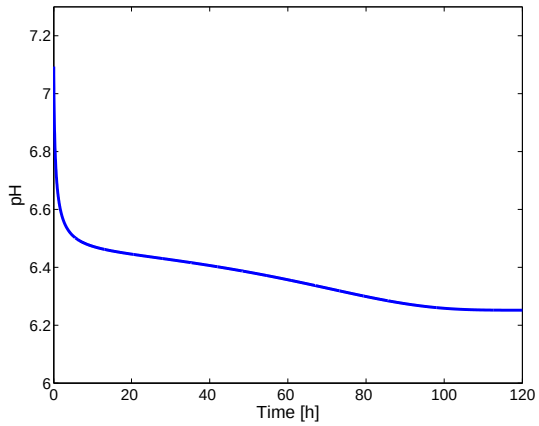

Figure 5.4: pH estimation from the model results

5.2.2 Temperature dependance

In this section we analyze the behavior of our model as a function of temperature. In order to estimate the maximum cell growth rate as a function of temperature, we need to measure cell concentration under non-limiting nutrients conditions. Under this hypothesis, in fact, the multiplicative factor related to the substrate concentrations is equal to 1 and the balance equation for the cells is uncoupled from the balance equations for the substrates. We obtain:

$$\frac{dX}{dt} = \mu_{max} X, \tag{5.1}$$

where

$$\mu_{max} = \mu_{opt} \exp\left(- \frac{(T - T_{opt})^2}{r^2} \right).$$

The equation (5.1) can be solved analytically and we obtain:

$$X(t) = X_0 \exp(\mu_{max} t) = X_0 \exp\left(\mu_{opt} \exp\left[-\frac{(T - T_{opt})^2}{r^2}\right] t\right),$$

where X_0 is the initial cell concentration. If we know the cell concentration as a function of time t and temperature T under non-limiting nutrients conditions, we can estimate the model parameters μ_{opt}, T_{opt} and r.

Whereas we don't have this kind of experimental results, we have to proceed in a different way: we estimate the model parameters μ_{opt}, T_{opt} and r from the value of μ_{max} estimated in [1] with the Gompertz model.

The maximum specific growth rate as a function of temperature that we obtain with this strategy is plotted in Figure 5.5, while the values of the parameters are showed in Table 5.1. For easy of reading, the values of temperature are expressed in Celsius degrees.

If we apply the gaussian model for temperature to the 0D model for cell growth, we obtain the results plotted in Figure 5.6 and in Figure 5.7. It is possible to observe that temperature influences both the maximum specific cell growth rate, the lag phase duration and the maximum cell concentration, as expected from experimental results (see section 2.4.1).

We can observe that when $T = 37°C$ we obtain the maximum cell concentration. When $T = 35°C$ the lag phase is longer and the maximum cell concentration at the end of the process is a bit lower. The final cell concentration decreases further when temperature increases up to $T = 39°C$. When temperature becomes lower than $35°C$ and higher than $39°C$, cell growth is highly inhibited, and for $T = 31°C$ and $T = 41°C$ it is nearly zero, as expected from experimental results (Figure 5.6).

Finally, in Figure 5.7 we can observe that the substrates and the toxic by-products concentrations at different temperatures essentially reflect cell dynamics.

5.2.3 $K_L a$ dependance

In this section we want to test the model at different values of the mass transfer parameters $K_L a$, with $T = 37°C$. The results are plotted in Figure 5.8 and in Figure 5.9.

Parameter	Value
T_{opt} [°C]	36.4
μ_{opt} [1/h]	1.882
r [Δ°C]	3.12

Table 5.1: Parameters of the Gaussian model

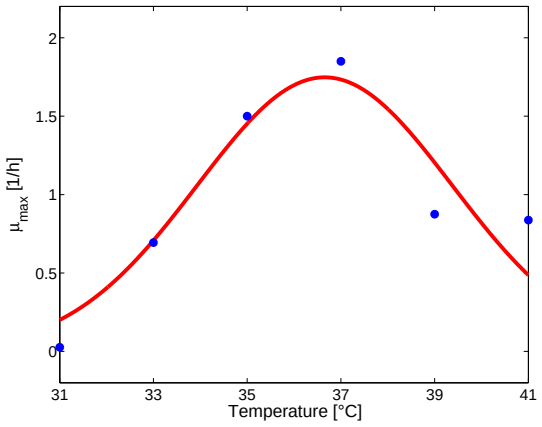

Figure 5.5: Maximum specific growth rate as a function of temperature

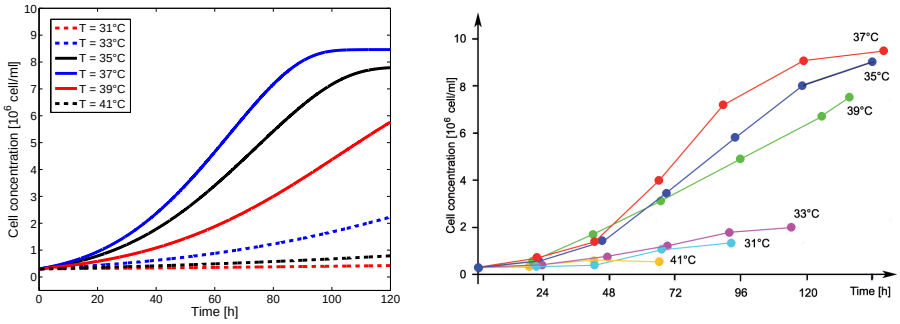

Figure 5.6: Cell growth as a function of temperature: model results (left) and experimental results (right)

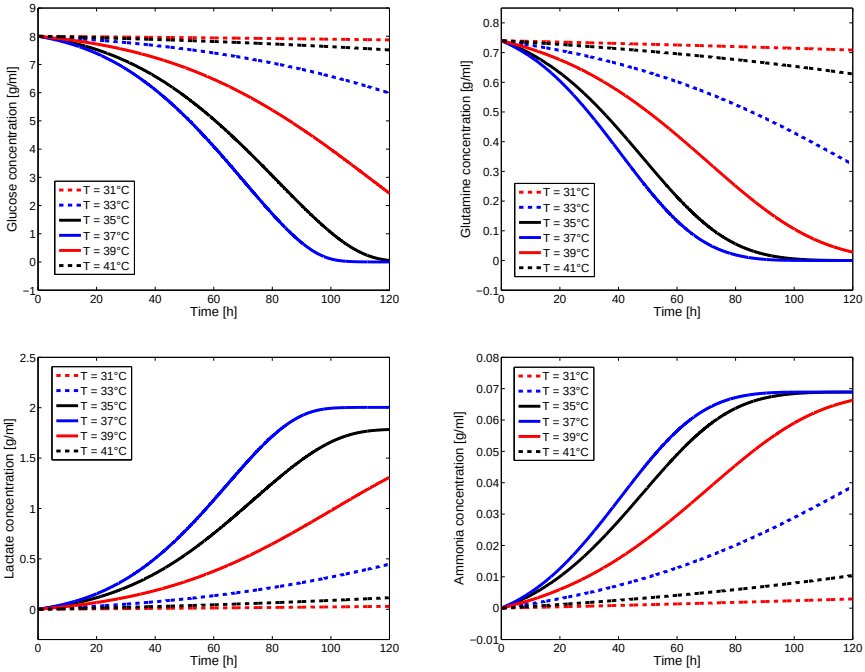

Figure 5.7: Cell growth model: results for different temperatures

We can observe that, as expected from experimental results [1], when K_La is equal to 0, that is when there is not exchange of oxygen and carbon dioxide between the culture medium and the atmosphere, the oxygen in the culture medium is consumed in a few hours. Consequently, there is no production of ammonia and consumption of glutamine, that is metabolized by cells only under aerobic conditions. At the same time, carbon dioxide produced in the first hours of the culture is not released to the atmosphere and it causes a remarkable reduction of the pH in the culture medium (Figure 5.10). Finally, whereas cells recover energy primarily from aerobic respiration, the maximum cell concentration that is reached when $K_La = 0$ is significantly lower respect to the concentration that is reached when the K_La becomes higher. From these observation we can infer why one of the aim of bioreactor design is the increment of the coefficient K_La of the culture system. An increment of the K_La, in fact, causes the increment of the maximum cell concentration reached during the culture period and helps to maintain the pH above toxic values.

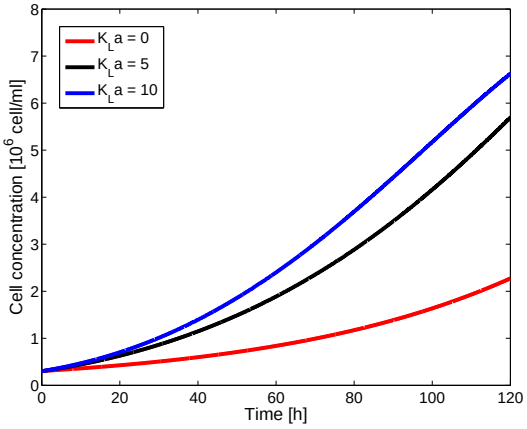

Figure 5.8: Cell growth as a function of the mass transfer coefficient K_La: model results

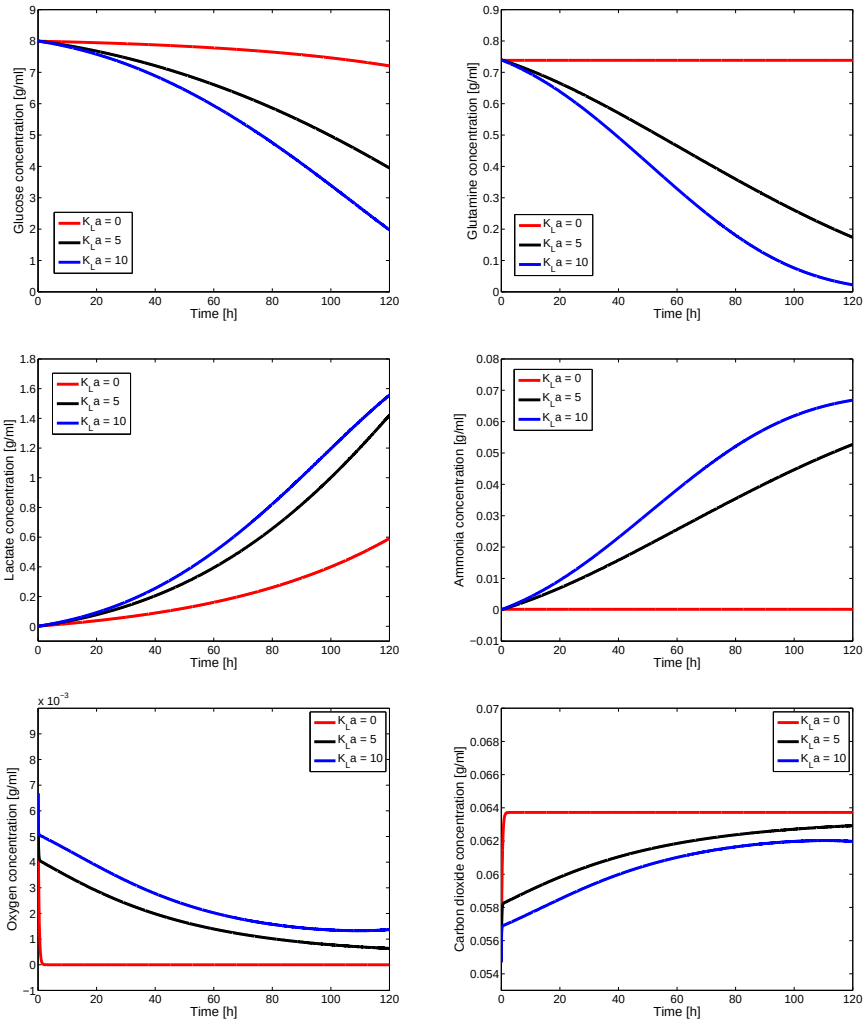

Figure 5.9: Model results as a function of the mass transfer coefficient K_La

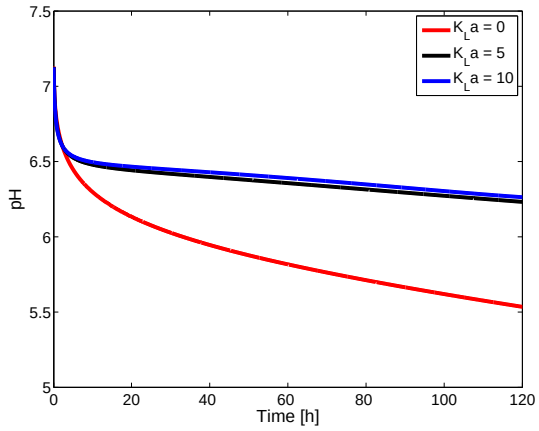

Figure 5.10: pH as a function of the mass transfer coefficient K_La: model results

5.3 1D model

In this section we test the 1D model and in particular we compare its results with the 0D model results. Whereas in the 1D model we are not considering the fluid motion and, consequently, the mass transfer is determined only by the boundary conditions and the diffusivity of each substance in water, we need to set the correct value of the mass transfer parameter K_La in the 0D model in order to make a significant comparison.

From experimental results [26] we know that when the fluid in the bioreactor is steady, the mass transfer coefficient is usually lower than 2 and depends only on the bioreactor geometry and the gas diffusivity. In Figure 5.12 and in Figure 5.13 we plot the results obtained with $K_L^{O_2}a = K_L^{CO_2} = 0.7$ and $T = 37°C$. Whereas the CultiFlask50 Bioreactor (Figure 5.11) that we are considering can be approximated with a cylinder with diameter equal to 30 mm and height equal to 115 mm, we obtain the desired culture volume of 10 ml if we suppose that the fluid in the bioreactor is about 3 cm deep.

One of the main difficulties in the comparison of the 1D model and the 0D model is related to the meaning of the values of concentration obtained with the 0D model and the measurement techniques adopted during the experiments.

Figure 5.11: CultiFlask50 Bioreactor

As explained in [26], the measurement of the concentration of the compounds in the culture medium is done in different ways. For example, the cell concentration is usually estimated by sampling the culture medium only on the surface of the liquid, while the oxygen concentration is estimated by sampling on the bottom of the bioreactor. Moreover, up to our knowledge, in the literature there are neither results about the spatial distribution of the concentrations in the bioreactor, nor results about the average concentrations in the volume. Therefore, it is not easy to make a comparison both between the 1D model and the 0D model and between the 1D model and the experimental results.

Consequently, we decide to compare the concentrations obtained from the 0D model as they were an averaged value in the bioreactor with the averaged concentrations obtained with the 1D model. Moreover, we consider also the minimum and the maximum values as reference concentrations.

In Figure 5.12 we can observe that the averaged cell concentration that we obtain by solving the 1D model is almost equal to the cell concentration that is estimated with the 0D model when we assume that the fluid is stationary. However we can see that the maximum cell concentration in the domain is much larger than the minimum cell concentration: in particular the cell concentration is quite uniform in the domain except in proximity of the surface (Figure 5.14), where the maximum cell concentration is reached. This behavior is related to the fast consumption of the oxygen by the cells and its low solubility and diffusivity in the culture medium. Whereas the

fluid is steady, the liquid that is far away from the surface is not oxygenated (Figure 5.15) and cell growth is thus inhibited. In conclusion cell growth is significant only in proximity of the interface between the culture medium and the surface (Figure 5.14). As a consequence, glucose and glutamine are mainly consumed near the surface, as well as lactate and ammonia are mainly produced in that zone of the domain (Figure 5.15).

In Figure 5.13 we can observe that, while there is correspondence between the averaged oxygen concentration in the 1D domain and the oxygen concentration obtained from the 0D model, the concentrations of carbon dioxide obtained with the two models are quite different and in particular the carbon dioxide estimated with the 0D model is lower than the one obtained with the 1D model. This behavior can be probably explained with the choice of the same $K_L a$ value for both oxygen and carbon dioxide. As observed in [26], in fact, the $K_L a$ value for the carbon dioxide is usually lower than the value for the oxygen, as seemingly predicted from the 1D model. We will focus on this problem in the next section.

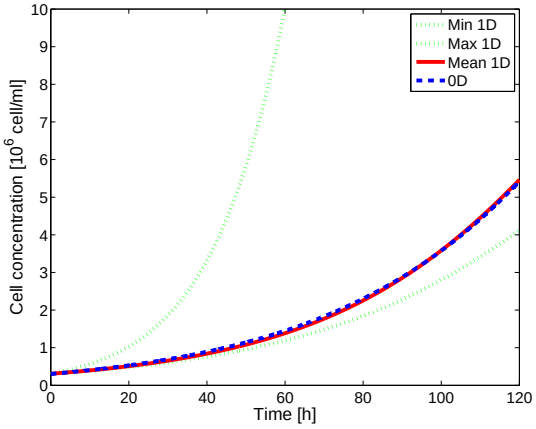

Figure 5.12: Cell growth: comparison between the 1D model and the 0D model

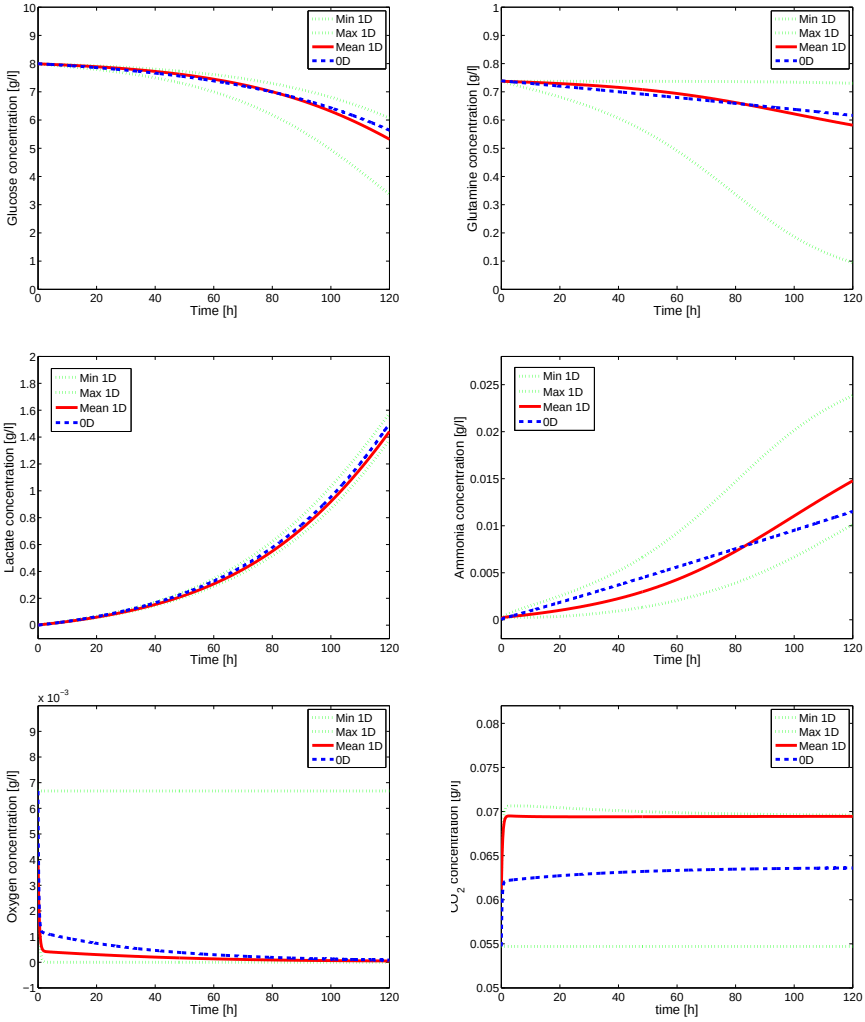

Figure 5.13: Comparison between the 1D model and the 0D model

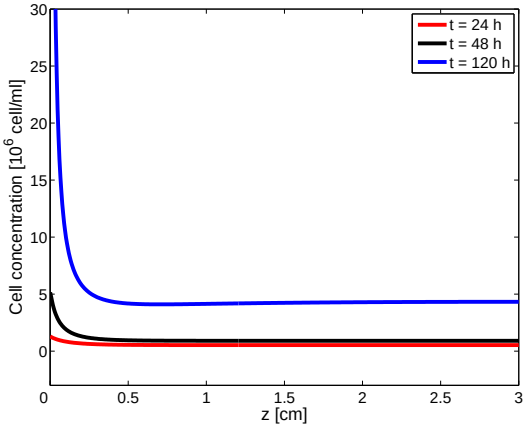

centering

Figure 5.14: 1D cell growth model: spatial dependance

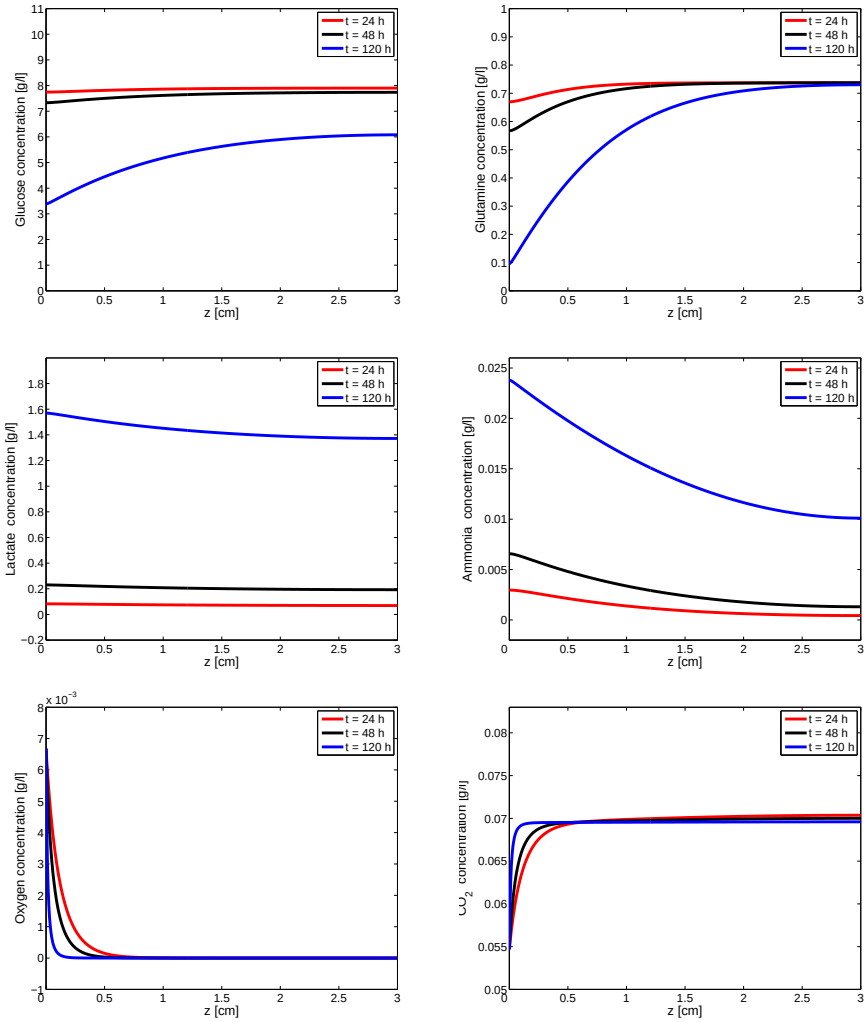

Figure 5.15: 1D model: spatial dependance

5.4 3D model

In this section we test the 3D model and we compare its results with the ones obtained with the 0D model. However we have to take into account that we are not considering the real geometry and the real hydrodynamics of the shaken bioreactor. Consequently, with these simulations we do not have the aim to reproduce the real process, but we want only to test the qualitative effects of transport on the global growth process.

We select the domain $\Omega = [-1, 1]^3$ [dm] and the following simple velocity field (Figure 5.16):

$$\mathbf{u} = \begin{bmatrix} 0 \\ -A\cos\left(\frac{\pi y}{2}\right)\sin\left(\frac{\pi z}{2}\right) \\ A\sin\left(\frac{\pi y}{2}\right)\cos\left(\frac{\pi z}{2}\right) \end{bmatrix}. \tag{5.2}$$

with $A \in R$ [m/s].

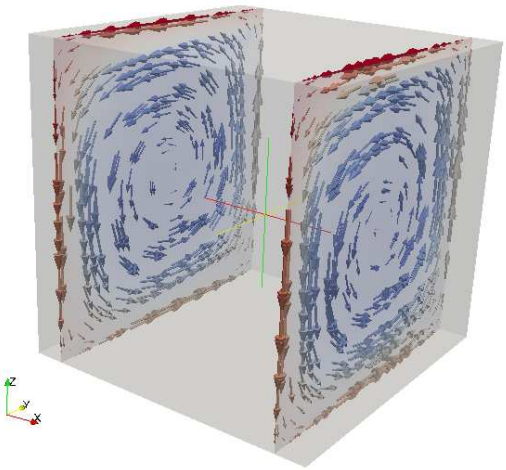

Figure 5.16: Velocity field (5.2)

As in the previous simulations, we don't know exactly the value of the $K_L a$ coefficient related to the geometry and the hydrodynamics that we are considering, however it is possible to make some significant comparisons. As in the previous section, the results obtained with the 0D model are compared with the averaged values of the concentrations in the domain Ω, as well as

with the minimum and the maximum values.

In Figure 5.17 we compare the results obtained from the 3D model and from the 0D model in the case of steady fluid. We can observe that the averaged cell concentration obtained with the 3D model with the considered operative setting corresponds to the one obtained from the 0D model with $K_L a \simeq 5$. In Figure 5.18 we can observe that the correspondence between the 3D model and the 0D model is quite good except for the carbon dioxide concentration: the values obtained with the 3D model are greater than the values obtained with the 0D model with $K_L a = 5$ for both the oxygen and the carbon dioxide, as previously observed also in the 1D model simulations. This result confirms the experimental observation that usually the mass transfer coefficient for the carbon dioxide is lower than the one for the oxygen [26]. We can observe that, while the substances concentrations, except for the oxygen and the carbon dioxide concentrations, are almost uniform in the culture medium, since the minimum and the maximum values are almost equal, the cell concentration varies quite a lot in the volume (Figure 5.25), as already observed for the 1D model. The maximum cell concentration that is reached after 120 hours is nearly the double than the minimum concentration. This behavior is related primarily to the different oxygen concentration in the culture volume: in the lower part of the domain the oxygen is soon consumed by the cells and consequently cell growth is inhibited (Figure 5.25). These results confirm what previously discussed in Section 3.5.2.

In Figure 5.19 we plot the results obtained with the 3D model when the transport field (5.2) with $A = 0.003$ m/s is applied. We can observe that the cell concentration obtained in the considered operative setting can be obtained from the 0D model with $K_L a \simeq 10$. This is confirmed also by the results showed in Figure 5.20. We can observe that, thanks to the fluid motion, the concentration of cells in the volume is almost uniform.

In Figure 5.21 we plot the results obtained with the 3D model when the transport field (5.2) with $A = 0.03$ m/s is applied. We can observe that the concentrations obtained with this transport field can be obtained from the 0D model with $K_L a \simeq 23$. We can observe that the maximum cell concen-

tration that is reached at the end of the growth phase is greater that the ones obtained in the previous cases. We can observe that also in this case the 0D model seems to underestimate the carbon dioxide concentration if we impose that the oxygen and the carbon dioxide have the same $K_L a$ value. From experimental results it is known that the mass transfer rate of CO_2 is about 10%−20% lower than the oxygen transfer rate. If we impose that $K_L^{CO_2} a = 0.8 \cdot K_L^{O_2} a$, we obtain the results plotted in Figure 5.23 and in Figure 5.24. We can observe that the carbon dioxide concentration obtained with the 3D model and the 0D model are now comparable, thus confirming what expected from experimental results.

In Figure 5.25 we compare the spatial distribution of cells, oxygen and carbon dioxide in the culture medium at the end of the process in the case of steady fluid (left) and with the effect of the transport field (right). In particular we plot the results in one section yz. We can observe that the oxygen and the carbon dioxide concentrations are highly affected by the fluid motion, that helps to oxygenate the lower part of the bioreactor and to make the cell concentration uniform in the volume.

In Figure 5.26 and 5.27 we plot the concentrations of oxygen and carbon dioxide respectively at four different time when the transport field with $A = 0.03$ m/s is applied. We can observe that, while the cell concentration remains uniform in the volume (Figure 5.23), the oxygen, starting from a uniform distribution, is consumed and almost exhausted only in the central part of the volume when cell growth is faster. Later on, when cell growth reaches the stationary phase, the oxygen concentration starts increasing. An analogous behavior is observed for the carbon dioxide concentration.

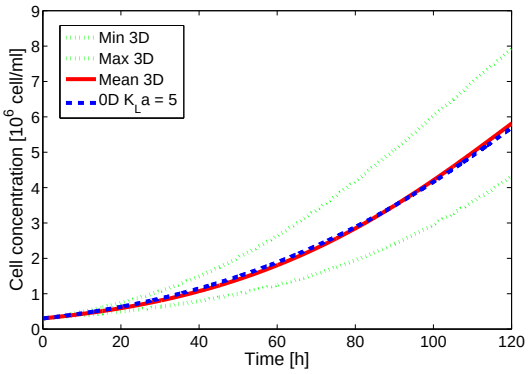

Figure 5.17: Cell growth: comparison between the 3D model and the 0D model with the steady fluid

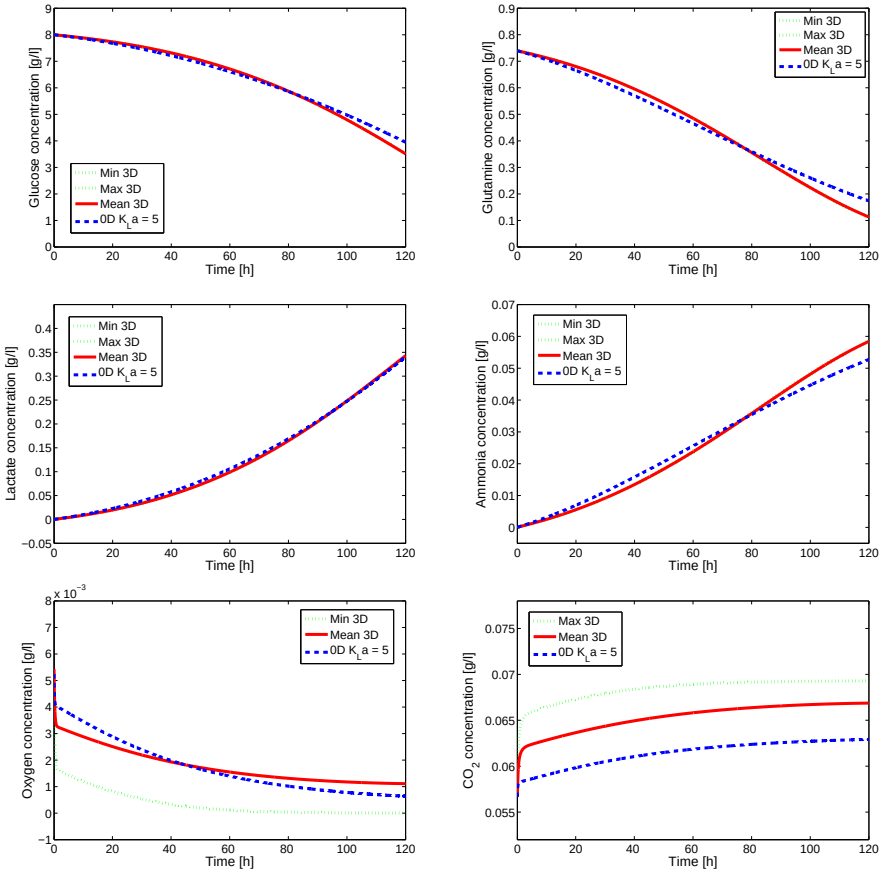

Figure 5.18: Comparison between the 3D model and the 0D model with the steady fluid

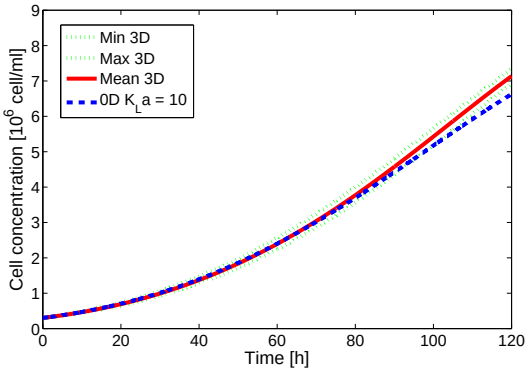

Figure 5.19: Cell growth: comparison between the 3D model and the 0D model (velocity field (5.2) with $A = 0.003$ m/s)

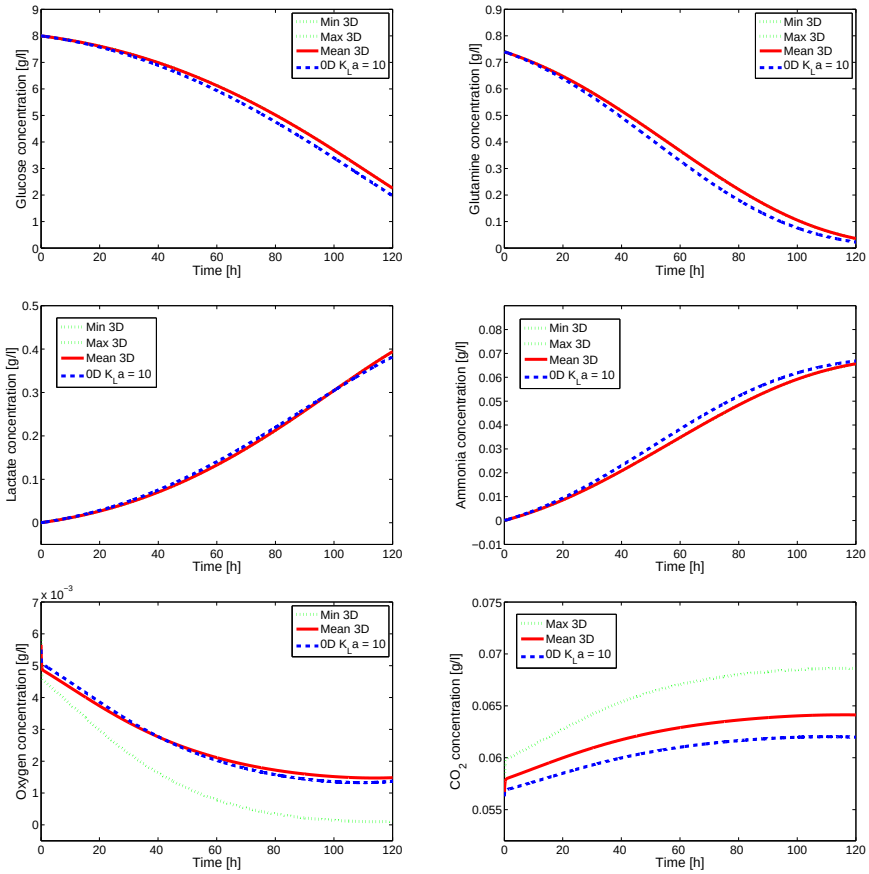

Figure 5.20: Comparison between the 3D model and the 0D model (velocity field (5.2) with $A = 0.003$ m/s)

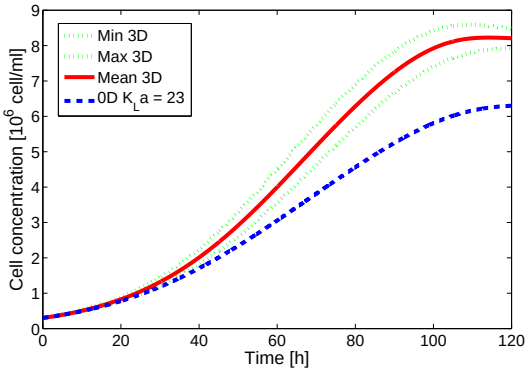

Figure 5.21: Cell growth: comparison between the 3D model and the 0D model (velocity field (5.2) with $A = 0.03$ m/s)

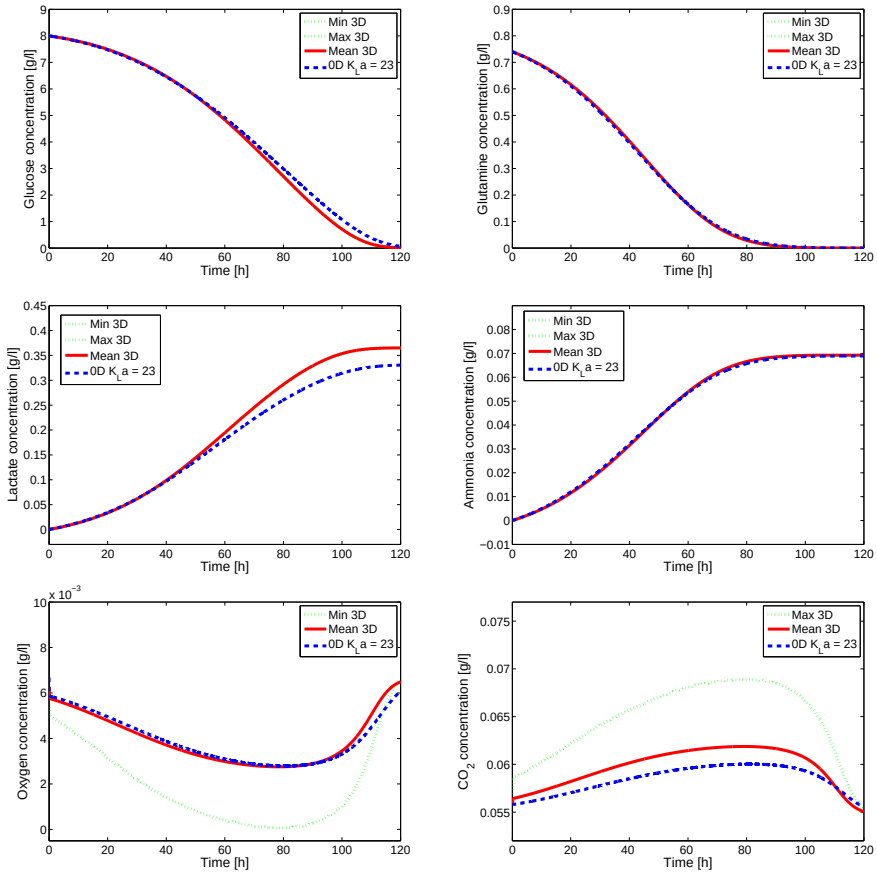

Figure 5.22: Comparison between the 3D model and the 0D model (velocity field (5.2) with $A = 0.03$ m/s)

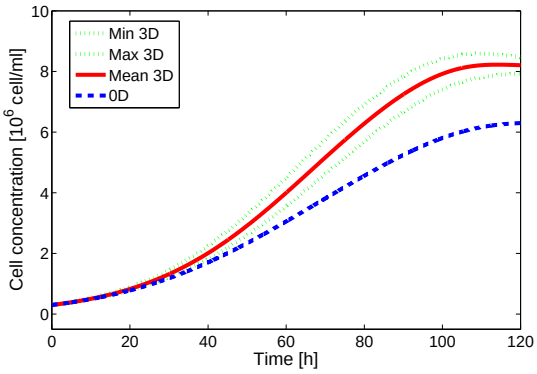

Figure 5.23: Cell growth: comparison between the 3D model and the 0D model (velocity field (5.2) with $A = 0.03$ m/s) and $K_L^{CO_2}a = 0.8 \cdot K_L^{O_2}a$

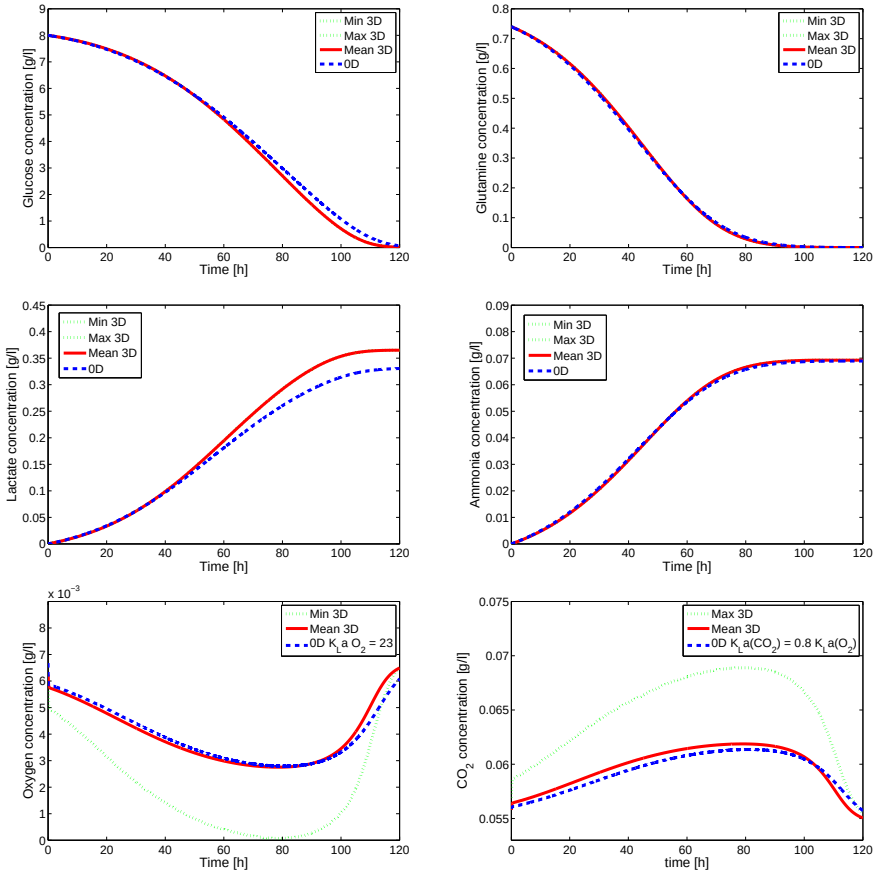

Figure 5.24: Comparison between the 3D model and the 0D model (velocity field (5.2) with $A = 0.03$ m/s) and $K_L^{CO_2}a = 0.8 \cdot K_L^{O_2}a$

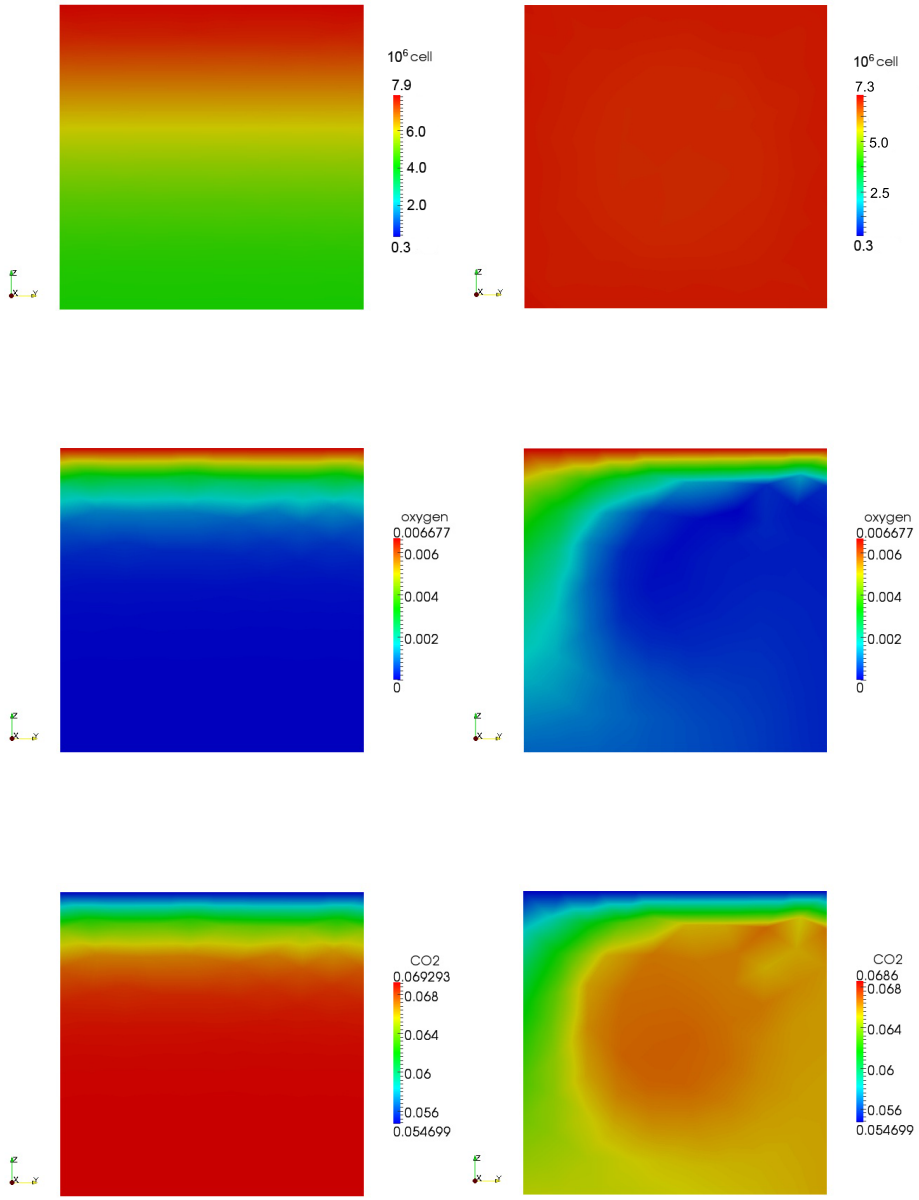

Figure 5.25: 3D model results: comparison between the steady fluid (left) and the transport field (5.2) (right) at $t = 120$ h

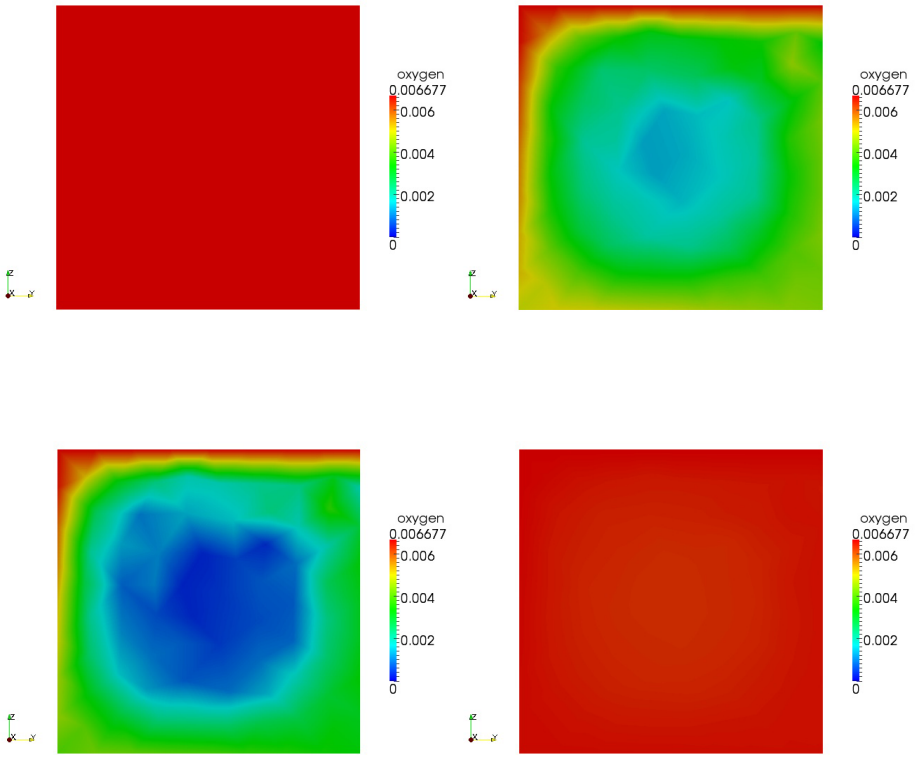

Figure 5.26: 3D model results: oxygen concentration at $t = 0$ h, $t = 40$ h, $t = 80$ h, $t = 120$ h with the transport field (5.2) with $A = 0.03$ m/s

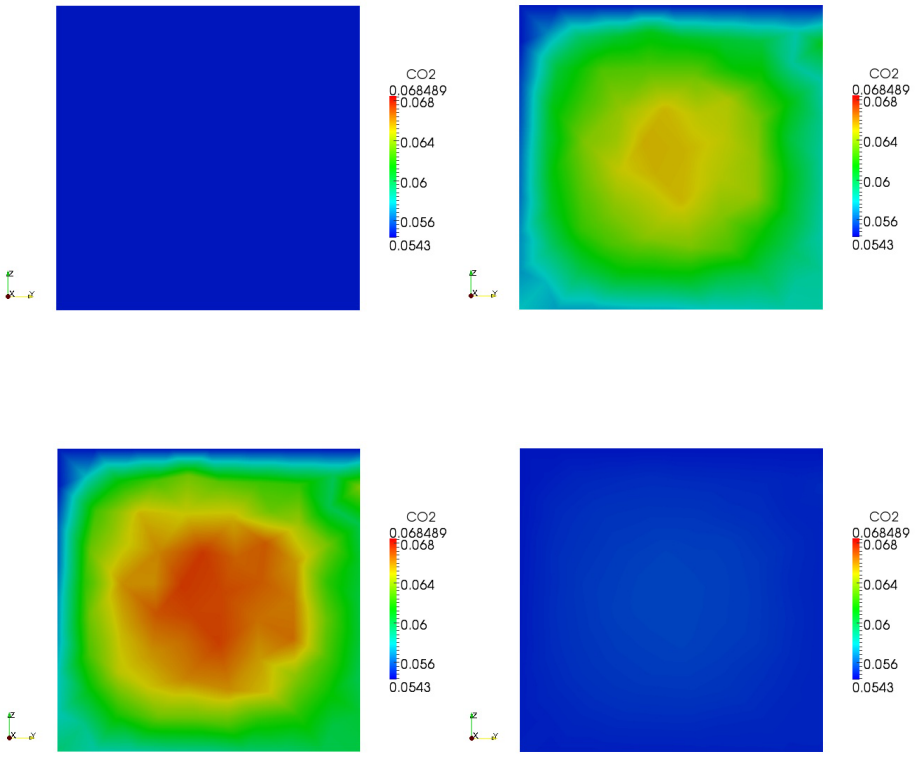

Figure 5.27: 3D model results: carbon dioxide concentration at $t = 0$ h, $t = 40$ h, $t = 80$ h, $t = 120$ h with the transport field (5.2) with $A = 0.03$ m/s

Closing remarks and future work

This work has been focused on the development of a new model for CHO cell growth under batch conditions, primarily based on the study of the cell metabolism.

In the first part, we have analyzed in a critical manner the state of the art on cell growth models, with the objective of detecting the advantages and the limits of the different approaches adopted in the literature.

We studied the main aspects of cell physiology, focusing in particular on cell metabolism and analyzing the effects of different environmental factors, like temperature, oxygen concentration and pH, on the cell behavior.

Then we analyzed the CHO cell culture system, focusing in particular on the relationship between the mode of the bioreactor operation and the properties of the culture environment. Whereas in the framework of the project carried out at LBTC and CMCS CHO cell growth is studied in shaken bioreactors under batch conditions, we introduced an appropriate model for the batch fermenter and in particular for the oxygen and carbon dioxide transfer between the culture medium and the atmosphere.

We proposed a 0D model for cell growth, in which the rate of cell production is based on the analysis of the cell metabolism. The knowledge of the metabolic reactions helps to couple the balance equation that describes the cell dynamics with the ones that describe the substrates consumption and the toxic by-products formation. In particular we considered glucose, glutamine and oxygen as main energy sources and lactate, ammonia and

carbon dioxide as main metabolic products.

We introduced the temperature as a independent factor that influences cell growth. We proposed a gaussian model such that, under optimal temperature conditions, we obtain the maximum growth rate that is possible under the actual substrates concentrations, whereas cell growth is inhibited when temperature exceeds the normal physiological range.

The 0D model is then extended in order to introduce the spatial dependance in the cell growth model. The 1D model that we proposed allows us to estimate the effect on cell growth dynamics of the distance from the culture medium surface.

Finally, we introduced a 3D model in which cell growth is affected by the fluid motion. However, here we don't consider the real hydrodynamics of the shaken bioreactor, but we only analyze the qualitative effects of the fluid transport on cell growth. The integration of the new cell growth model with the real free-surface hydrodynamics is currently under development at CMCS.

The models introduced were tested and the results obtained were qualitatively compared with the experimental results. It is necessary to highlight, however, that further experimental measurement will be required for a full validation of the model. The parameters values have been selected, when it was possible, in the ranges of values proposed in the literature. Despite that, the results obtained with the proposed models are encouraging. The different scale models are currently being tested by LBTC in order to perform a calibration based on additional experiments.

Firstly, the 0D model reproduces the three main phases of the growth curve, namely the lag phase, the exponential phase and the stationary phase. Moreover, the maximum cell concentration that is reached is a quite good estimation of the real concentration obtained from experiments under the same operative conditions. The estimated concentrations of ammonia and lactate are comparable with the ones measured during experiments. Moreover the 0D model seems to reproduce quite well the real cell dynamics under different conditions of temperature and mass transfer rate.

Later on, the 1D model and the 3D model were tested. Whereas, up

to our knowledge, in the literature there are not results about the spatial dependance of cell concentration, the results obtained with these models were compared only with the 0D model's results.

Analyzing the results of the 1D model, we observed that, because of the low oxygen solubility and the absence of mixing related to the fluid motion, the oxygen is rapidly consumed and the medium that is far away from the liquid surface is badly oxygenated. Consequently cell growth is inhibited except in the proximity of the surface, where the maximum cell concentration is reached.

The same results were obtained with the 3D model in the case of steady fluid. On the contrary, if a transport field is imposed, the compounds mixing is enhanced and consequently the concentrations become almost constant in the bioreactor volume. The fluid motion helps to oxygenate the lower part of the culture medium, thus enhancing cell growth and permitting to reach an averaged cell concentration that is greater than in the case of steady fluid. Moreover, the averaged concentrations obtained with the 3D model are comparable with the ones obtained with the 0D model under the same operative conditions and with the corresponding mass transfer coefficient.

The results obtained with the 3D model show that, as expected, if the fluid is moving, the concentrations of cells and metabolic compounds tend to become homogeneous in the bioreactor volume, and that the averaged values in the volume are close to those obtained with the 0D model. We could use the 3D model to simulate and optimize the operating setting, e.g. velocity and geometry, in order to maximize the mixing and to make the concentrations as much homogeneous as possible in the culture medium. If the operative setting of the bioreactor is optimized, than we can proceed by estimating the corresponding mass transfer coefficient and by simulating the cell growth process using the less expensive 0D model. However we need to highlight that the current 3D cell growth model is not considering the effect of shear stresses on cells viability. In shaken bioreactors, in fact, well-mixed conditions are generally obtained with turbulent regimes of motion, which are characterized by high shear-stress. As a consequence better results would probably be obtained by solving the full 3D cell growth model with the real free-surface hydrodynamics introducing the effect of shear-stress on cells vi-

ability.

In conclusion, we want to highlight that an accurate validation of the models is necessary. In order to do that, appropriate experimental results are needed in order to estimate the effect of each considered factor on cell growth. Wherear the factors that influence cell growth in our model are independent the one from the others, each of them should be studied when all the other factors are not limiting. In particular it is necessary to estimate the effect of aerobic glucose oxidation, anaerobic glucose consumption and glutamine aerobic oxidation on the cell growth rate. Moreover, as mentioned in the previous chapter, the effect of different temperatures should be studied under non limiting-nutrient conditions. Finally, further improvements can also be envisaged thanks to the coupling of the cell growth model with the real bioreactor hydrodynamics, that is now being implemented at CMCS.

Ringraziamenti

Sono giunta finalmente a scrivere la pagina più importante, una pagina dedicata a tutte le persone che in questi anni mi hanno aiutato a raggiungere questo importante traguardo.

Il primo e sincero ringraziamento va al Dott. Nicola Parolini, per avermi seguito con pazienza e disponibilità in questi mesi.

Desidero ringraziare il Prof. Alfio Quarteroni ed il Prof. Marco Discacciati, che mi hanno ospitato presso il CMCS dell'EPFL di Losanna e che mi hanno dato in questo modo la possibilità di lavorare in un ambiente molto stimolante. In particolare ringrazio Samuel, che ha condiviso con me, oltre all'ufficio, i "segreti" di LifeV. Un Grazie affettuoso a Matteo e Laura, per avermi accolto e per avermi incoraggiato durante questa trasferta.

Ringrazio il Laboratorio di Biotecnologie Cellulari (LBTC) dell'EPFL ed in particolare la Dottoressa Stéphanie Tissot, che con pazienza ha risposto alle mie numerose e-mail ed ha chiarito ogni mio dubbio sui processi di crescita cellulare.

Ringrazio tutti gli Ingegneri Matematici che hanno condiviso con me questo percorso, in particolare Grazie a Laura e Claudia, con le quali ho affrontato e superato gli ostacoli di questi anni.

Grazie a Giovanni, che non ho ancora conosciuto di persona, ma che ha fatto resuscitare il mio portatile quando avevo quasi perso le speranze.

Grazie a Matteo, che mi ha aiutato a installare LifeV prima della mia partenza, e che anche a distanza è sempre stato disponibile per aiutarmi.

Il Grazie più grande è per i miei genitori, che da sempre hanno creduto in me, mi hanno sostenuta nei momenti di difficoltà e consolata nei momenti di sconforto, come solo una mamma e un papà sanno fare. Grazie al mio fratellino (ma se dico fratellone forse si capisce di più...) per aver sopportato i miei schizzi di pazzia.

Un Grazie speciale alle mie amiche di sempre, Alessandra, Elisa e Paola, per i nostri "Martedì Sera", per le "Corse al Regalo" e per gli "Appuntamenti Disneyani", quelli passati e ovviamente per quelli futuri.

Per concludere, Grazie Leonardo. Per ogni istante condiviso e per il tuo Amore. Il Politecnico ha voluto che anche il giorno della Laurea rientrasse tra i giorni condivisi! Come hai detto tu, un altro Segno...

Bibliography

[1] Broccard G., *"Development of a predictive model for cell growth in shaken bioreactors as a function of the effects of temperature, oxygen transfer rate and seeding concentration"*, Master Thesis, LBTC/EPFL, 2009

[2] Buchanan R.L., Whiting R.C., *"A classification of models for predictive microbiology"*, Food Microbiol., 10: 175-177, 1993

[3] Burman E., Hansbo P., *"Edge stabilization for Galerkin approximations of convection-diffusion-reaction problems"*, Comput. Methods Appl. Mech. Engrg., 193: 1437-1453, 2004

[4] De Sanctis D., Perrone M., *"Numerical analysis of fluid dynamics and oxygen diffusion in shaking bioreactors"*, Master Thesis, Università degli Studi di Roma "Tor Vergata", 2007

[5] Dunn I.J., Heinzle E., Ingham J., Prenosil J.E., *"Biological reaction engineering"*, Wiley-VCH Verlag, 2003

[6] Fourestey G., Deparis S., Formaggia L., Gerbeau J.F., Prud'homme C., *"LifeV developer manual"*, `http://www.lifev.org`, 2010

[7] Furukawa K., Ohsuye K., *"Effect of culture temperature on a recombinant CHO cell line producing a C-terminal α-amidating enzyme"*, Cytotechnology, 26: 153-164, 1998

[8] Gompertz B., *"On the nature of the function expressive of the law of human mortality, and on a new mode of determining the value of life contingencies"*, Philos. Trans. R. Soc. Lond., 115: 513-585, 1825

[9] Hauser H., Wagner R., *"Mammalian cell biotechnology in protein production"*, W. de Gruyter, 1997

[10] Herbert D., *"Continuous culture of microorganisms; some theoretical aspects"*, in Malek I., *"Continuous cultivation of microorganisms; a symposium"*, pp. 45-52, Czech Academy of Science, 1958

[11] Hinshelwood C.N., *"Influence of temperature on the growth of bacteria"*, in "The chemical kinetics of the bacterial cell", Clarendon press, 254-257, 1946

[12] Jayapal K.P., Wlaschin K.F., Hu W.S., Yap M.G.S., *"Recombinant protein therapeutics from CHO cells - 20 years and counting"*, Chem. Eng. Prog., 103: 40-47, 2007

[13] Kovarova K., Zehnder A.J.B., Egli T., *"Temperature-dependent growth kinetics of Escherichia Coli ML 30 in glucose-limited continuous culture"*, J. Bacteriol., 178: 4530-4539

[14] Kovarova K., Egli T., *"Growth kinetics of suspended microbial cells: from single-substrate-controlled growth to mixed-substrate kinetics"*, Microbiol. Mol. Biol. Rev., 62(3): 646-666, 1998

[15] Lewis W.K., Withman W.G., *"Principles of gas absorption"*, Ind. Eng. Chem., 16(12): 1215-1220, 1924

[16] Lu S., Sun X., Zhang Y., *"Insight into metabolism of CHO cells at low glucose concentration on the basis of the determination of intracellular metabolites"*, Process Biochem., 40: 1917-1921, 2005

[17] Malthus T., *"An essay on the principle of population"*, (1798 1st edition) with a "A summary view", and introduction by Professor Antony Flew, Penguin Classics, 1830

[18] McKellar R.C., Lu X., *"Modeling microbial responses in food"*, CRC Series in Contemporary Food Science, 2004

[19] Monod J., *"Recherches sur la croissance des cultures bacteriennes"*, Ed. Hermann and Cie, 1942

[20] Penfold W., Norris D., *"The relation of concentraion of food supply to generation time of bacteria"*, J. Hyg, 12: 253-256, 1912

[21] Quarteroni A., *"Modellistica numerica per problemi differenziali"*, Springer-Verlag Italia, 2006

[22] Rotin D., Robinson B., Tannock I.F., *"Influence of hypoxia and an acid environment on the metabolism and viability of cultured cells: potential implications for cell death in tumors"*, Cancer Rer., 46(6): 2821-2826, 1986

[23] Seth G., Hossler P., Yee J.C., Hu W.S., *"Engineering cells for cell culture bioprocessing - Physiological fundamentals"*, Adv. Biochem. Engin./Biotechnol., 101: 119-164, 2006

[24] Schoonen W.G.E.J., Wanamarta A.H., Van der Klei-Van Moorsel J.M., Jakobs C., Joanje H., *"Respiratory failure and stimulation of glycolysis in Chinese hamster ovary cells exposed to normobaric hyperoxia"*, J. Biol. Chem., 265: 11118-11124, 1990

[25] Smolke C.D., *"The metabolic pathway engineering handbook"*, CRC Press, 2010

[26] Tissot S., *"Experimental results on CHO cell growth"*, Internal report, LBTC/EPFL, 2010

[27] Van Impe J.F., Nicolaï B.M., Martens T., De Baerdemaeker J., Vandewalle J., *"Dynamic mathematical model to predict microbial growth and inactivation during food processing"*, Appl. Environ. Microbiol., 58(9): 2901-2909, 1992

[28] Verhulst P.F., *"Notice sur la loi que la population poursuit dans son accroissement"*, Correspondance mathématique et physique 10: 113-121, 1838

[29] Waite G.N., Waite L.R., *"Applied cell and molecular biology for engineers"*, McGraw-Hill, 2007

[30] Xing Z., Bishop N., Leister K., Li Z.J., *"Modeling kinetics of a large-scale fed-batch CHO cell culture by Markov Chain Monte Carlo method"*, Biotechnol. Prog., 26: 208-219, 2010

[31] Zhang X., Bürki C.A., Stettler M., De Sanctis D., Perrone M., Discacciati M., Parolini N., DeJesus M., Hacker D.L., Quarteroni A., Wurm F.M., *"Efficient oxygen transfer by surface aeration in shaken cylindrical containers for mammalian cell cultivation at volumetric scales up to 1000 L"*, Biochemical Engineering Journal, 45: 41-47, 2009

[32] Zwietering M.H., De Koos J.T., Hasenack .E., De Wit J.C., Van't Riet K., *"Modeling of bacterial growth as a function of temperature"*, Appl. Environ. Microbiol., 57(4): 1094-1101, 1991

[33] Zwietering M.H., Jongenburger I., Rombouts F.M., Van't Riet K., *Modeling of the bacterial growth curve*, Appl. Environ. Microbiol., 56(6): 1875-1881, 1990

[34] Zwietering M.H., Wijtzes T., De Wit J.C., Van't Riet K., *"A decision support system for prediction of the microbial spoilage in foods"*, J. Food Prot., 55: 973-979, 1992